

REVIEW ARTICLE

Open Access

# Intrinsically soft electronics using conducting nanomaterials and liquid metals

Sung-Hyuk Sunwoo<sup>1,2,3</sup>, Hye Jin Kim<sup>2,4</sup>, Jae Hyuk Kim<sup>1</sup>, Dong Chan Kim<sup>5,6</sup> and Dae-Hyeong Kim<sup>1,2,7,8</sup> 

## Abstract

Flexible electronics have significantly influenced modern daily life, particularly in personalized, human-centric applications, due to their ability to conform to curved surfaces. Building on this adaptability, researchers are now focusing on developing stretchable electronic devices that promise next-generation form factors, offering unprecedented user experience and functionalities. Current approaches employ rigid electronic materials configured in strain-accommodating geometries, achieving a high level of technological maturity by leveraging well-established technologies. However, these strategies face limitations, particularly in terms of long-term durability under repeated deformation, primarily due to their reliance on non-stretchable components. To overcome these limitations and facilitate durable deformation, intrinsically stretchable electronic materials have emerged as a promising solution. This review highlights recent advancements in intrinsically soft electronics, with a particular focus on stretchable conductors based on metallic components. Key elements of intrinsically stretchable conductors are discussed, including elastomers used as stretchable substrates, and metallic ingredients such as low-dimensional metallic nanomaterials and liquid metals. Additionally, we explore various assembly and patterning techniques for these materials. Practical applications of metal-based intrinsically soft conductors are highlighted, and this review concludes with an outlook on the prospects and potential challenges for these emerging technologies.

## Introduction

Recent advancements in electronics have propelled modern human civilization forward in transformative ways. Innovations in materials science and semiconductor processing have enabled the creation of electronic devices that are not only smaller in size but also vastly superior in performance. For example, the computational power of modern mobile phones far exceeds that of the Apollo 11 mission's onboard computer, while being remarkably compact<sup>1</sup>. These advancements have paved the way for the development of wearable and implantable electronics, technologies that seamlessly integrate with the human body.

Applications of these devices span from medical and biological monitoring to sports, entertainment, and industrial operations, enhancing both functionality and efficiency.

Traditional electronic materials, such as metals and silicon, have been instrumental in these achievements due to their excellent electrical properties and ease of processing<sup>2,3</sup>. Moreover, processing those materials in ultra-thin, sub-micrometer scale and patterning them with the structures, which absorb mechanical stress, enabled flexibility and even stretchability<sup>4–7</sup>. However, this methodology is constrained by limited deformation capabilities and susceptibility to mechanical fatigue during repeated use<sup>8,9</sup>.

To overcome these challenges, recent research has shifted toward developing intrinsically soft and stretchable materials<sup>8,10</sup>. These materials not only withstand extensive deformation but also retain their performance under repeated mechanical stresses<sup>11,12</sup>. For instance, hydrogels, liquid metals (LMs), and polymer composites with conductive fillers have emerged as promising

Correspondence: Dong Chan Kim ([dckim@gachon.ac.kr](mailto:dckim@gachon.ac.kr)) or Dae-Hyeong Kim ([dkim98@snu.ac.kr](mailto:dkim98@snu.ac.kr))

<sup>1</sup>Department of Chemical Engineering, Kumoh National Institute of Technology, Gumi, Republic of Korea

<sup>2</sup>Center for Nanoparticle Research, Institute for Basic Science (IBS), Seoul, Republic of Korea

Full list of author information is available at the end of the article  
These authors contributed equally: Sung-Hyuk Sunwoo, Hye Jin Kim

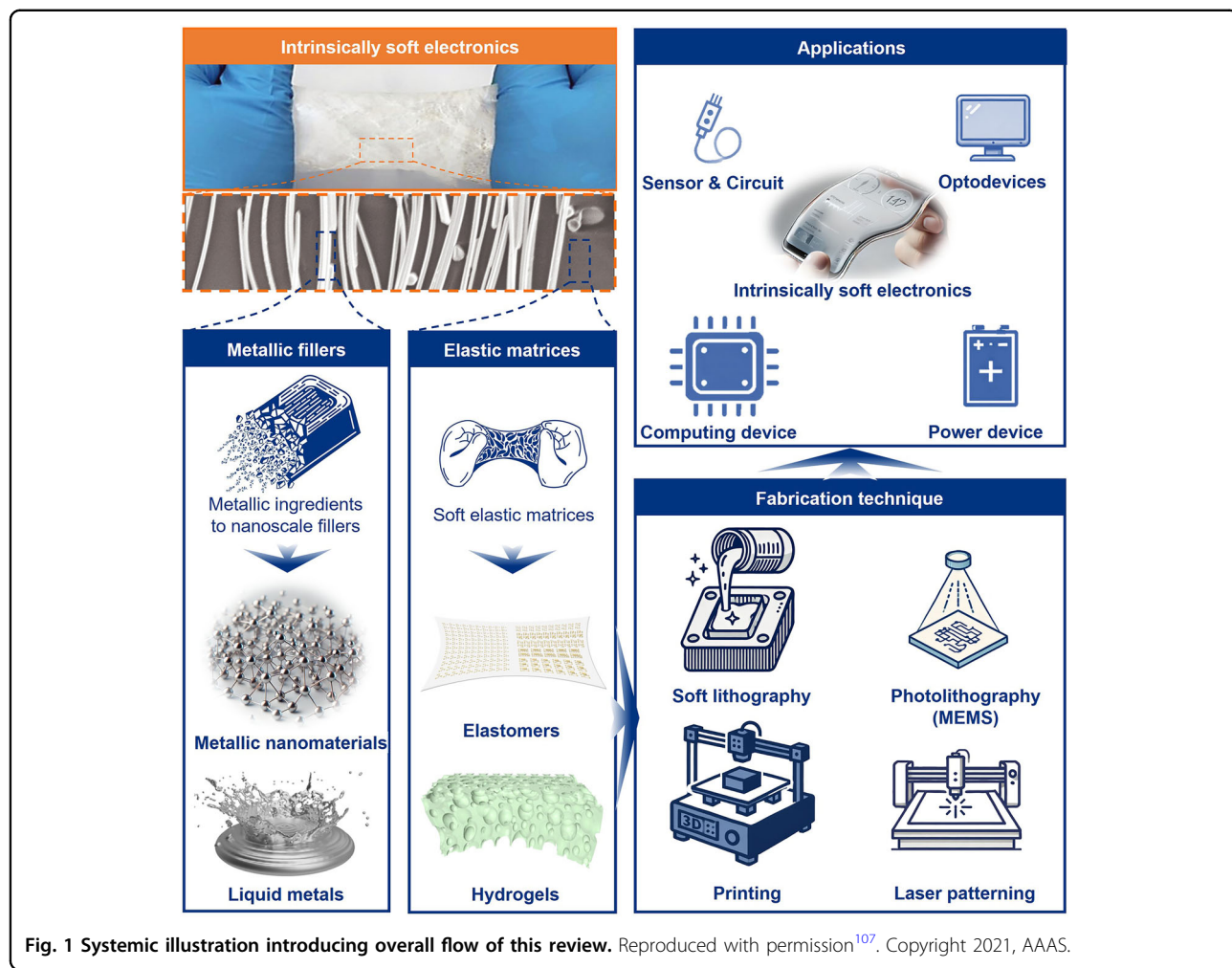


Fig. 1 Systemic illustration introducing overall flow of this review. Reproduced with permission<sup>107</sup>. Copyright 2021, AAAS.

candidates due to their unique combination of softness, stretchability, and excellent electrical properties<sup>13</sup>. Such materials are particularly valuable in biomedical and industrial applications, where flexibility and biocompatibility are critical<sup>14</sup>.

This study reviews the latest research trends and future directions for intrinsically soft electronic materials, with a focus on metal-based systems (Fig. 1). It first examines structural engineering strategies for imparting stretchability to traditional rigid materials, analyzing their advantages and limitations. Next, it introduces cutting-edge intrinsically soft metallic materials, detailing their properties and how they overcome the constraints of rigid counterparts. The discussion then shifts to fabrication techniques and structural designs that enhance the performance and durability of these materials. Finally, the study highlights applications of these materials in electronic components such as circuits, displays, energy storage devices, and computing systems, illustrating their potential to revolutionize the field of flexible electronics.

## Complications of conventional flexible electronics

The development of flexible electronics has revolutionized applications in wearable devices, medical implants, and soft robotics. However, conventional approaches encounter critical limitations, particularly under highly deformable or stretchable conditions. The primary strategy has relied on ultrathin materials capable of conforming to non-planar surfaces while preserving functionality. Despite their potential, these methods are hindered by the intrinsic rigidity of the materials and the intricate mechanical and electrical design processes needed to maintain performance under strain. This chapter delves into these challenges, analyzing the strategies employed and their associated limitations.

## Strategies for flexible electronics

Flexible electronics have primarily achieved mechanical compliance by employing ultrathin materials, enabling devices to conform to curved or dynamic surfaces without significantly compromising electrical properties<sup>15</sup>. Thin metal films, often deposited and patterned on flexible

substrates like polyimide (PI) or parylene, exemplify this approach. The primary advantage of ultrathin materials is their ability to reduce bending stiffness, allowing for substantial flexibility even when rigid materials are utilized. However, while effective for addressing flexibility in bending, this strategy falls short when dealing with complex deformations such as stretching or twisting, key requirements for next-generation applications like epidermal electronics and biomedical implants.

### Structural designs for stretchable electronics using ultrathin materials

To address the limitations of ultrathin materials, various structural designs have been employed to enhance the stretchability of flexible electronics. These designs enable rigid materials to withstand greater mechanical strain without compromising their electrical performance. Four major approaches are commonly used:

#### *In-plane serpentine structure*

In-plane serpentine structures utilize wavy or serpentine patterns for conductive traces, enabling stretchability by allowing the material to unfold under tensile stress. This geometric configuration accommodates mechanical deformation while the conductive material itself remains rigid, thus enhancing flexibility (Fig. 2a)<sup>16</sup>. However, a key limitation of this approach is the significant space required for serpentine patterns, which reduces the effective functional density of the device.

For instance, Jiao et al. developed a vertical serpentine structure to achieve flexibility and stretchability using intrinsically rigid materials<sup>17</sup>. This structure was fabricated on a silicon-based platform, where functional nodes were interconnected through serpentine designs to provide mechanical compliance. The process involved photolithography and etching on a silicon wafer to create the base for the serpentine interconnects, which were subsequently encapsulated in multiple layers of Parylene-C. This encapsulation protected the conductive layers while allowing the structure to stretch and bend without compromising electrical performance. The resulting vertical serpentine conductor exhibited exceptional mechanical properties, withstanding up to 350% strain while maintaining electrical stability. Experimental results indicated less than a 2% change in electrical resistance under 300% strain (Fig. 2b), and the structure endured over 100 stretching cycles at 100% strain without significant degradation, demonstrating its durability.

#### *Out-of-plane buckling structure*

Out-of-plane buckling structures enable stretchability by leveraging vertical deformations. When a thin, rigid film is bonded to a pre-stretched elastomer and subsequently released, the film forms out-of-plane wrinkles or

buckles (Fig. 2c)<sup>18</sup>. This configuration accommodates strain without stretching the material itself, effectively maintaining conductivity during deformation. However, controlling the uniformity and direction of buckling patterns remains challenging.

For example, Xu et al. employed this technique by bonding silicon microstructures onto a pre-stretched elastomer substrate<sup>19</sup>. Upon releasing the pre-strain, the silicon structures buckled into three-dimensional (3D) geometries, enabling mechanical strain accommodation without fracturing (Fig. 2d). The structures maintained electrical continuity and mechanical stability under cyclic strains of up to 100% over 1,000 cycles, demonstrating their durability for stretchable electronics.

#### *Coiled structure and helical structure*

The coiled and/or helical structure, often applied to wires and fibers, involves creating a spring-like configuration that extends and compresses under strain. This configuration offers significant stretchability while maintaining electrical continuity (Fig. 2e)<sup>20</sup>. The downside of this design as electronic materials is that it introduces inductance and resistance variations under different strain conditions, which can lead to signal distortion in high-frequency applications (Fig. 2f)<sup>21</sup>.

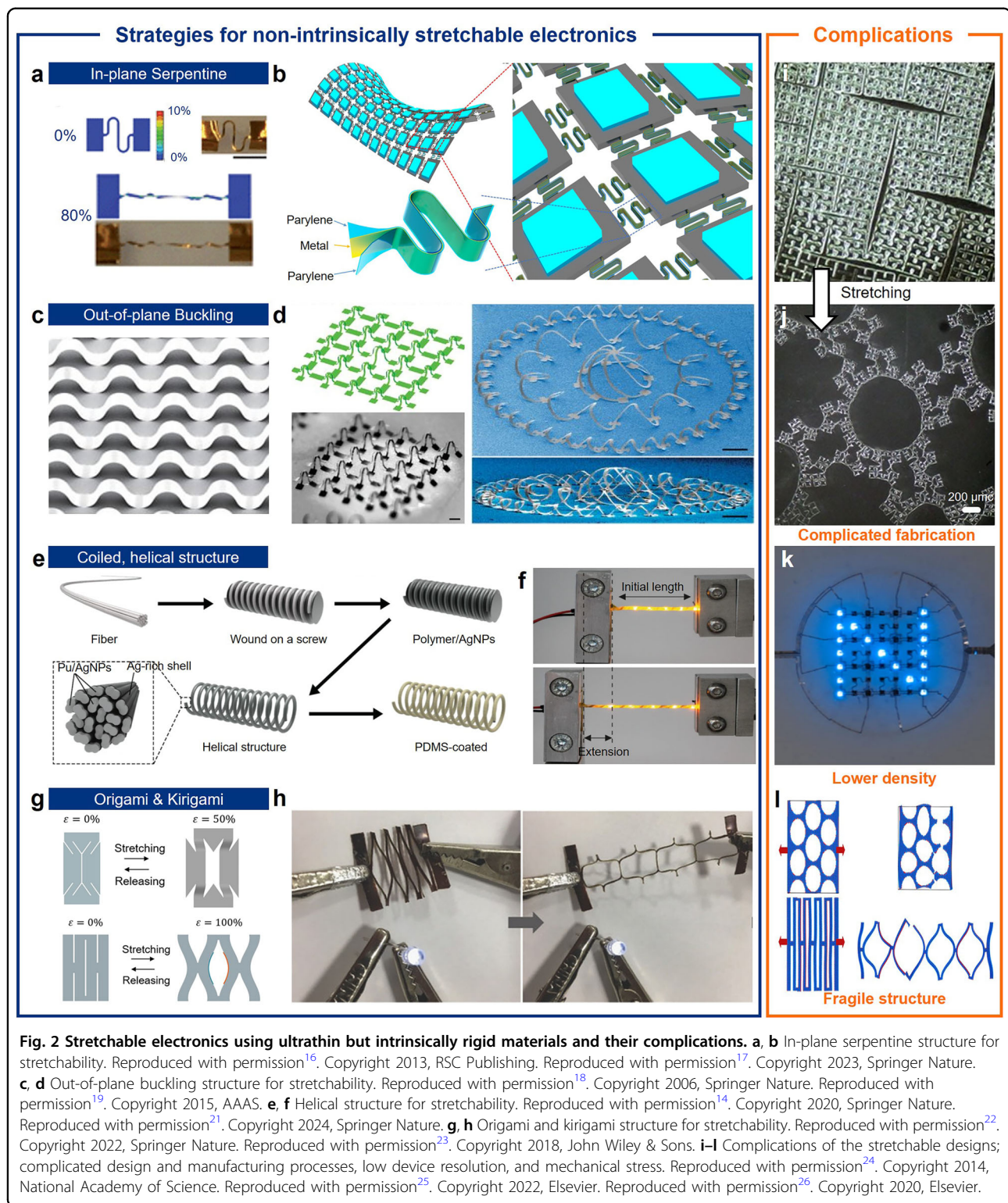
#### *Origami and Kirigami design*

Origami and kirigami techniques utilize folding and cutting patterns in thin films to enable stretchability, accommodating significant mechanical deformation without damaging the material (Fig. 2g)<sup>22</sup>. These designs are particularly effective for applications requiring large strains, though they can reduce functional density and complicate fabrication processes.

For example, Guan et al. implemented a kirigami-inspired design to transform non-stretchable polymer conducting nanosheets (NSs) into highly stretchable materials<sup>23</sup>. By introducing precise cuts into a polymer sheet containing Poly(3-butylthiophene-2,5-diyl) conductive nanowires (NWs) embedded in a robust polymer matrix, the structure achieved up to 2000% strain by deforming along the cut lines. The NSs retained stable electrical performance over 1000 cycles of 2000% strain, with conductivity improving to  $4.002 \text{ S/cm}$  after iodine doping, compared to the original  $2.2 \times 10^{-3} \text{ S/cm}$  (Fig. 2h).

#### *Drawbacks of structural design strategies*

While structural design strategies offer innovative ways to impart stretchability to rigid materials, these approaches are fundamentally limited by the intrinsic rigidity of the materials themselves. Metals, semiconductors, and other stiff components encounter significant challenges under repetitive mechanical strain, constraining their



long-term reliability and applicability in soft electronic devices.

One major limitation is the complexity of adapting rigid materials for stretchable applications. Geometric designs

often require intricate patterns and thin-film architectures, necessitating advanced fabrication techniques that involve multiple deposition, patterning steps, and even transfer<sup>24</sup>. These processes are not only technically

demanding but also time-intensive and costly, adding significant barriers to scalability and widespread adoption (Fig. 2i, j).

Another drawback arises from the need for 3D deformation in inherently 2D materials. Accommodating such deformations requires the inclusion of marginal spaces in the design, leading to increased size and reduced functional density (Fig. 2k)<sup>25</sup>. For instance, serpentine structures used in stretchable displays demand additional spacing, which decreases pixel density, diminishing image resolution and overall device performance. This trade-off between stretchability and functional density remains a critical challenge for applications requiring high precision and compact designs.

Moreover, reducing the thickness of rigid materials to enhance flexibility compromises their mechanical robustness (Fig. 2l)<sup>26</sup>. Under repetitive mechanical strain, such as cyclic stretching or bending, stress accumulates within the material, eventually leading to fatigue, micro-cracking, or delamination at interfaces. These issues degrade performance and shorten the device's operational lifespan. Even in commercially available flexible electronics, hinge regions often experience accelerated mechanical degradation due to repeated stress.

Despite advancements in structural design, these limitations underscore the necessity of alternative approaches. Intrinsically soft materials offer a promising solution by eliminating the reliance on geometric adaptations to achieve stretchability. By addressing the fundamental challenges posed by rigid materials, intrinsically soft electronics can enable devices that are not only stretchable but also robust, functional, and reliable over extended periods.

### **Intrinsically stretchable substrate/encapsulation materials**

As electronics evolve towards wearable, implantable, and soft robotic applications, the demand for highly stretchable and deformable materials, particularly those suitable for use as substrates and encapsulation layers, has become increasingly critical<sup>27</sup>. Conventional electronics rely on rigid or semi-rigid substrates, which significantly limit their performance in environments requiring high flexibility and adaptability. In contrast, intrinsically soft materials offer an innovative solution by combining high elasticity with mechanical compliance, enabling electronic devices to withstand stretching, twisting, and bending without compromising functionality.

Soft electronics typically involve conductive components, which serve as circuits, and insulating materials, which function as substrates or encapsulation layers. To achieve truly intrinsically soft electronics, both conductive and insulating materials must exhibit comparable softness. This chapter delves into a range of intrinsically soft

insulating materials, including flexible polymers, elastomers, and hydrogels, that are widely utilized as substrates or encapsulation layers in soft electronics, highlighting their properties and applications.

#### **Flexible polymers**

Flexible polymers, such as polyimide and parylene, have long been considered for use in flexible electronics due to their mechanical flexibility and ease of processing. While not inherently stretchable, these polymers can serve as flexible substrates for thin-film electronics or in combination with more elastic materials.

#### **Parylene**

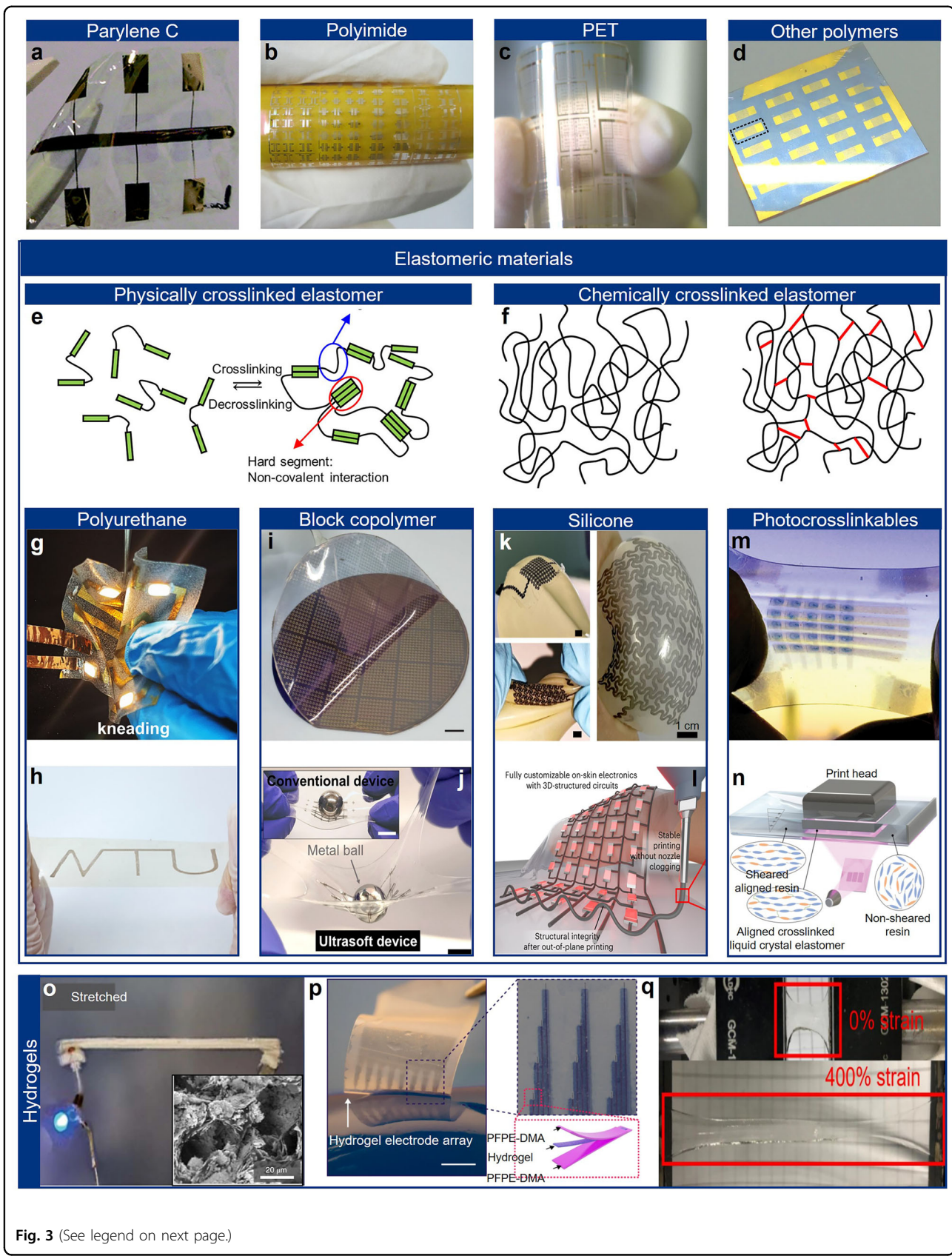
Parylene is a widely utilized material in flexible electronics, valued for its exceptional dielectric properties and chemical resistance. Its vapor-phase deposition process enables the formation of conformal, pinhole-free coatings, making it ideal for applications requiring electrical insulation and protection from environmental factors like moisture and chemicals<sup>28</sup>. Parylene's inherent flexibility further enhances its suitability for scenarios where devices must endure mechanical deformation.

For example, Werkmeister and Nickel investigated the use of Parylene-N and Parylene-C as substrates and gate dielectrics in organic thin-film transistors<sup>29</sup>. The chemically vapor-deposited Parylene-N film demonstrated an impressively low surface roughness of approximately 4 nm. Utilizing the lift-off technique, a gold layer and a pentacene layer were deposited onto the parylene substrate to construct the electronic components. The resulting organic thin-film transistor exhibited remarkable mechanical flexibility, maintaining consistent performance even under deformation with a bending radius as small as 1 mm (Fig. 3a). This highlights Parylene's potential in advanced flexible electronic applications.

#### **Polyimide (PI)**

PI is a high-performance polymer renowned for its excellent thermal stability (−296 to 400 °C), mechanical robustness, and flexibility<sup>30</sup>. These properties make PI a preferred choice for applications such as flexible printed circuit boards (FPCBs), where it serves as a reliable substrate for thin metal interconnects. Its outstanding thermal resistance ensures durability in high-temperature environments, while its mechanical flexibility makes it ideal for wearable electronics requiring minimal bending stiffness.

For example, Jin et al. developed flexible surface acoustic wave resonators using vertically-aligned zinc oxide (ZnO) nanocrystals deposited on PI film. The ZnO nanocrystal film, with a thickness of 1.7–4 μm, was sputtered onto a 100 μm-thick PI substrate<sup>31</sup>. The



(see figure on previous page)

**Fig. 3 Intrinsically stretchable substrate and encapsulation materials.** **a–d** Flexible polymers. Reproduced with permission<sup>29</sup>. Copyright 2013, RSC Publishing. Reproduced with permission<sup>31</sup>. Copyright 2013, Springer Nature. Reproduced with permission<sup>34</sup>. Copyright 2020, Springer Nature. Reproduced with permission<sup>23</sup>. Copyright 2022, Springer Nature. **e, f** Physically (e) and chemically (f) crosslinked elastomers. Reproduced with permission<sup>37</sup>. Copyright 2021, John Wiley & Sons. **g, h** Thermoplastics. Reproduced with permission<sup>43</sup>. Copyright 2024, Springer Nature. Reproduced with permission<sup>44</sup>. Copyright 2023, Springer Nature. **i, j** Block-copolymers. Reproduced with permission<sup>46</sup>. Copyright 2023, Springer Nature. Reproduced with permission<sup>45</sup>. Copyright 2023, Springer Nature. **k, l** Silicones. Reproduced with permission<sup>54</sup>. Copyright 2024, Springer Nature. Reproduced with permission<sup>44</sup>. Copyright 2023, Springer Nature. **m, n** Photocrosslinkable elastomers. Reproduced with permission<sup>57</sup>. Copyright 2020, Springer Nature. Reproduced with permission<sup>58</sup>. Copyright 2021, AAAS. **o–q** Intrinsically soft hydrogel substrate. Reproduced with permission<sup>62</sup>. Copyright 2019, Springer Nature. Reproduced with permission<sup>63</sup>. Copyright 2023, Springer Nature.

resulting resonator exhibited remarkable flexibility, maintaining its functionality even when wrapped around a finger. This demonstrates polyimide's potential for use in flexible electronics, sensors, and lab-on-a-chip devices, highlighting its capability to endure substantial mechanical deformation while preserving performance (Fig. 3b).

#### Polyethylene terephthalate (PET)

Polyethylene terephthalate (PET) is widely used in flexible electronics due to its transparency, mechanical strength, and cost-effectiveness<sup>32,33</sup>. Its optical clarity and flexibility make it a popular choice for applications like flexible displays and touchscreens. However, PET's low stretchability and limited thermal and chemical stability restrict its use in environments requiring significant elongation or harsh conditions. For instance, Li et al. fabricated large-scale, transparent molybdenum disulfide (MoS<sub>2</sub>)-based transistors and logic circuits on PET substrates (Fig. 3c) by transferring a wafer-scale MoS<sub>2</sub> monolayer onto indium tin oxide (ITO) and aluminum oxide (Al<sub>2</sub>O<sub>3</sub>)-treated PET<sup>34</sup>. The resulting devices demonstrated durability, maintaining functionality after 1,000 bending cycles at 2% strain.

#### Other flexible polymers

In addition to parylene, polyimide, and PET, polymers such as polycarbonate (PC)<sup>35</sup> and polyether ether ketone (PEEK)<sup>36</sup> have been explored for flexible electronics due to their balance of flexibility, strength, and durability. These materials are suitable for applications in flexible circuits, displays, and biomedical devices. For instance, Quereda et al. fabricated a tungsten disulfide (WS<sub>2</sub>) photodetector on a transparent polycarbonate film through a simple direct rubbing technique with WS<sub>2</sub> micropowder (Fig. 3d)<sup>37</sup>. The polycarbonate substrate, chosen for its abrasion resistance, supported the fabrication process without degradation. The photodetector demonstrated a responsivity of 114 mA/W and a fast response time of ~70 μs, with stable performance under 0.7% uniaxial elongation.

#### Elastomeric materials

Elastomers are a class of polymers that are intrinsically stretchable, offering both high elasticity and mechanical compliance. These materials can undergo large strains (up to several hundred percent) without permanent deformation, making them ideal for applications in soft electronics where significant mechanical deformation is required. Elastomers can be broadly classified into physically crosslinked elastomers and chemically crosslinked elastomers, each with a crosslinking mechanism, distinct properties, and fabrication processes.

#### Physically crosslinked elastomers

Physically crosslinked elastomers rely on physical inter-chain interactions, such as hydrogen bonding and electrostatic forces, to maintain their structure<sup>38,39</sup>. These materials typically consist of soft segments, which provide stretchability by unfolding under mechanical deformation, and hard segments, which ensure structural integrity through inter-chain interactions (Fig. 3e). The ratio of soft to hard segments dictates the material's overall softness and stretchability. Compared to chemically crosslinked elastomers, physically crosslinked variants exhibit greater plasticity and stretchability due to their lower crosslinking density and reversible bonding mechanisms. Additionally, their capacity to accommodate nanofillers makes them well-suited as nanocomposite matrices. However, their weak resistance to heat and chemicals limits their durability in harsh environments.

**Polyurethane (PU)** Polyurethane (PU) is a physically crosslinked elastomer valued for its high elasticity and toughness, making it a popular material in wearable electronics, sensors, and soft robotics. Its ability to endure high strain without mechanical failure makes it particularly suitable for harsh environments<sup>40,41</sup>. However, PU's sensitivity to moisture and humidity can affect its long-term mechanical properties. Despite this limitation, PU remains a versatile and easily tunable material for soft electronics due to its mechanical robustness and ease of processing<sup>42</sup>.

For example, Cao et al. developed stretchable electrodes with anti-friction properties by forming hydrogen bonds between hydrophilic PU and wet gold grains, achieving a robust interfacial binding strength of 1,243.4 N/m—significantly higher than polydimethylsiloxane (PDMS) or styrene-ethylene-butylene-styrene (SEBS) substrates (Fig. 3g)<sup>43</sup>. The Au/PU device demonstrated excellent electrical conductivity (<500  $\Omega/\square$ ) even after 1100 friction cycles at 130 kPa and maintained low electrical resistance ( $1.09 \times 10^{-3} \Omega \cdot \text{m}$ ) under 400% strain. This versatile electrode was successfully used as a bioelectrode and an anti-friction pressure sensor array.

Lv et al. introduced a sustainable PU-based printed conductor using vegetable oil-derived polyols crosslinked through carbamate-oxime and hydrogen bonds<sup>44</sup>. This PU/Ag composite exhibited a conductivity of 12,833 S/cm, stretchability of 350%, and low hysteresis (0.333) after 100% cyclic stretching (Fig. 3h). As a proof of concept, the composite was implemented in a soft smart gripper for fruit maturity sensing, detecting ripeness via impedance spectroscopy and transmitting signals to a pneumatic actuator for automated gripping. Additionally, the composite was recyclable, allowing separation into reusable PU and Ag flakes through solvent dissolution and centrifugation.

**Block-copolymers** Block copolymers, such as styrene-butadiene-styrene (SBS) and SEBS, are widely used as physically crosslinked elastomers due to their combination of mechanical strength and stretchability<sup>45</sup>. These materials consist of alternating hard and soft segments, where the hard blocks provide reinforcement, and the soft blocks contribute to elasticity, making them ideal for flexible conductive composites and stretchable electrodes.

For example, Koo et al. developed intrinsically soft transistors by integrating semiconducting carbon nanotubes (CNTs), microcracked gold nanomembranes, and a chemically vapor-deposited elastic polymer dielectric on a SEBS substrate (Fig. 3i)<sup>46</sup>. The dielectric material, designed with soft (isononyl acrylate) and hard (trimethyl-trivinyl cyclotrisiloxane) segments, maintained stretchability while ensuring high uniformity and stable electrical performance. The transistor array, comprising 1000 devices on a wafer, demonstrated functionality under 40% strain for over 1000 cycles and supported logic operations such as NAND, NOR, and XOR gates.

In another study, Li et al. incorporated a soft SEBS interlayer with a Young's modulus of 2.83 MPa to create tissue-level modulus devices, including transistors and sensors (Fig. 3j)<sup>45</sup>. The SEBS layer, combined with polyacrylamide (PAAm) hydrogel, exhibited significantly reduced stiffness compared to SEBS-PDMS composites. A stretchable polymer semiconductor and CNTs network

were deposited onto the SEBS-PAAm substrate, resulting in a soft transistor with an on/off ratio of  $10^4$  and stable charge-carrier mobility ( $\sim 0.7 \text{ cm}^2/\text{Vs}$ ) after 1000 cycles at 100% strain. The device's tissue-like softness enabled conformal skin contact without delamination during mechanical deformation.

### Chemically crosslinked elastomers

Chemically crosslinked elastomers are characterized by irreversible inter-chain interactions formed through covalent bonds. These crosslinks are typically initiated by external triggers, such as crosslinking agents or UV radiation, depending on the mechanism employed (Fig. 3f)<sup>38,47</sup>. The strong covalent bonds provide exceptional resistance to chemical, mechanical, and thermal stimuli, making these elastomers highly durable. However, the dense crosslinking limits nanofiller incorporation and reduces plasticity, often resulting in a higher modulus compared to their physically crosslinked counterparts<sup>48</sup>.

**Silicone (PDMS, Ecoflex)** Silicone elastomers, particularly PDMS and Ecoflex, are widely utilized in soft electronics due to their softness, with Young's modulus values of 43.3 kPa for Ecoflex and 353 kPa for PDMS—comparable to that of human skin (25–260 kPa)<sup>49</sup>. PDMS is prized for its biocompatibility, optical transparency, and chemical inertness, making it a versatile material for substrates, encapsulation layers, and dielectric applications<sup>50,51</sup>. Its elasticity enables stretching up to several hundred percent without permanent deformation<sup>52</sup>. Ecoflex, being softer, is often used in applications requiring extreme deformability, such as soft robotics and wearable sensors.

A key strength of silicone elastomers is their processability; PDMS can be molded into complex shapes via soft lithography, ideal for microfluidics, flexible circuits, and stretchable sensors. However, limitations like poor adhesion and high gas permeability (55  $\mu\text{m}$  for  $\text{CO}_2$  and He)<sup>53</sup> necessitate surface modifications or composite designs to enhance performance.

For instance, Lu et al. developed a laser-induced graphene (LIG)-PDMS composite, increasing the stretchability of brittle LIG from 20% to 220% using an adhesive hydrogel transfer process (Fig. 3k)<sup>54</sup>. The LIG-hydrogel electrode on PDMS demonstrated high biocompatibility and antibacterial properties, serving as wearable sensors for mechanical, humidity, and electrocardiography (ECG) monitoring. Its softness enabled its application as an implantable epicardial monitor on rodent hearts. Similarly, Lee et al. created a printable conductive elastomer composite combining Ag particles, multi-walled CNTs, and PDMS, achieving high stretchability (150%) and conductivity (6682 S/cm)<sup>55</sup>. Printed into freestanding 3D

structures with 100  $\mu\text{m}$  resolution (Fig. 3l), the composite functioned as on-skin electrodes for temperature sensing and feedback displays, maintaining performance under 40% strain.

**Photocrosslinkable elastomers** Photocrosslinkable elastomers represent a promising class of materials for soft electronics, offering precise control over mechanical properties and geometry through UV-induced chemical crosslinking. These materials are particularly suited for applications requiring high-resolution patterning, such as microelectronics and microfluidic devices, due to their tunable stiffness, elasticity, and stretchability. A commonly used example, pure polyurethane acrylate (PUA), exhibits a Young's modulus of 1.4 MPa<sup>56</sup>. Fabrication involves spin-coating or printing liquid precursors onto substrates, followed by UV curing, enabling intricate, flexible patterns. While promising, further research is necessary to optimize their mechanical and electrical performance for practical applications.

For instance, Liu et al. developed a fully stretchable organic light-emitting electrochemical cell array and thin-film transistor using a PUA-AgNWs electrode, poly(3,4-ethylenedioxythiophene):polystyrene sulfonate (PEDOT:PSS) hole injection layer, and diamethacrylate-modified perfluoropolyether dielectric<sup>57</sup>. The UV-crosslinked dielectric layer demonstrated resistance to mechanical deformation and chemical exposure, with a high breakdown voltage of over 100 V at a thickness below 200 nm, highlighting its potential for stretchable organic thin-film transistors (Fig. 3m). The integrated device achieved 30% stretchability without delamination or cracking and exhibited a turn-on current density of  $\sim 2 \text{ mA/cm}^2$ .

In another study, Li et al. introduced photopatternable liquid crystal elastomer (LCE) actuators using digital light processing<sup>58</sup>. During fabrication, shear printing aligned the liquid crystal in the resin tray, followed by photocrosslinking with projected UV light (Fig. 3n). The resulting LCE exhibited thermal actuation properties, reconfiguring its crosslinking network in response to heat. This enabled behaviors such as locomotion and weight lifting, showcasing its potential for optoelectric sensing and actuation in soft robotics.

## Hydrogels

Hydrogels are water-swollen polymers with tunable mechanical properties and high biocompatibility, making them ideal for elastic electronics<sup>59,60</sup>. Their tissue-like softness and conformability enable seamless integration with biological tissues, making them valuable for wearable devices, bioelectronics, and implantable sensors. Hydrogels serve as substrates, dielectric layers, or encapsulation

materials, offering flexibility and adaptability to various shapes<sup>61</sup>.

One advantage of hydrogels is their adjustable mechanical properties, controlled by crosslinking density, polymer composition, or water content. This tunability ensures compatibility with biological tissues, minimizing mechanical mismatch in bioelectronic applications. Hydrogels' swelling behavior can also enable self-healing or adaptive responses to environmental changes like humidity or temperature. Commonly used hydrogels include polyvinyl alcohol (PVA) for mechanical strength and encapsulation, PAAm for high elasticity, and polyethylene glycol for biocompatibility and resistance to protein adsorption. Advanced hydrogels, such as those with nanofillers or double-network structures, offer enhanced toughness and stability.

Despite their benefits, hydrogels face challenges, including susceptibility to drying and residual ionic conductivity, which can cause signal leakage or noise in dielectric applications. Strategies like composite designs or hydrophobic coatings mitigate these issues, extending hydrogel functionality in practical devices.

For instance, Ohm et al. developed a conductive hydrogel composite with a soft modulus of 10 kPa and conductivity of 374 S/cm using 5 vol.% Ag flakes forming a percolation network in a PAAm-alginate matrix<sup>62</sup>. The composite exhibited stable electrical performance under 250% strain and minimal resistance change over 100 stretching cycles, making it suitable for neural electrodes and actuators. Integrated with a shape-memory alloy, the hydrogel powered a swimming robot with a speed of 40 mm/s (Fig. 3o).

Liu et al. created a conductive hydrogel for neuro-modulation by removing ionic liquid from an ionic liquid-PEDOT:PSS hydrogel<sup>63</sup>. The resulting material achieved a conductivity of 47.4 S/cm, stretchability of 20%, and a Young's modulus of 32 kPa. It maintained stable impedance under deformation and withstood 10,000 stretching cycles with minimal resistance changes. Using photolithography, the hydrogel was patterned with 100  $\mu\text{m}$  resolution and exhibited high charge storage capacity (164  $\text{mC/cm}^2$ ), making it effective for low-voltage sciatic nerve stimulation in rodents (Fig. 3p).

Huang et al. enhanced hydrogel mechanics for soft electronics by developing a double-network polyacrylamide-calcium alginate hydrogel<sup>64</sup>. This design enabled 400% strain without damage due to its interconnected porous structure. Replacing water with glycerol increased the Young's modulus from 77.5 to 252 kPa, improving stability in low-humidity conditions. The organohydrogel retained over 80% of its weight after 36 hours, proving its suitability for wearable sensors in variable environments (Fig. 3q).

**Table 1** Characteristic summary of metallic and liquid metal-based fillers.

Category	Example Material	Electrical Conductivity	Percolation Threshold	Pros	Cons
0D Metallic Nanofillers	<b>AgNPs</b>	Medium (~ $10^4$ – $10^5$ S/m)	High (~20–40 vol%)	High conductivity; Easy dispersion; Printable inks	Poor percolation; Aggregation; Oxidation issues
	<b>AuNPs</b>	Medium (~ $10^4$ – $10^5$ S/m)	High (~20–40 vol%)	Excellent biocompatibility; Chemical stability	Poor percolation; High cost;
	<b>CuNPs</b>	Medium (~ $10^4$ – $10^5$ S/m)	High (~20–40 vol%)	Cost-effective; Good conductivity	Poor percolation; Oxidation sensitivity
1D Metallic Nanofillers	<b>AgNWs</b>	Very High (~ $10^5$ – $10^6$ S/m)	Low (~1–5 vol%)	Excellent percolation; High stretchability; Low filler loading	Junction instability under cyclic strain
	<b>AuNWs</b>	High (~ $10^5$ – $10^6$ S/m)	Low (~1–5 vol%)	Stable; Biocompatible; Oxidation-resistant	Expensive; Low aspect ratio
	<b>CuNWs</b>	Very High (~ $10^5$ – $10^6$ S/m)	Low (~1–5 vol%)	Cost-effective; High conductivity	Oxidation sensitivity; Junction degradation
2D Metallic Nanofillers	<b>AuNSs</b>	High (~ $10^5$ – $10^6$ S/m)	Medium (~5–10 vol%)	High surface area; Stable conductivity; Biocompatibility	High cost; Small size
	<b>Silver flakes</b>	Very High (~ $10^5$ – $10^6$ S/m)	Medium (~5–10 vol%)	Good conductivity; Effective percolation	Aggregation; Non-transparency
Liquid Metals (LMs)	<b>EGaIn</b>	Very High (~ $10^6$ S/m)	N/A (Liquid)	Ultra-high stretchability; Self-healing; Reconfigurable	Leakage issues; Oxide skin formation; Patterning complexity
	<b>Galinstan</b>	Very High (~ $10^6$ S/m)	N/A (Liquid)	Non-toxic; High conductivity; Low melting point	Oxide layer; Leakage; High surface tension
	<b>Gallium</b>	Very High (~ $10^6$ S/m)	N/A (Liquid)	High conductivity; Reconfigurable	Oxide formation; Leakage

## Conductive metallic nanomaterials for intrinsically soft nanocomposites

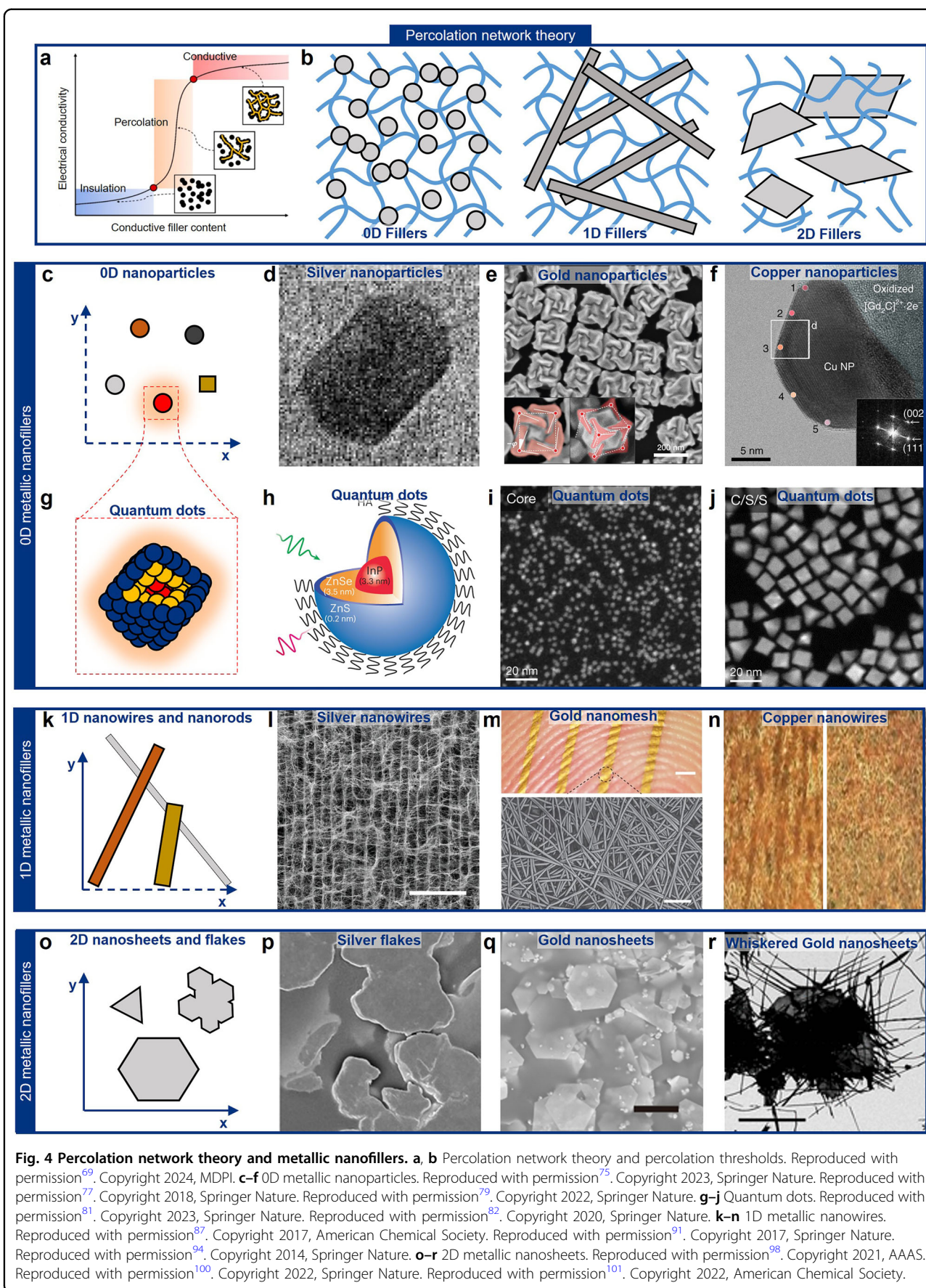
The advancement of intrinsically soft electronics relies on the development of materials that combine high electrical conductivity with exceptional deformability. Metallic nanomaterials, including zero-dimensional (0D) nanoparticles (NPs), one-dimensional (1D) NWs, and two-dimensional (2D) NSs, play a pivotal role in creating conductive and stretchable composites. By embedding these nanomaterials into elastomeric or other soft matrices, conductive networks are formed that preserve electrical performance under mechanical deformation. This chapter explores the unique properties, advantages, and fabrication techniques of metallic nanomaterials, focusing on their integration into soft electronics<sup>65</sup>. Additionally, methods to functionalize and enhance these nanocomposites for improved performance, such as electric conductivity, stretchability, and biocompatibility, are discussed, emphasizing their potential in next-

generation electronic applications. The summary discussing characteristics of the metallic nanomaterials and LMs are presented in Table 1.

## Percolation network theory and nanocomposites

Understanding the role of metallic nanomaterials in soft electronics begins with the concept of a percolation network. Percolation theory explains how conductive fillers, dispersed within an insulating matrix (such as an elastomer), form continuous pathways for electrical conduction once their concentration surpasses a critical threshold—the percolation threshold<sup>66,67</sup>. Below this threshold, the material remains non-conductive, but exceeding it establishes a conductive network, enabling current flow (Fig. 4a, b)<sup>68,69</sup>.

In metallic nanocomposites, achieving an effective percolation network with minimal filler content is crucial. The geometry<sup>70</sup>, size, and distribution of metallic fillers significantly influence the percolation threshold and



composite conductivity<sup>71</sup>. Furthermore, these factors impact the mechanical properties of the composite, including stretchability and durability, by governing the interactions between the fillers and the matrix. Careful optimization of these parameters facilitates the development of soft, conductive nanocomposites suitable for diverse applications, such as sensors, circuits, and energy storage devices<sup>72</sup>.

### Metallic nanofillers

Metallic nanofillers are the core components used to create percolation networks in soft, conductive composites. These fillers can be classified into three main categories based on their dimensionality: 0D NPs, 1D NWs, and 2D NSs. Each of these forms of nanomaterials offers unique properties that can be leveraged to optimize the performance of soft electronics.

#### 0D metallic nanoparticles (NPs)

Metallic NPs are 0D nanomaterials with small aspect ratios, characterized by their ability to infiltrate polymeric matrices or fill gaps between other nanomaterials without compromising functionality (Fig. 4c)<sup>73</sup>. However, their small size and low aspect ratio make it challenging for NPs alone to form effective percolation networks<sup>74</sup>. Consequently, nanoparticles are often used as secondary or additive fillers to enhance the properties of nanocomposites, complementing primary fillers that establish the percolation network. While they are limited in independently forming conductive networks, nanoparticles contribute additional functionalities without significantly affecting the composite's mechanical or electrical performance.

**Silver nanoparticles (AgNPs)** Silver nanoparticles (AgNPs) are extensively utilized in flexible and soft electronics due to their excellent electrical conductivity and relatively low cost (Fig. 4d)<sup>75</sup>. Common applications include conductive inks for printed electronics, wearable sensors, and flexible circuits. Their nanoscale size, typically below 100 nm, provides a high surface area-to-volume ratio, facilitating interactions with the surrounding matrix and supporting the formation of conductive networks<sup>76</sup>. As secondary fillers, AgNPs effectively stabilize connections between primary fillers, enhancing the inter-filler network.

Despite their advantages, AgNPs face limitations due to their low aspect ratio, which results in conductivity being dominated by inter-filler resistance rather than intra-filler pathways. This characteristic reduces their effectiveness in conductive networks, especially under repeated mechanical deformation, where disruptions in inter-filler contact can compromise electrical connectivity. Additionally, AgNPs are prone to oxidation, which degrades their

electrical properties over time, and their potential cytotoxicity raises concerns for bioelectronic applications.

**Gold nanoparticles (AuNPs)** Gold nanoparticles (AuNPs) are highly valued as 0D metallic fillers due to their exceptional electrical conductivity, chemical stability, and biocompatibility (Fig. 4e)<sup>77</sup>. Although costlier than silver, AuNPs excel in applications where biocompatibility and long-term reliability are critical, such as biomedical devices, biosensors, and implantable electronics<sup>78</sup>. Unlike many metallic NPs, AuNPs resist oxidation, preserving their electrical properties over extended periods and ensuring durability in demanding environments.

In addition to their stability and conductivity, AuNPs exhibit remarkable optical properties driven by localized surface plasmon resonance. This phenomenon causes free electrons to resonate with light at specific wavelengths, producing intense absorption and scattering effects. These optical characteristics enable their use as highly sensitive optical sensors, where shifts in plasmon resonance wavelength can detect environmental changes, making them invaluable in cancer diagnostics and molecular imaging.

AuNPs also offer extensive versatility in surface functionalization, facilitating the attachment of biomolecules, drugs, or targeting agents. Functionalization with thiol or amine groups enhances their stability and compatibility in biological environments, supporting applications such as targeted drug delivery and biosensors, where precise molecular recognition is essential.

**Copper nanoparticles (CuNPs)** Copper nanoparticles (CuNPs) offer a cost-effective alternative to AgNPs and AuNPs, delivering comparable electrical conductivity at a significantly lower price (Fig. 4f)<sup>79</sup>. Their high thermal conductivity further enhances their utility in energy storage devices, conductive adhesives, and printed electronics<sup>79</sup>. Additionally, CuNPs exhibit a degree of biocompatibility and biodegradability, making them suitable for environmentally sustainable applications, including transient and bioelectronic devices.

A major limitation of CuNPs is their susceptibility to oxidation, which significantly degrades their electrical performance. Exposure to air or moisture increases resistance and can result in a complete loss of conductivity, posing challenges for stable, long-term use. To mitigate this, protective coatings or stabilizing agents, such as polymers, graphene, or silver layers, are applied to prevent oxidation. These stabilization strategies preserve the NPs' conductivity and enable reliable performance in demanding applications.

The combination of electrical and thermal conductivity broadens the application scope of CuNPs, particularly in

systems requiring efficient heat dissipation, such as flexible electronics. Their relative abundance, low toxicity, and biodegradability further position CuNPs as a sustainable choice, aligning with the growing emphasis on environmentally conscious materials in advanced electronic technologies.

**Platinum nanoparticles (PtNPs)** Platinum nanoparticles (PtNPs) are distinguished among 0D metallic nanomaterials for their exceptional catalytic activity, chemical stability, and high conductivity, making them indispensable in applications such as fuel cells, catalysis, sensors, and biosensing<sup>80</sup>. While their high cost, owing to platinum's status as a precious metal, limits widespread commercial use, the unparalleled efficiency and durability of PtNPs often justify their expense in specialized applications.

The defining feature of PtNPs is their superior catalytic activity. Platinum's ability to facilitate redox reactions without degradation makes it invaluable for fuel cells, where it catalyzes the hydrogen oxidation and oxygen reduction reactions. The nanoscale size of PtNPs further enhances their performance by providing a high surface area, enabling efficient energy conversion in fuel cells and other energy systems. Compared to other metals, PtNPs deliver significantly greater catalytic efficiency, making them indispensable in high-performance energy applications.

In addition to their catalytic properties, PtNPs exhibit exceptional chemical stability. Unlike copper, which oxidizes readily, or silver, which tarnishes over time, platinum resists oxidation and corrosion even in harsh chemical or thermal environments. This stability ensures the reliability and longevity of devices like catalytic converters and high-temperature fuel cells. Furthermore, PtNPs are biocompatible and robust, making them suitable for long-term biological applications, including biosensors and drug delivery systems.

Despite these advantages, the high cost and scarcity of platinum pose significant limitations. PtNPs are generally reserved for applications where their unique properties are essential, as their economic and environmental costs hinder broader adoption. Additionally, while PtNPs exhibit high conductivity, their lack of plasmonic properties limits their use in optical applications. These challenges highlight the importance of optimizing PtNPs usage and exploring sustainable alternatives for broader applications.

**Quantum dots (QDs)** QDs are nanoscale semiconductor particles that exhibit unique optical and electronic properties due to quantum confinement effects, which occur when the particle size is smaller than the exciton Bohr radius (Fig. 4g). This confinement restricts electron

and hole motion, creating discrete energy levels instead of the continuous bands seen in bulk materials. Consequently, QDs can absorb and emit light at specific wavelengths determined by their size, composition, and surface structure. This tunable photoluminescence, combined with high brightness and photostability, makes QDs valuable for applications in displays, solar cells, bioimaging, and sensing (Fig. 4h)<sup>81</sup>.

QDs are typically composed of semiconductor materials, with cadmium selenide (CdSe), cadmium sulfide (CdS), and lead sulfide (PbS) being among the most widely used due to their favorable bandgap properties. However, concerns over cadmium and lead toxicity have driven interest in more environmentally friendly alternatives, such as indium phosphide (InP) and carbon-based QDs (Fig. 4i, j)<sup>82</sup>. To enhance optical performance and stability, core-shell structures are often employed; for example, a CdSe core with a zinc sulfide (ZnS) shell improves photostability and quantum yield by reducing surface defects and protecting the core from environmental degradation.

### 1D metallic nanowires (NWs)

Metallic NWs and nanorods, collectively referred to as NWs, are 1D nanomaterials characterized by high aspect ratios. Their directional geometry facilitates the formation of percolation networks with minimal filler content, making them effective as primary fillers in conductive composites (Fig. 4k)<sup>83</sup>. NWs also integrate seamlessly into polymeric matrices, maintaining structural integrity while ensuring electrical connectivity under mechanical strain. This unique property enables NWs to slide and rearrange within the matrix, preserving conduction during stretching or bending, which is essential for soft electronics.

NWs share many material properties with metallic NPs but offer the added advantage of precise control over their dimensions. Template-assisted synthesis uses porous templates like anodic aluminum oxide to define NWs' length and diameter through controlled metal deposition. The polyol process employs solvents like ethylene glycol (EG) and capping agents such as polyvinylpyrrolidone (PVP) to drive anisotropic growth, particularly effective for AgNWs and CuNWs. Seed-mediated growth introduces seed particles into a growth solution, enabling controlled elongation of AuNWs by adjusting seed concentration and reaction conditions. These methods allow customization of NWs' properties for diverse applications, including flexible electronics, transparent conductive films, and catalytic systems.

**Silver nanowires (AgNWs)** AgNWs share many material characteristics with AgNPs<sup>72,84</sup>. Their high conductivity and aspect ratio make AgNWs some of the most

extensively studied one-dimensional metallic nanomaterials for soft and stretchable electronics<sup>85</sup>. AgNWs form efficient percolation networks at low filler concentrations, resulting in flexible and stretchable conductive composites with low percolation thresholds. These properties make them ideal for applications such as transparent electrodes, flexible touchscreens, and stretchable circuits<sup>52,86</sup>.

For example, Qian et al. fabricated ultralight, conductive silver aerogels using AgNWs (Fig. 4l)<sup>87</sup>. AgNWs with diameters of 50–100 nm and lengths of 40–80  $\mu\text{m}$ , synthesized via the polyol process, served as building blocks for the aerogels. The process involved freezing an AgNW suspension, lyophilizing it to form a porous network, and sintering at 250 °C under hydrogen gas to weld the NWs' junctions. The resulting aerogel demonstrated an ultralight density of 4.8 mg/cm<sup>3</sup>, electrical conductivity of 51,000 S/m, and a Young's modulus of 16.8 kPa, highlighting its exceptional softness and conductivity.

**Gold nanowires (AuNWs)** AuNWs offer advantages similar to AgNWs, including excellent conductivity, but with superior chemical stability and biocompatibility, making them suitable for stretchable biosensors, implantable devices, and flexible circuits<sup>88</sup>. However, their high cost limits commercial scalability, confining their use to high-performance devices where stability and biocompatibility justify the expense.

A major challenge with AuNWs is achieving a high aspect ratio comparable to AgNWs or CuNWs due to gold's unstable surface diffusion and lack of protective oxidation. Consequently, Au is often synthesized as nanorods rather than true NWs. A promising solution involves coating high-aspect-ratio NWs with gold, as seen in Au-AgNWs, which combine Ag's conductivity with Au's stability<sup>89,90</sup>. However, creating one-dimensional networks of pure Au remains more complex.

For example, Miyamoto et al. developed ultrathin, lightweight, and stretchable gold nanomeshes directly laminable onto human skin without irritating (Fig. 4m)<sup>91</sup>. This process involved electrospinning PVA nanofibers into a mesh structure, coating it with a 70–100 nm gold layer, and dissolving the PVA scaffold with water to leave a conductive gold network. The nanomesh exhibited exceptional biocompatibility and electrical resistivity of  $5.3 \times 10^{-7}$   $\Omega\cdot\text{m}$ , comparable to bulk gold. Although lacking an elastomeric matrix, the nanomesh maintained conductivity under up to 48% strain and remained stable over 500 cycles of 25% strain stretching.

**Copper nanowires (CuNWs)** CuNWs present a low-cost alternative to AgNWs and AuNWs, offering excellent electrical and thermal conductivity while being

synthesized through relatively inexpensive methods<sup>92</sup>. These properties make CuNWs attractive for applications in stretchable circuits, sensors, and energy devices<sup>93</sup>. However, their susceptibility to oxidation significantly reduces conductivity over time. To address this, protective coatings or polymer encapsulation are commonly employed, enabling CuNWs to remain viable for large-scale, cost-effective soft electronics, particularly in consumer electronics and energy storage.

Won et al. developed an annealing-free, scalable CuNWs-based stretchable electrode using a cost-effective process (Fig. 4n)<sup>94</sup>. CuNWs, averaging 66 nm in diameter and 50  $\mu\text{m}$  in length, were synthesized via a chemical reaction between copper chloride and a capping agent, followed by vacuum filtration to form a conductive film. This film was transferred onto a 40% pre-stretched PDMS substrate, achieving a sheet resistance of 6–12  $\Omega/\text{sq}$ . While pristine copper films failed under 25% strain, the CuNWs/PDMS film withstood strains up to 90%. Additionally, the PDMS substrate was molded into a helical structure to further enhance strain absorption. The helical CuNWs/PDMS electrode exhibited a minimal relative resistance change of 3.9 under 700% strain and maintained functionality after 100 cycles of 100% strain.

## 2D metallic nanosheets (NSs)

2D metallic NSs offer unique advantages for applications requiring flat, conductive networks or films due to their broad, plate-like structures and large surface area, which enhance charge and heat transfer (Fig. 4o)<sup>95</sup>. While NSs excel in forming 2D conductive films, integrating them into 3D percolation networks within elastomeric matrices poses challenges. Aggregation tendencies and their flat geometry can hinder dispersion and disrupt elastomer crosslinking, complicating the balance between conductivity and mechanical integrity.

Several methods are utilized to synthesize metallic NSs while maximizing surface area and ensuring uniform thickness. Liquid-phase exfoliation, a widely used method, involves exfoliating bulk metals into thin sheets using solvents and sonication. Optimizing solvent and surfactant selection minimizes aggregation and enhances dispersion in polymer matrices. Chemical vapor deposition (CVD) enables precise control over NSs' thickness and lateral dimensions by depositing vaporized metal precursors onto substrates, producing high-quality, defect-free films. Wet chemical synthesis offers versatility, reducing metal salts in solution with surfactants or capping agents to guide 2D growth, allowing for NSs with tunable surface chemistries and improved compatibility with elastomers.

**Silver flakes** Silver flakes, as 2D metallic nanomaterials, provide a distinctive approach to achieving conductivity in flexible and stretchable composites<sup>96</sup>. Their large lateral dimensions enable the formation of continuous conductive pathways at low filler concentrations, making them ideal for conductive adhesives, flexible circuits, and printed electronics. Even under mechanical strain, silver flakes maintain electrical contact through sliding mechanisms<sup>97</sup>. However, challenges such as high cost and susceptibility to oxidation limit their broader application.

For example, Lv et al. developed a stretchable Ag flake electrode enhanced by human sweat (Fig. 4p)<sup>98</sup>. Silver flakes dispersed in hydrophilic PUA (HPUA) were used to create conductive ink directly printable onto hydrophilic textiles. Exposure to sweat facilitated a chloride ion-mediated surfactant removal process, improving inter-flake connectivity and reducing resistance from 3.02 to 0.62  $\Omega$ . This sweat-induced sintering also enhanced the electrode's durability, maintaining resistance below 5  $\Omega$  through 500 cycles of 30% stretching and showing stable conductivity under 120% strain. The Ag flake-HPUA electrode demonstrates strong potential for wearable electronics, such as soft batteries and current collectors, due to its softness and performance improvements under real-world conditions.

**Gold nanosheets (AuNSs)** AuNSs have gained attention for their exceptional conductivity and chemical stability, making them ideal for biomedical devices, sensors, and flexible electronics<sup>99</sup>. Their 2D structure facilitates the formation of robust percolation networks with high conductivity and durability under mechanical deformation. Despite their advantages, the high cost of gold limits widespread application.

Heo et al. developed elastomeric electrodes incorporating interconnected AuNSs optimized for mechanical resilience and cyclic stretching<sup>100</sup>. The AuNSs, synthesized via a solution-based process, were transferred onto a PDMS matrix using a hot-pressing method, which removed surface ligands and improved interlayer contact (Fig. 4q). This process produced electrodes with a sheet resistance as low as 0.15  $\Omega/\text{sq}$ , increasing only slightly to 1.8  $\Omega/\text{sq}$  under 50% strain. The electrodes demonstrated exceptional durability, maintaining performance over 100,000 stretching cycles. Using these AuNS-based elastomeric electrodes, Heo et al. fabricated resilient electronic devices, including transistors, inverters, and NOR/NAND logic gates, achieving stable field-effect mobilities of 19.8  $\text{cm}^2/\text{V}\cdot\text{s}$  even under deformation. These electrodes also proved effective in soft robotic systems, where integrated electronic components retained functionality during various grip motions, highlighting their potential for wearable devices and robotics.

Lim et al. introduced whiskered AuNSs (W-AuNSs) to enhance percolation networks in stretchable electronics<sup>101</sup>. Featuring whisker-like extensions, W-AuNSs exhibited a significantly lower percolation threshold (1.56 vol%) compared to conventional AuNSs. Nanocomposites incorporating W-AuNSs achieved a conductivity of 91 S/cm at a 2.13% filler volume fraction and maintained stretchability up to 200% elongation at 7.9 vol%. These W-AuNSs also demonstrated stable performance under cyclic testing, with minimal resistance variation. When applied as bioelectrodes for electrophysiological monitoring and stimulation, W-AuNSs provided consistent, high-performance results under mechanical strain, showcasing their suitability for wearable biomedical applications.

### Functionalization of metallic nanocomposites

To enhance the performance of metallic nanocomposites, several functionalization techniques have been developed. These techniques aim to improve the electrical conductivity, mechanical properties, and stability of the composites by modifying the structure, composition, or arrangement of the metallic nanofillers.

### Secondary fillers

The incorporation of secondary fillers, such as carbon-based nanomaterials, metallic NPs, and ionic liquids, significantly enhances the mechanical strength, stretchability, and conductivity of metallic nanocomposites (Fig. 5a). These fillers infiltrate the gaps between primary fillers or within the polymeric matrix, supporting the percolation network and introducing additional functionalities, such as improved electrochemical performance, antibacterial properties, and reactive oxygen species scavenging. This synergy enables tailored composites optimized for specific applications.

For instance, Sunwoo et al. developed a stretchable nanocomposite integrating Ag–Au core-shell NWs with platinum black (Pt black) as a secondary filler to enhance electrochemical properties for epicardial recording and stimulation<sup>89</sup>. The addition of 13 wt% Pt black increased the charge storage capacity (CSC) eightfold to 25 mC/cm<sup>2</sup> and reduced impedance from 2348 to 112  $\Omega$  at 40 Hz (Fig. 5b). This composite achieved a high signal-to-noise ratio (SNR) of 20.05 dB and maintained durable performance under strain. When implanted in an epicardial mesh, it enabled synchronized biventricular pacing and stable heart rate modulation in rodent models, demonstrating its potential for advanced cardiac support devices.

In situ-formed metallic NPs offer a homogeneous distribution within the matrix, enhancing the performance of nanocomposites. Matsuhisa et al. reported a printable elastic conductor with in situ-generated AgNPs formed

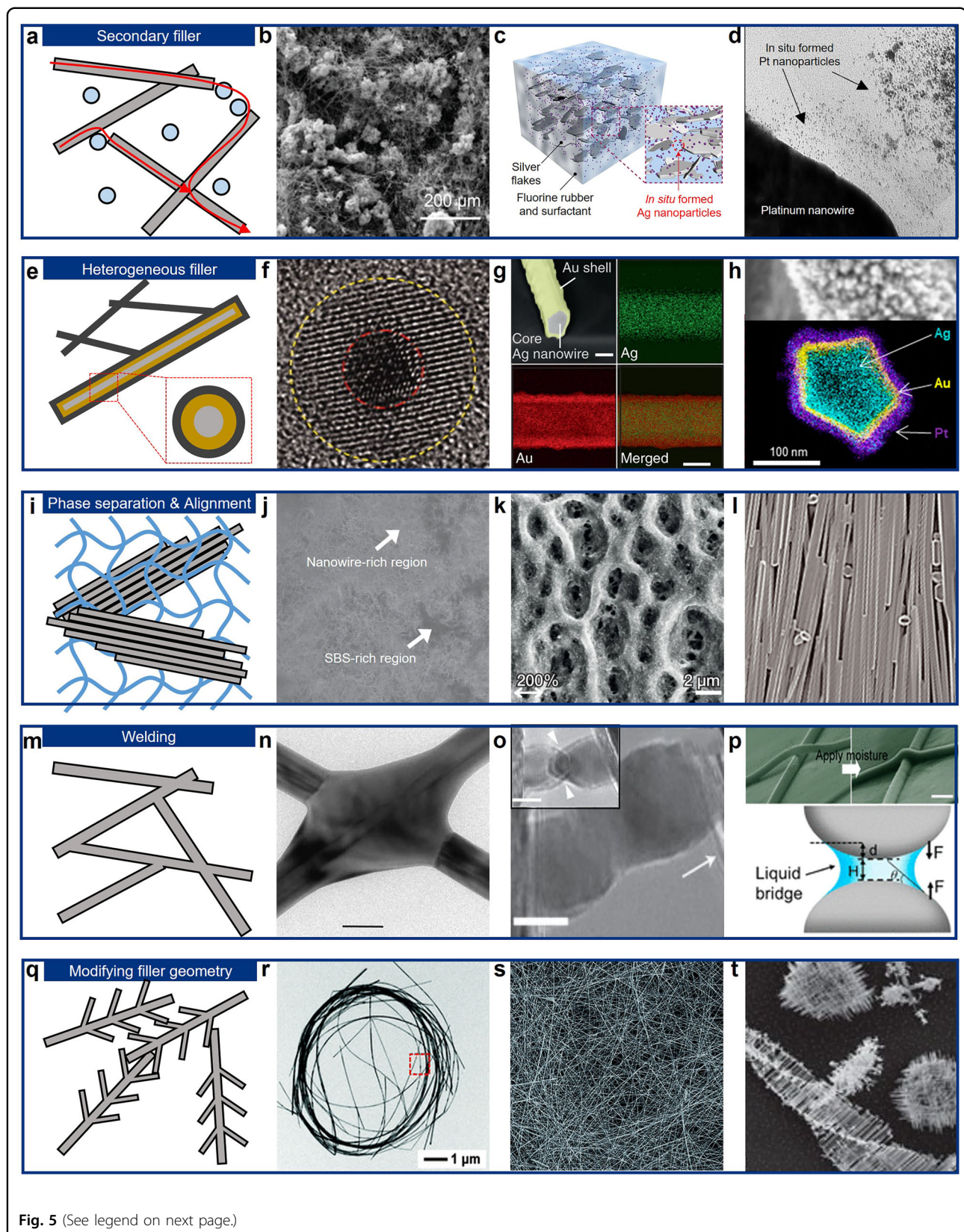


Fig. 5 (See legend on next page.)

(see figure on previous page)

**Fig. 5 Functionalization of metallic nanocomposites.** **a-d** Applying secondary filler. Reproduced with permission<sup>89</sup>. Copyright 2019, John Wiley & Sons. Reproduced with permission<sup>102</sup>. Copyright 2017, Springer Nature. Reproduced with permission<sup>103</sup>. Copyright 2023, American Chemical Society. **e-h** Applying heterogeneous fillers. Reproduced with permission<sup>104</sup>. Copyright 2010, AAAS. Reproduced with permission<sup>105</sup>. Copyright 2018, Springer Nature. Reproduced with permission<sup>103</sup>. Copyright 2023, American Chemical Society. **i-l** Phase separation and alignment of the fillers. Copyright with permission<sup>105</sup>. Copyright 2018, Springer Nature. Reproduced with permission<sup>106</sup>. Copyright 2013, Springer Nature. Reproduced with permission<sup>107</sup>. Copyright 2021, AAAS. **m-p** Nanofiller welding techniques. Reproduced with permission<sup>108</sup>. Copyright 2012, Springer Nature. Reproduced with permission<sup>109</sup>. Copyright 2010, Springer Nature. Reproduced with permission<sup>110</sup>. Copyright 2017, American Chemical Society. **q-t** Modifying geometry of the fillers. Reproduced with permission<sup>111</sup>. Copyright 2017, RSC Publishing. Reproduced with permission<sup>112</sup>. Copyright 2018, RSC Publishing. Reproduced with permission<sup>113</sup>. Copyright 2008, Springer Nature.

during thermal processing<sup>102</sup>. The AgNPs bridged the gaps between Ag flakes, bolstering conductivity to 6,168 S/cm at 0% strain and 935 S/cm at 400% strain (Fig. 5c). This composite was utilized in fully printed stretchable sensor networks for pressure and temperature monitoring on dynamic surfaces, highlighting its potential for flexible electronics.

Similarly, a study incorporating in situ-formed PtNPs into an SEBS matrix demonstrated improved conductivity and structural integrity<sup>103</sup>. The homogeneously dispersed PtNPs enhanced the percolation network, achieving a conductivity of 11,000 S/cm, stretchability of 480%, and low impedance (166.5  $\Omega$  at 1 kHz) (Fig. 5d). When applied in a rat model, the nanocomposite electrode provided stable biosignal recording, arrhythmia management, and efficient pacing with reduced capture thresholds, underscoring its suitability for advanced bioelectronic devices.

#### Heterogeneous filler

Incorporating multiple fillers into composites often constrains the performance of primary fillers. To address this, heterogeneous fillers, which integrate multiple materials into a single nanostructure, have emerged as an effective alternative. These fillers combine the strengths of different materials, enhancing overall composite performance. Techniques such as core-sheath structures and doped nanomaterials are commonly employed, with each component contributing distinct properties.

For example, Zhang et al. used a nonepitaxial growth method to synthesize hybrid core-shell NPs, addressing lattice mismatch issues between core and shell materials<sup>104</sup>. This solution-phase process sequentially deposited metals to form core-shell structures, enhancing stability and electronic properties due to the integration of materials with different crystalline structures (Fig. 5f). These advancements have broadened applications in electronics, catalysis, and energy storage.

In another study, Choi et al. developed AgNW-Au core-sheath NWs to achieve high conductivity, stretchability, and biocompatibility<sup>105</sup>. Au was galvanically deposited on AgNWs to prevent oxidation, forming a composite integrated into an SBS elastomer (Fig. 5g). The material

achieved conductivity of 41,850 S/cm, enhanced to 72,600 S/cm with heat rolling, and stretchability up to 266%, increasing to 840% under strain. The Au coating reduced Ag ion leaching, improving biocompatibility. This composite demonstrated stable performance under strain and oxidative conditions, making it suitable for wearable and implantable bioelectronics.

Sunwoo et al. further advanced this approach with an Ag–Au–Pt core-shell-shell NWs composite incorporating in situ synthesized PtNPs<sup>103</sup>. This design leveraged silver's high conductivity, gold's biocompatibility, and platinum's low impedance (Fig. 5h). The embossed Pt shell increased surface area, enhancing charge transfer and lowering impedance, while PtNPs within the matrix improved percolation network efficiency. The composite achieved a conductivity of 11,000 S/cm and 500% stretchability, with dual Au–Pt coatings reducing silver ion leaching. Tested in bioelectronic applications, the material demonstrated excellent signal clarity and lower capture thresholds during in vivo cardiac monitoring, highlighting its potential for advanced biosignal monitoring and cardiac rhythm management.

#### Phase separation and filler alignment

Controlling phase separation and alignment of metallic nanofillers within a matrix significantly enhances composite performance (Fig. 5i). Phase separation allows selective localization of nanofillers, creating efficient percolation networks, while alignment of fillers like AgNWs or AuNWs along the direction of mechanical strain improves conductivity and stretchability. Techniques such as mechanical stretching and magnetic field alignment are commonly used to achieve these effects.

For instance, Choi et al. leveraged phase separation during solvent drying to enhance the properties of an Ag–Au nanocomposite<sup>105</sup>. By introducing hexylamine, phase separation formed microstructured regions enriched with Ag–Au NWs and SBS elastomer (Fig. 5j). This microstructure reduced the composite's Young's modulus and improved softness, enabling stretchability up to ~266% while maintaining high conductivity (41,850 S/cm). Without hexylamine, the composite exhibited lower stretchability and a homogenous structure, demonstrating

the critical role of phase separation in balancing mechanical and electrical properties.

Kim et al. employed vacuum-assisted flocculation (VAF) to integrate citrate-stabilized AuNPs into a PU matrix, enhancing phase separation and self-organization<sup>106</sup>. This approach produced composites with stretchability up to 486%, as NPs formed conductive pathways under strain (Fig. 5k). VAF composites exhibited larger PU domains, optimizing stretchability, while layer-by-layer composites offered higher initial conductivity (11,000 S/cm) due to uniform NPs dispersion. SAXS and TEM analysis revealed that NPs alignment under strain improved conductivity by lowering the percolation threshold.

Jung et al. developed a highly conductive and stretchable AgNWs nanomembrane using a float assembly method<sup>107</sup>. This process aligned AgNWs at the water–oil interface through Marangoni flow, creating a compact monolayer embedded in an ultrathin elastomer membrane (Fig. 5l). The aligned network achieved exceptional conductivity (165,700 S/cm) and stretchability, withstanding strains over 1,000%. This structural design efficiently dissipated strain through elastomeric regions, making the nanomembrane suitable for advanced soft electronic applications.

#### **Welding of metallic nanofillers**

Welding techniques, such as thermal annealing and chemical welding, significantly enhance the connectivity between metallic nanofillers by reducing contact resistance and boosting composite conductivity (Fig. 5m)<sup>87</sup>. These methods are particularly beneficial for NW networks, where individual wires can lose contact under mechanical strain.

Garnett et al. developed a self-limited plasmonic welding technique for AgNWs junctions using light-induced plasmonic heating to generate localized heat at contact points<sup>108</sup>. This process, driven by a tungsten halogen lamp, achieved epitaxial recrystallization at junctions without damaging surrounding areas (Fig. 5n). Junction resistance was reduced by over three orders of magnitude within 60 seconds, yielding electrical performance comparable to continuous NWs. The self-limiting nature of the process prevented over-welding, ensuring structural integrity.

Lu et al. demonstrated cold welding of ultrathin AuNWs without localized heating<sup>109</sup>. By applying minimal mechanical pressure, single-crystalline AuNWs (3–10 nm in diameter) were seamlessly bonded via surface atom diffusion and oriented attachment (Fig. 5o). Welded junctions maintained crystal orientation and exhibited mechanical strength (~580 MPa) and resistivity (~298.1 Ω·nm) comparable to pristine NWs. The technique was also applicable to Ag–Ag and Au–Ag junctions,

highlighting its versatility for nanoscale interconnects in electronic systems.

Liu et al. introduced a capillary-force-induced cold welding method for AgNW films<sup>110</sup>. Moisture applied to the films created liquid bridges at junctions, drawing wires together as the liquid dried (Fig. 5p). This simple process reduced sheet resistance from  $2.25 \times 10^5 \Omega/\text{sq}$  to 179 Ω/sq while maintaining optical transparency (<1% change). Treated films showed enhanced flexibility, enduring up to 100% strain with minimal resistance increase (~1.5 times), demonstrating the technique's effectiveness for flexible electronics.

#### **Filler geometry modification**

Modifying the geometry of metallic nanofillers offers a promising route to enhance their performance in soft electronics by improving filler contact and optimizing the percolation network (Fig. 5q). Branched or curved NWs, for instance, provide additional contact points between fillers, enhancing conductivity and mechanical compliance. These geometrical modifications enable tailored nanocomposites suited for applications like stretchable sensors and flexible circuits.

Lim et al. demonstrated the formation of curved AgNWs through a spray-coating process that induced elasto-capillary interactions<sup>111</sup>. High-speed spraying generated micrometer-sized liquid droplets, within which AgNWs were elastically deformed into curved shapes as the droplets dried, forming AgNW rings instead of linear structures (Fig. 5r). The curved networks, embedded in a PDMS matrix, exhibited exceptional durability, maintaining stable resistance over 5000 cycles of 30% strain. In contrast, traditional linear AgNW networks showed breakage and increased resistance under similar conditions, highlighting the superior electromechanical stability of the curved structures.

Another approach involved synthesizing ultra-long AgNWs exceeding 100 μm via a solvothermal method, yielding a high aspect ratio critical for efficient percolation network formation<sup>112</sup>. The extended lengths reduced inter-NWs junctions, minimizing resistive losses and enhancing connectivity (Fig. 5s). These AgNW films, applied as transparent conductive layers on PET substrates, achieved a low sheet resistance of ~19 Ω/sq and high optical transmittance (88%). The dense, stable networks outperformed conventional materials like ITO in both flexibility and durability.

Zhu et al. explored chiral branched PbSe NWs grown through the Eshelby Twist, which combined vapor-liquid-solid and screw dislocation-mediated mechanisms<sup>113</sup>. The resulting structures exhibited branching and chiral motifs, with perpendicular branches twisting around central NWs due to axial dislocations (Fig. 5t). While not directly tested for percolation networks, these branched configurations

suggest improved connectivity and enhanced electron transport potential, ideal for applications requiring robust, interconnected NW networks.

### Liquid metals (LMs)

LMs represent a unique class of materials for intrinsically soft electronics, combining metallic conductivity with fluid-like mechanical properties<sup>114</sup>. These materials offer exceptional electrical conductivity, comparable to traditional solid metals, which is essential for efficient circuit operation. Their fluid nature provides intrinsic deformability, enabling them to conform to various shapes and withstand mechanical forces such as stretching, twisting, or compressing. These properties make LMs particularly suitable for applications in soft robotics, wearable electronics, and flexible sensors, where conventional rigid materials are inadequate.

Despite these advantages, LMs face several challenges in practical applications. Certain LMs, such as mercury, are toxic<sup>115</sup>, while others, like cesium, are radioactive<sup>116</sup>, or highly flammable, such as sodium-potassium alloys<sup>117</sup>. Additionally, surface oxidation can hinder the electrical properties of some LMs. Furthermore, precise patterning and reliable encapsulation methods are critical to prevent leakage and ensure safe operation across diverse environments. The following sections explore the most commonly used LMs, their inherent limitations, and the innovative techniques developed to integrate them into soft electronic devices effectively.

### Commonly used LMs

Several LMs are commonly used in soft electronic applications. These metals are typically chosen based on their electrical properties, melting points, and ease of processing. The most prominent examples include gallium and its alloys, such as eutectic gallium-indium (EGaIn) and gallium-indium-tin (Galinstan).

### Gallium

Gallium (Ga) is a widely used liquid metal in soft electronics, primarily due to its low melting point of 29.76 °C, allowing it to remain liquid at or near room temperature (Fig. 6a)<sup>118</sup>. Gallium's relative abundance, low toxicity, and high electrical conductivity make it a safer and efficient alternative to hazardous materials like mercury. These properties render gallium ideal for applications such as stretchable circuits, flexible antennas, and wearable sensors.

A key challenge with pure gallium is its tendency to form a thin oxide layer when exposed to air. This nanometer-scale oxide layer increases electrical resistance, potentially limiting gallium's effectiveness in applications requiring ultra-low resistivity. However, the oxide layer also enhances structural integrity, enabling the

formation of stable liquid metal structures. Strategies such as encapsulation and surface treatments have been developed to control oxide formation and optimize gallium's performance in electronic devices.

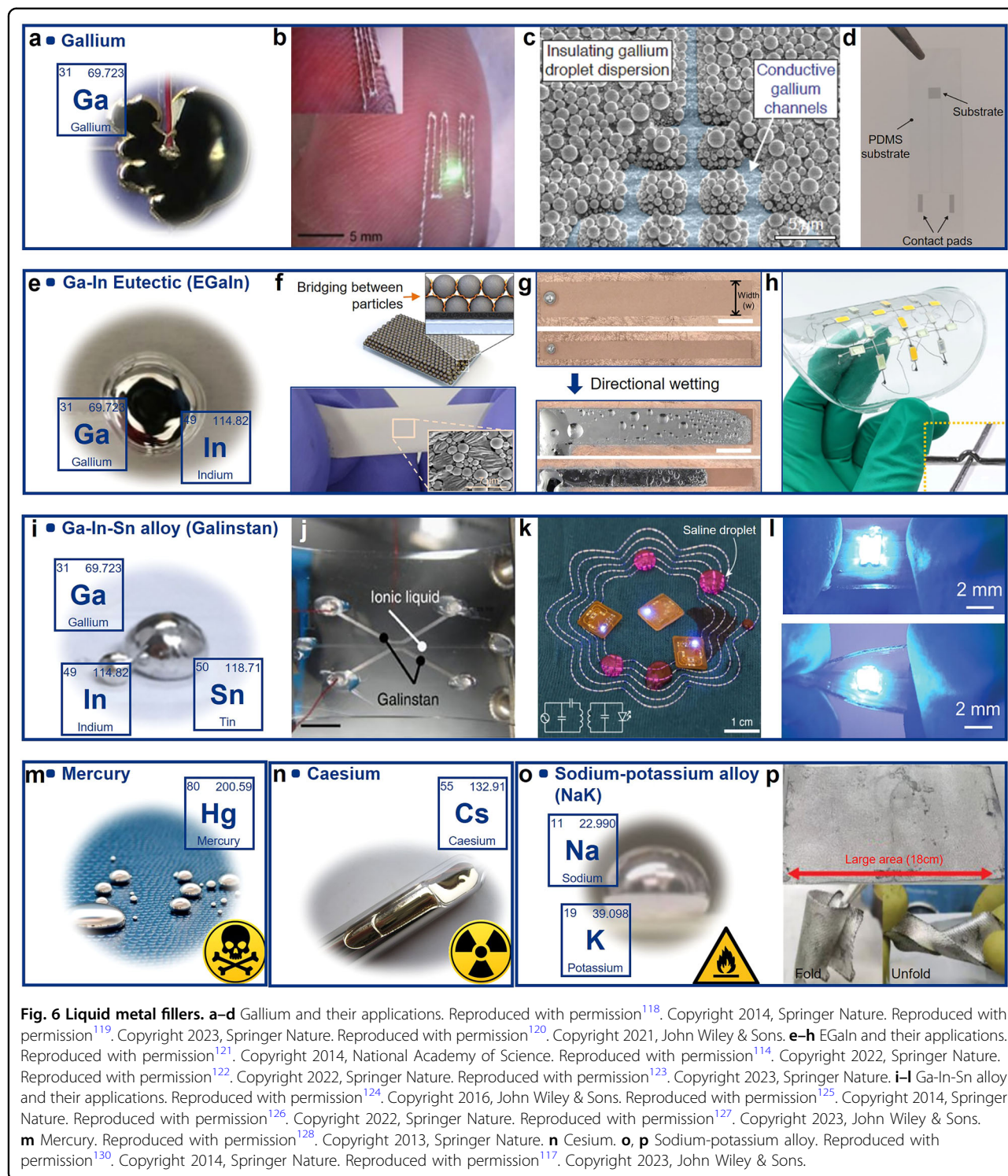
For instance, Wang et al. introduced supercooled liquid gallium (SLGa) to create intrinsically stretchable electronics<sup>119</sup>. Encapsulating gallium with low-surface-energy materials like PDMS prevented crystallization, maintaining its liquid state down to -22 °C. This enabled the fabrication of stretchable circuits and ECG patches capable of stable operation in cold conditions and underwater environments. Using spray-printing, uniform SLGa microelectrode arrays with low impedance and high conformability to human skin were created. These circuits demonstrated stable resistance under strains up to 50%, highlighting their suitability for flexible and wearable electronics (Fig. 6b).

In another study, Dejace et al. developed highly stretchable and transparent electronics by patterning microscale gallium conductors within a PDMS substrate<sup>120</sup>. Through soft lithography and thermal evaporation, high-aspect-ratio gallium channels as narrow as 2 μm were fabricated, achieving up to 89.6% optical transparency at 550 nm and a sheet resistance as low as 4.3 Ω/sq. This precise patterning enabled scalable designs for large-area applications (Fig. 6c). The patterned conductors exhibited stable electrical performance under strain, with resistance increasing by less than 0.2-fold after 50% strain cycles. By adjusting the grid pitch, the transparency and conductivity of the gallium structures were fine-tuned, making them suitable for wearable and transparent electronics (Fig. 6d).

### EGaIn (eutectic gallium-indium)

EGaIn, a eutectic alloy of gallium (75%) and indium (25%), has a melting point of approximately 15.7 °C, making it liquid at room temperature (Fig. 6e)<sup>121</sup>. Compared to pure gallium, EGaIn offers enhanced properties such as lower viscosity and improved stability. Its high electrical conductivity and ease of processing make it ideal for applications in stretchable electronics, soft robotics, and flexible circuits. While EGaIn forms a thin oxide layer upon air exposure, which acts as a self-passivating barrier to further oxidation, this layer can also pose challenges for consistent conductivity, particularly in high-frequency applications. Nevertheless, its low toxicity compared to other LMs makes EGaIn highly suitable for wearable and biomedical devices.

For instance, Lee et al. utilized meniscus-guided printing to create high-resolution patterns of polyelectrolyte-attached liquid metal particles prepared from EGaIn (Fig. 6f)<sup>114</sup>. This technique enabled stable, post-processing-free patterning with resolutions as fine as 50 μm. The printed films exhibited an initial conductivity



of  $1.5 \times 10^6$  S/m and endured up to 500% strain while maintaining minimal resistance changes under 10,000 cycles of testing. This versatile approach allowed direct printing on substrates like PDMS and hydrogels, facilitating applications in wearable e-skin and customizable ECG sensors.

In another study, Kim et al. introduced an imbibition-induced selective wetting method to pattern EGaIn on microstructured copper surfaces (Fig. 6g)<sup>122</sup>. Using HCl vapor to remove the oxide layer, the researchers achieved uniform, oxide-free coating and precise patterns without complex processing. The resulting EGaIn films

demonstrated stable conductivity, maintaining low resistance under 70% strain with a gauge factor of 2.6. Durability was further confirmed through 4,000 cycles of 30% strain.

Additionally, researchers developed 3D flexible electronics using the regulated plasticity of a Ga–10In alloy (gallium with 10% indium by weight) (Fig. 6h)<sup>123</sup>. By exploiting its solid–liquid phase transition, the alloy was shaped into complex 3D conductive structures in its solid form and encapsulated in the elastomer. Above 22.7 °C, the alloy transitioned to a liquid state, ensuring flexibility and temperature stability. These 3D circuits demonstrated robust performance, with strain sensors achieving a gauge factor exceeding 2000 and maintaining electrical connections after 20,000 bending cycles, showcasing their potential for advanced stretchable devices.

#### **Galinstan (gallium-indium-tin alloy)**

Galinstan, a eutectic alloy of gallium, indium, and tin, remains liquid at sub-zero temperatures due to its exceptionally low melting point of approximately 11 °C (Fig. 6i)<sup>124</sup>. Its non-toxic, environmentally friendly properties make it suitable for applications in medical devices, consumer products, and thermal management systems. Galinstan shares similarities with gallium and EGaIn, forming a surface oxide layer upon air exposure. However, its low viscosity and high fluidity make it ideal for deformable conductive materials, such as stretchable interconnects, flexible displays, and fluidic sensors.

For instance, Ota et al. developed deformable liquid-state heterojunction sensors using Galinstan within PDMS microfluidic channels (Fig. 6j)<sup>125</sup>. By pairing Galinstan with ionic liquids and controlling channel dimensions, they created stable liquid–liquid junctions. The sensors exhibited high flexibility, with stable electrical properties under 90% strain, and achieved a temperature sensitivity of 3.9% per °C, outperforming conventional solid-state sensors. They also showed high responsiveness to humidity (1.7% per 1% increase) and oxygen concentration (1.0% per 1% increase).

In another example, Lin et al. fabricated flexible, conductive textiles by injecting Galinstan into perfluoroalkoxy alkane tubing, forming liquid metal fibers with a conductivity of  $3.46 \times 10^6$  S/m (Fig. 6k)<sup>126</sup>. These fibers were embroidered onto fabrics to create durable electronic textiles capable of withstanding 10,000 bending cycles and multiple washes. The textiles enabled wireless communication and power transfer, achieving a quality factor of 44.4 at 13.56 MHz for textile-based inductors, outperforming conventional threads.

Guo et al. utilized Galinstan for flexible strain sensors by embedding the liquid metal within PDMS microchannels fabricated using a PVA microridge mold (Fig. 6l)<sup>127</sup>. Pre-stretching the PDMS increased the channel's contact area,

enhancing performance. The sensors demonstrated linear sensitivity with a gauge factor of ~1, low hysteresis, and excellent durability ( $\Delta R/R_0 < 0.8$ ) over 10,000 cycles under 75% strain.

#### **Other LMs**

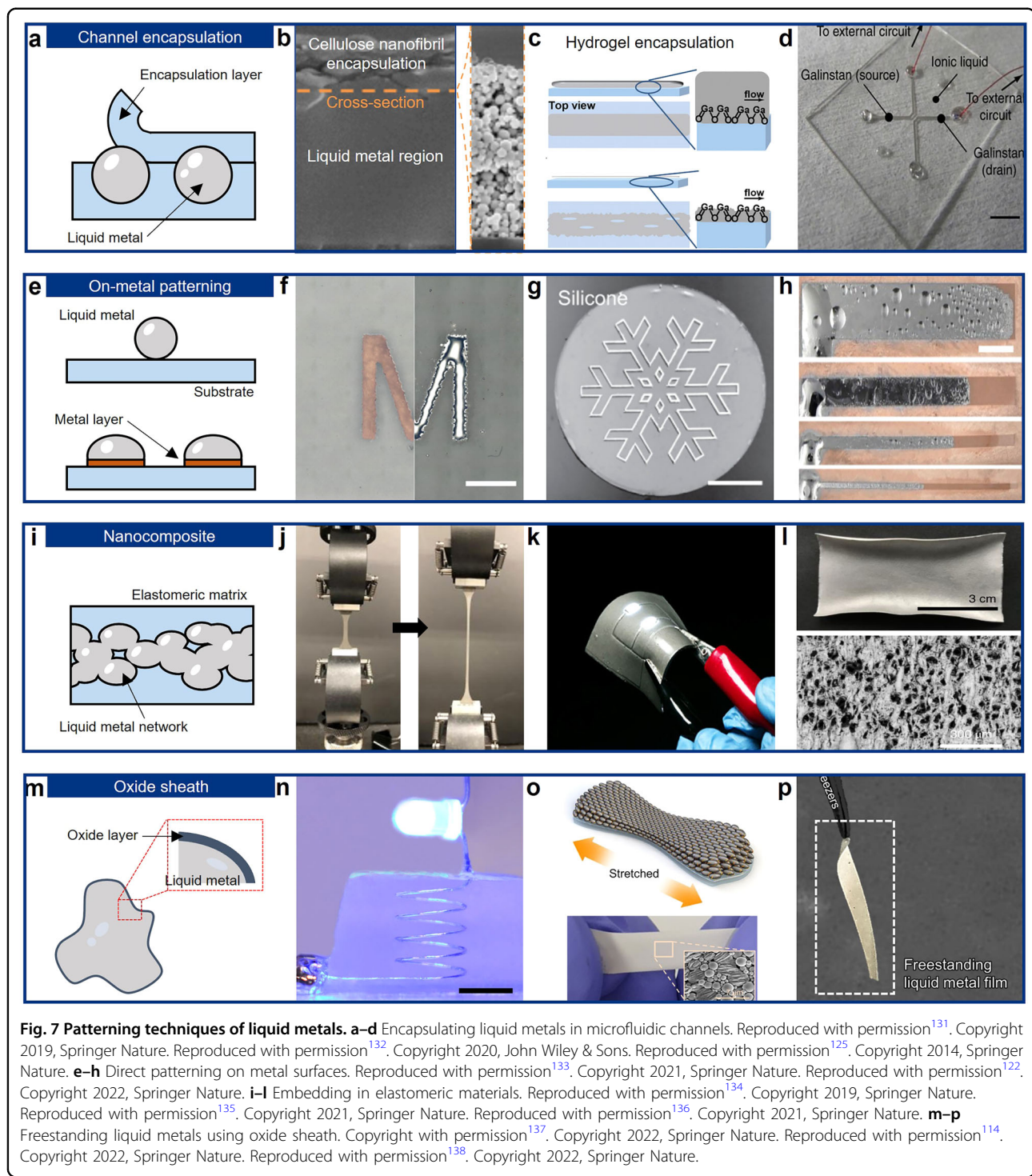
Although gallium-based metals are the most commonly used, other LMs have been investigated for specific applications. Mercury (Hg), for instance, has historically been employed in electronic devices because of its high conductivity and low melting point (Fig. 6m)<sup>128</sup>. However, its toxicity and environmental hazards have significantly curtailed its use in modern applications<sup>115</sup>. Cesium (Cs), liquid at 28.5 °C, offers potential for low-temperature applications but is highly reactive, making handling difficult (Fig. 6n)<sup>116</sup>. Similarly, the sodium-potassium alloy (NaK) is liquid at room temperature and is used in controlled environments, such as in specialized chemical or nuclear systems, due to its extreme reactivity (Fig. 6o, p)<sup>117,129,130</sup>. While these metals exhibit unique properties, their use in soft electronics remains limited because of safety concerns and the practicality of safer alternatives like gallium-based alloys.

#### **Challenges of LMs in soft electronics**

LMs, owing to their intrinsic fluidity and high surface tension, pose practical challenges including aggregation, leakage, and unstable conductivity under mechanical deformation. To address these issues, several strategies have been developed. Encapsulation within microfluidic elastomeric channels, typically using PDMS, effectively confines liquid metals, preventing undesired leakage and enhancing structural stability under strain. Another robust approach involves forming a native oxide skin on LMs, which stabilizes their shape and suppresses aggregation by providing a mechanically supportive and self-limiting barrier. Recent advances have employed polymer grafting methods, such as poly(methyl methacrylate) surface modification, to enhance dispersion and prevent coalescence of LM droplets within polymer matrices. Additionally, composite approaches embedding LM micro- or NPs within elastomeric substrates further improve mechanical stability and conductivity retention upon stretching. These encapsulation and composite formation techniques collectively enable precise patterning, stable electrical performance, and reliable mechanical deformability, facilitating broader practical adoption of liquid-metal-based intrinsically soft electronic devices.

#### **Patterning techniques of liquid metals**

One of the most significant challenges in working with liquid metals is the development of reliable patterning techniques that allow for precise control over their shape and placement within electronic devices. Liquid metals, by



nature, are prone to spreading and leaking, making it essential to develop methods for their encapsulation and confinement. In this section, we discuss various patterning techniques, including encapsulation in microfluidic channels, surface patterning on metal layers, liquid metal nanocomposites, and self-oxidation methods.

#### Encapsulation in channels

Encapsulating liquid metals within microfluidic channels is a widely used approach for controlling their flow and shape in soft electronics (Fig. 7a). This method involves fabricating predefined channels within an elastomeric matrix, such as PDMS, and injecting liquid metal

into these channels. The elastomeric matrix confines the liquid metal, preventing leakage and maintaining its position along designated pathways. This encapsulation approach is particularly advantageous in stretchable circuits, where liquid metals serve as conductive traces, connecting electronic components while tolerating significant mechanical deformation. The liquid metal can flow and adapt to the stretching or bending of the elastomeric matrix, preserving conductivity even under strain. Additionally, encapsulation minimizes surface oxidation, enhancing the liquid metal's long-term stability and performance.

For instance, Li et al. developed a method for encapsulating liquid metal droplets using biological nanofibrils to create stable conductive channels while preventing leakage (Fig. 7b)<sup>131</sup>. In this process, EGaIn droplets were dispersed in a nanofibril suspension, forming a bilayer structure through evaporation-induced sintering. The resulting structure featured a conductive EGaIn-rich layer beneath an insulating nanofibril-rich layer, enabling conductivity up to  $8.9 \times 10^5$  S/m and strain tolerance of 200% with minimal resistance increase. Additionally, the bilayer structure exhibited an electromagnetic shielding efficiency exceeding 12 dB for a 20-μm-thick layer in the X-band range.

In another approach, researchers micropatterned EGaIn onto a chemically cross-linked hydrogel, achieving autonomous surface reconciliation and high deformability (Fig. 7c)<sup>132</sup>. By leveraging the interaction between hydroxyl groups on the hydrogel and the native  $\text{Ga}_2\text{O}_3$  layer on EGaIn, the liquid metal adhered strongly to the hydrogel surface. Using a 3D-printed mold, patterns with resolutions as fine as 100 μm were created. These patterned hydrogels exhibited exceptional stretchability, tolerating strains of up to 1500% while maintaining a low resistance (initial resistance  $\sim 2 \Omega$ , increasing to  $\sim 4.6 \Omega$  at maximum strain). After 1400 cycles of 700% strain, resistance variation remained stable, demonstrating durability suitable for wearable applications.

Ota et al. introduced a technique for encapsulating liquid metal within microchannels to form liquid–liquid heterojunctions (Fig. 7d)<sup>125</sup>. Using a PDMS microfluidic template with channels approximately 30 μm wide and 31 μm high, galinstan was confined alongside various ionic liquids. Controlled injection prevented intermixing, creating stable junctions. The encapsulated galinstan maintained high conductivity ( $3.4 \times 10^6$  S/m) and endured 90% strain without compromising performance. These configurations enabled the development of flexible sensors capable of measuring temperature, humidity, and oxygen levels with excellent durability under mechanical deformation.

### Patterning on metal electronics

Another technique for patterning liquid metals involves directly depositing or printing the metal onto pre-patterned surfaces, such as metal layers or flexible substrates. For example, liquid metals can be selectively deposited onto chemically treated copper surfaces, where they adhere spontaneously, forming conductive pathways. This method is particularly effective for creating flexible circuits, antennas, and sensors. Compared to encapsulation methods, surface patterning provides higher precision in defining liquid metal geometries. However, controlling the wetting behavior of the liquid metal on the substrate is crucial. Surface treatments, including chemical etching or plasma activation, are often employed to enhance adhesion and prevent the uncontrolled spreading of the liquid metal.

In one approach, Zhu et al. developed a solution-based technique for patterning liquid metal onto an elastomeric substrate by employing a series of chemical modifications to achieve precise and durable features (Fig. 7f, g)<sup>133</sup>. The process began with the application of a sacrificial screen-printed mask to define the desired patterns on a SEBS substrate. A polydopamine layer was then deposited to act as a base for subsequent copper plating. Immersion of the substrate in a silver nitrate solution catalyzed the electroless deposition of copper, forming a metallic film. Galinstan liquid metal was selectively deposited onto the copper, taking advantage of its high wettability contrast with the SEBS substrate. The resulting patterns exhibited resolutions as fine as 100 μm and a conductivity of  $4.15 \times 10^4$  S/cm. These features demonstrated exceptional stretchability, retaining conductivity under strains of up to 1000% and maintaining consistent performance through repeated mechanical cycles, underscoring their potential for flexible electronic applications.

In another example, researchers achieved selective patterning of liquid metal, specifically EGaIn, onto chemically modified metallic microstructures through an imbibition-induced wetting process (Fig. 7h)<sup>122</sup>. The method involved preparing a copper-coated microstructured substrate and exposing it to HCl vapor to remove the oxide layer from the EGaIn. This treatment enabled spontaneous wetting of the liquid metal on the metallic surface. By employing a microstructured PDMS substrate coated with copper, patterned posts and pyramids were created to control EGaIn's spreading behavior. Within 30 seconds, the contact angle reduced to nearly 0°, resulting in uniform wetting across the patterned regions. This approach achieved precise micro-scale resolution without external force and demonstrated excellent durability. The patterned EGaIn structures retained electrical conductivity under strain, with stable resistance changes even after multiple stretching cycles.

### Liquid metal nanocomposites in elastomeric matrix

Embedding liquid metals within an elastomeric matrix to form liquid metal nanocomposites is a promising strategy for developing stretchable electronics (Fig. 7i). In this approach, liquid metal droplets are dispersed throughout the elastomer, combining the high conductivity of liquid metals with the elasticity of the matrix. When strained, the droplets rupture, creating new conductive pathways that preserve electrical connectivity even under extreme deformation. These nanocomposites have been widely applied in soft sensors, stretchable interconnects, and flexible energy devices, offering materials capable of stretching, compressing, and bending without significant loss of electrical performance.

One example involves embedding EGaIn nanodroplets in an elastomeric matrix using surface-initiated atom transfer radical polymerization for effective dispersion (Fig. 7j)<sup>134</sup>. Poly(methyl methacrylate) was grafted onto the EGaIn nanodroplets through radical polymerization, achieving a stable, homogeneous distribution within the polymer matrix and reducing droplet size to  $\sim 200$  nm. This uniform dispersion prevented coalescence and ensured consistent conductivity. The composite exhibited an electrical conductivity of  $8.9 \times 10^5$  S/m, maintained its performance under up to 300% elongation, and demonstrated suitability for flexible electronics, such as soft robotics and stretchable sensors.

In another study, researchers developed a liquid metal–elastomer composite using a scalable embossing technique with a styrene–isoprene–styrene elastomer matrix and micron-sized EGaIn droplets (Fig. 7k)<sup>135</sup>. The droplets were dispersed in the SIS matrix and selectively connected through a compressive embossing load, forming conductive pathways. The process allowed precise control over trace resistance, yielding an initial conductivity of 150 S/cm that increased to 45,400 S/m under 1200% strain. The composite demonstrated exceptional mechanical resilience, with strain-invariant resistance under stretching and stability over multiple cycles, making it ideal for reconfigurable, recyclable electronics in soft robotics and wearable devices.

In a further example, EGaIn was incorporated into an electrospun SBS fiber mat to create a highly permeable, stretchable conductor (Fig. 7l)<sup>136</sup>. Electrospinning was followed by coating the SBS mat with EGaIn, which was then pre-stretched to 1,800% strain to form a porous, mesh-like structure. This design achieved an initial conductivity of 10,000 S/m, which increased to 1,800,000 S/m with higher EGaIn loading. The composite maintained remarkable electrical stability, with resistance increasing by only 4.1% under strains of up to 1800%, highlighting its potential for wearable and soft electronic applications.

### Self-oxidation and freestanding

A recent approach to utilizing liquid metals in stretchable electronics leverages the natural oxide layer or thin polymeric skins that form on their surface to create freestanding structures (Fig. 7m). This self-oxidation process produces a solid skin around the liquid metal, enabling stable, self-supporting conductive patterns. The oxide or polymeric skin prevents uncontrolled flow, making it possible to shape the liquid metal into intricate structures. While the oxide layer increases resistance, limiting its use in ultra-low-resistance applications, this method excels in scenarios prioritizing mechanical flexibility and deformability over conductivity.

For example, Wu et al. demonstrated the fabrication of freestanding liquid metal structures through suspension printing, stabilizing the metal with an oxide layer formed during extrusion<sup>137</sup>. Using a yield-stress acrylamide/nanoclay suspension with hydrogen peroxide as the support bath, they enabled high-fidelity 3D printing of Galinstan-based liquid metal. The hydrogen peroxide induced rapid  $\text{Ga}_2\text{O}_3$  formation, stabilizing the liquid metal and preventing droplet formation due to surface tension. This technique achieved continuous filaments with diameters of  $\sim 150$   $\mu\text{m}$  and high spatial resolution (Fig. 7n). Embedded constructs within a hydrogel matrix demonstrated remarkable mechanical resilience, enduring tensile deformation up to 500%.

In another study, researchers developed semi-solid-state liquid metal structures using polyelectrolyte-attached skins to create freestanding and stretchable electronic components (Fig. 7o)<sup>114</sup>. Employing a meniscus-guided printing process, they printed polyelectrolyte-coated liquid metal microgranular particles onto diverse substrates with resolutions as fine as 50  $\mu\text{m}$ . This method required no post-processing and achieved an initial conductivity of  $1.5 \times 10^6$  S/m. The ink formulation minimized interparticle repulsion, facilitating compact assembly during printing. The resulting structures retained conductivity under 500% strain and withstood over 10,000 stretching cycles with minimal resistance changes.

Another innovative approach introduced freestanding liquid metal thin-film conductors (FS-GaIn) by integrating AgNWs into a Ga-In alloy and utilizing a selective laser process (Fig. 7p)<sup>138</sup>. Vacuum filtration produced a uniform LM-AgNWs thin film, which was patterned via laser sintering. This process induced multiphase sintering between the liquid metal and NWs, forming a robust oxide shell for structural stability. Subsequent etching removed unsintered regions, yielding a substrate-free conductor. The FS-GaIn film exhibited an initial conductivity of  $5.79 \times 10^5$  S/m and maintained functionality under strains up to 1358%. Remarkably, the conductor experienced only a tenfold resistance increase at

maximum strain and endured over 10,000 stretching cycles at 100% strain with negligible resistance fluctuations.

### Unconventional patterning process of intrinsically soft materials

Creating intricate patterns from intrinsically soft materials is essential for advancing deformable electronics that remain functional under mechanical strain. Traditional patterning processes often prove unsuitable for these materials due to their distinctive mechanical properties. To overcome these challenges, unconventional patterning techniques have been developed, enabling precise structuring of soft materials while preserving their flexibility and stretchability. This chapter examines innovative approaches such as inkjet printing, 3D printing, photolithography, soft lithography, and laser patterning, which have been adapted to address the limitations of conventional methods. These advancements allow for the seamless integration of soft materials with metallic components, enabling the fabrication of complex and functional structures. By leveraging these cutting-edge techniques, next-generation soft electronics with enhanced functionality and durability are becoming increasingly achievable.

#### Printing technologies

Printing techniques, such as inkjet printing and 3D printing, represent additive manufacturing techniques that have gained popularity for fabricating soft electronics due to their precision, scalability, and compatibility with soft materials.

#### Inkjet printing

Inkjet printing is a versatile, non-contact technique for patterning conductive inks and functional materials directly onto substrates. In soft electronics, it enables the deposition of conductive patterns using metallic NPs, conductive polymers, or liquid metals<sup>139</sup>. Its primary advantages include high-resolution patterning without the need for complex masks or etching processes<sup>140,141</sup>, as well as rapid prototyping and customization, making it suitable for flexible and stretchable electronics<sup>142</sup>.

The process involves ejecting tiny ink droplets from a nozzle onto the substrate, with parameters like droplet size, ejection speed, and substrate surface energy carefully adjusted to achieve precise patterns. This method is particularly effective for creating conductive traces on flexible substrates, such as PDMS or polyimide. Metallic NPs-based inks are commonly used due to their high conductivity after sintering. However, the sintering process must be controlled to prevent damage to heat-sensitive substrates. Inkjet printing is also compatible with

stretchable polymers and biomaterials, making it a promising tool for fabricating bioelectronic devices.

#### 3D printing

3D printing, or additive manufacturing, enables the layer-by-layer fabrication of complex 3D structures, making it particularly valuable for creating intricate geometries in soft and stretchable electronics<sup>143,144</sup>. This technique has been adapted to produce stretchable conductive circuits, flexible sensors, and complete electronic devices that are challenging to fabricate using traditional methods. A key advantage of 3D printing is its ability to directly create structures like serpentine patterns or helical coils, which enhance stretchability<sup>145,146</sup>. It also supports the deposition of conductive inks or metallic materials onto elastomeric substrates, forming deformable conductive traces. Additionally, 3D printing facilitates the fabrication of structural components, such as encapsulation layers and flexible scaffolds, that improve the mechanical stability of soft devices. By precisely controlling material deposition, this technique integrates multiple functional components into customized devices for applications like wearable electronics and implantable sensors<sup>147,148</sup>.

For example, an omnidirectionally printable elastic conductor, comprising silver particles and PDMS, was successfully 3D printed<sup>55</sup>. Using an emulsion-based ink with diethylene glycol, the composite exhibited solid-like behavior upon extrusion, maintaining clear 3D spiral structures (Fig. 8a–d). The printed composite demonstrated elasticity without additional encapsulation, allowing it to conform to external stimuli and recover elastically. The printing resolution, adjustable by nozzle size, reached as low as 100 μm. After the diethylene glycol evaporated, the composite showed numerous pores, which concentrated silver at the surface, forming a highly localized conductive layer. This increased conductivity, with stable  $R/R_0$  values below 5 under 100% strain. Even after 3000 cycles of 50% strain,  $R/R_0$  values remained under 3. Directly printed on a skin-like substrate, the composite was integrated with mini light-emitting diodes (LEDs) and microcontroller units, demonstrating its potential for wearable sensors and feedback displays.

#### Photolithography

Photolithography, a well-established technique in semiconductor manufacturing, has been adapted to enable precise patterning of thin films for soft electronics (Fig. 8e)<sup>149</sup>. While conventional photolithography is challenging to apply to intrinsically soft materials due to their mechanical properties<sup>3,150</sup>, advancements in soft-compatible resists and substrates have made it feasible. This process involves coating a photosensitive resist onto a substrate, exposing it to light through a mask, and

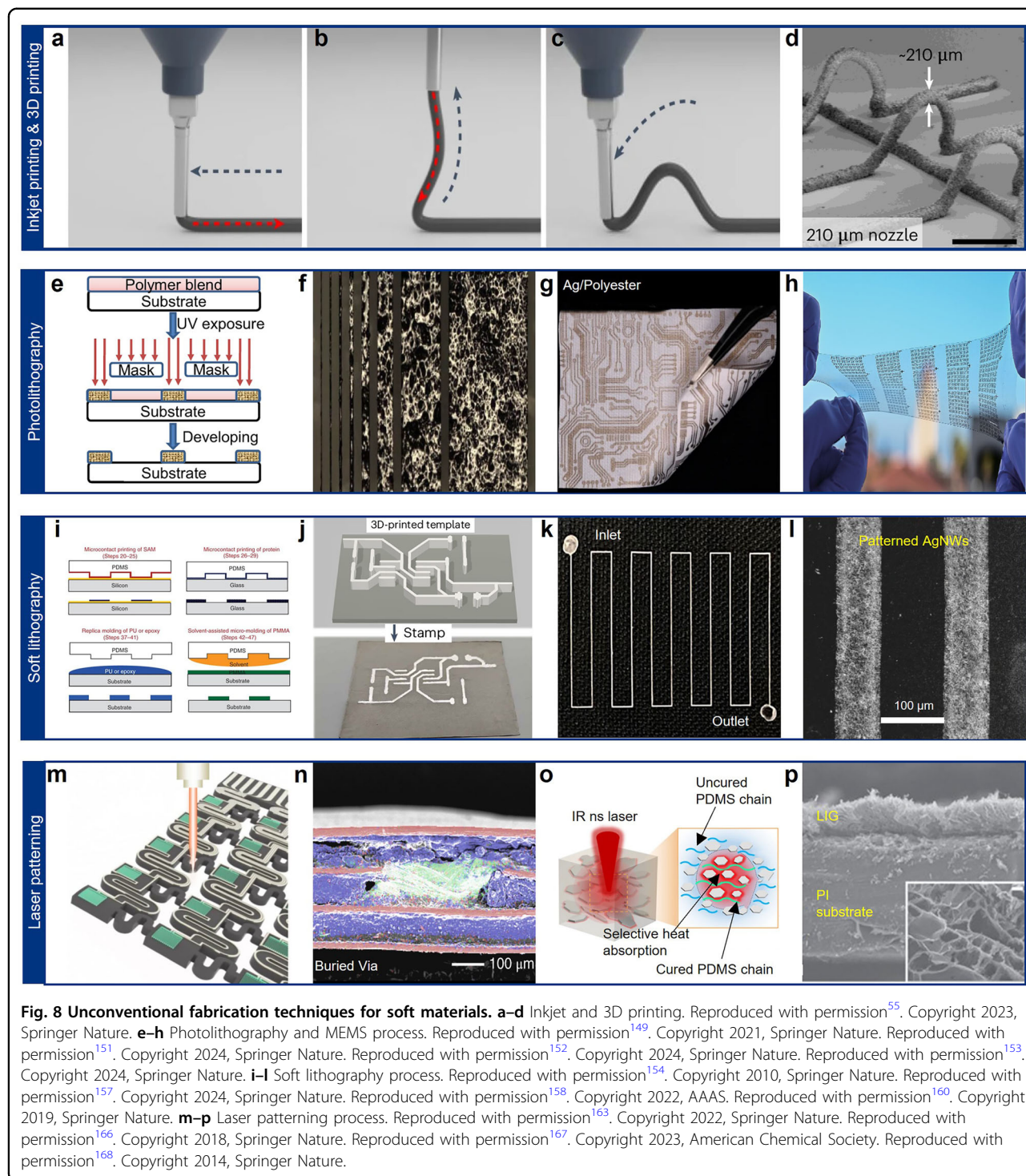


**Fig. 8 Unconventional fabrication techniques for soft materials.** **a-d** Inkjet and 3D printing. Reproduced with permission<sup>55</sup>. Copyright 2023, Springer Nature. **e-h** Photolithography and MEMS process. Reproduced with permission<sup>149</sup>. Copyright 2021, Springer Nature. Reproduced with permission<sup>151</sup>. Copyright 2024, Springer Nature. Reproduced with permission<sup>152</sup>. Copyright 2024, Springer Nature. Reproduced with permission<sup>153</sup>. Copyright 2024, Springer Nature. **i-l** Soft lithography process. Reproduced with permission<sup>154</sup>. Copyright 2010, Springer Nature. Reproduced with permission<sup>157</sup>. Copyright 2024, Springer Nature. Reproduced with permission<sup>158</sup>. Copyright 2022, AAAS. Reproduced with permission<sup>160</sup>. Copyright 2019, Springer Nature. **m-p** Laser patterning process. Reproduced with permission<sup>163</sup>. Copyright 2022, Springer Nature. Reproduced with permission<sup>166</sup>. Copyright 2018, Springer Nature. Reproduced with permission<sup>167</sup>. Copyright 2023, American Chemical Society. Reproduced with permission<sup>168</sup>. Copyright 2014, Springer Nature.

developing the exposed regions to form patterns. Conductive materials, such as metallic NWs or LMs, can then be deposited onto these patterns. Recent developments in elastomeric photoresists have improved the stretchability and durability of these patterns, maintaining integrity under mechanical strain.

For example, Kang et al. introduced a molecularly tailored elastomeric substrate compatible with photolithography<sup>151</sup>. They used a dual-island structure of PUA and polyepoxy acrylate, enabling stable patterning with resolutions down to  $\sim 10 \mu\text{m}$  (Fig. 8f). Using a CMOS-compatible lift-off process, they patterned EGaIn liquid

metal interconnections, achieving excellent electrical stability. The devices maintained consistent conductivity under 50% strain and withstood 10,000 cycles of 30% strain without significant degradation.

Wang et al. developed an in-textile photolithography method to fabricate precise conductive patterns on textile substrates<sup>152</sup>. This method used polymer-assisted metal deposition to anchor metal layers onto textile fibers, followed by double-sided photolithography for uniform patterning (Fig. 8g). The technique achieved sub-100  $\mu\text{m}$  resolution and produced conductive tracks with linear resistance as low as 22  $\Omega/\text{cm}$  for 200  $\mu\text{m}$ -wide features. These patterns remained conductive after 10,000 bending cycles (bending radius 4.7 mm) and 20 wash cycles, demonstrating robustness for wearable applications.

Zhong et al. presented a high-resolution photolithographic approach using stretchable elastomers integrated with conductive materials<sup>153</sup>. They combined semiconducting CNTs with a high- $\kappa$  nitrile-butadiene rubber dielectric layer, achieving patterning resolutions down to  $\sim 0.8 \mu\text{m}$  (Fig. 8h). Metallic CNTs/palladium source-drain electrodes enhanced electrical performance, resulting in low contact resistance and effective charge injection. The devices exhibited exceptional electrical properties, with field-effect mobility exceeding 20  $\text{cm}^2/\text{V}\cdot\text{s}$  under 100% strain and device densities reaching 100,000 transistors per  $\text{cm}^2$ .

### Soft lithography

Soft lithography, which utilizes elastomeric stamps or molds to pattern materials, has become a vital tool in fabricating soft electronics (Fig. 8i)<sup>154</sup>. Unlike traditional photolithography that relies on rigid masks, soft lithography employs flexible molds made from soft materials such as PDMS, enabling the patterning of materials on non-planar surfaces. This flexibility makes it particularly effective for applications involving soft and deformable materials, including conductive polymers, hydrogels, and other stretchable components used in bioelectronics, soft robotics, and flexible sensors<sup>154,155</sup>.

One widely used approach in soft lithography is microcontact printing, where a PDMS stamp transfers functional materials onto a substrate<sup>156</sup>. The stamp, inked with materials such as metallic NPs or LMs, is pressed onto the surface to create conductive patterns. This technique is scalable and ideal for fabricating large-area flexible electronics. Zheng et al. fabricated a nanofiber membrane with semi-embedded liquid metal micro-particles via electrospinning. A 3D-printed stamp was used to rupture the particles locally, forming conductive paths under pressure<sup>157</sup>. Through electrospinning, semi-embedded liquid metal particles were integrated into a TPU nanofiber membrane, and a 3D-printed stamp was used to rupture the particles under localized pressure. This process formed continuous conductive paths within

the membrane (Fig. 8j). The patterned LMNM achieved a resolution of 50  $\mu\text{m}$  and exhibited excellent electrical properties, with a sheet resistance as low as 1  $\Omega/\text{sq}$  at 40% liquid metal content, corresponding to a conductivity of approximately  $2.13 \times 10^6 \text{ S/m}$ . The membrane also demonstrated remarkable elasticity, retaining stable resistance over 30,000 cycles at 100% strain, underscoring its potential for wearable and stretchable electronics.

Another soft lithography technique, replica molding, uses PDMS molds to shape soft materials into complex geometries<sup>158</sup>. Liu et al. employed micromolding in capillaries to fabricate fine patterns of AgNWs on elastomeric substrates<sup>159</sup>. By guiding an AgNW solution through microchannels within a PDMS mold, they achieved highly uniform patterns with a resolution of approximately 20  $\mu\text{m}$  (Fig. 8k). The resulting structures demonstrated excellent conductivity of  $6.3 \times 10^6 \text{ S/m}$  and maintained their electrical properties under 20% strain, making them suitable for flexible sensors and transparent electrodes.

In addition, a “coat-and-print” method has been developed to simplify patterning processes for soft electronics<sup>160</sup>. Li et al. used this approach to create AgNW patterns by spin-coating a dense conductive network onto a substrate, followed by inkjet-printing a PMMA protective layer to define the desired pattern. Excess AgNWs were removed through wet wiping, and the PMMA was dissolved, leaving behind precise conductive patterns (Fig. 8l). This method achieved a resolution of 60  $\mu\text{m}$  and produced patterns with sheet resistance values between 7.1 and 30  $\Omega/\text{sq}$ . The AgNW patterns retained conductivity after over 1000 bending cycles with a radius as small as 3.5 mm, demonstrating their robustness and compatibility with flexible substrates for applications such as wearable antennas and transparent touchscreens.

### Laser patterning

The laser ablation technique has emerged as a promising method for patterning soft electronic materials, offering several advantages, including time and cost efficiency, a reliable and scalable patterning process, and precise control over material properties and structures. Additionally, it eliminates the need for masks or molds, further streamlining the fabrication process<sup>161,162</sup>. By using a focused laser beam, this method can selectively modify material properties or remove material from a surface to create high-precision patterns (Fig. 7m)<sup>163</sup>. The process is particularly suited for soft and stretchable materials, enabling direct patterning without causing mechanical damage, thanks to its non-contact nature<sup>164</sup>. Additionally, laser patterning achieves sub-micrometer precision by focusing the laser beam into a small spot, making it possible to create intricate features that are challenging to replicate using other patterning techniques<sup>165</sup>.

For example, Huang et al. demonstrated laser ablation to form microstructured conductive pathways on a silicone elastomer, showcasing the capability of lasers in directly patterning soft materials<sup>166</sup>. Using a nanosecond-pulsed laser at a 1,064 nm wavelength, they selectively ablated a black-dye-modified silicone elastomer to increase laser absorption and improve patterning efficiency. This technique provided fine control over the depth and diameter of the ablation, achieving a resolution of approximately 45  $\mu\text{m}$ . The resulting conductive pathways exhibited a low resistance of 68.7  $\text{m}\Omega$ , which remained stable under strains of up to 138% elongation. The structure also demonstrated exceptional durability, retaining electrical performance through over 2000 stretching cycles. This approach highlights the potential for integrating precise, multilayered circuits into stretchable electronics for wearable devices and flexible robotics (Fig. 7n).

In another study, Song et al. utilized photothermal lithography to achieve high-resolution patterning of stretchable electronic circuits using a nanosecond-pulsed laser<sup>167</sup>. By selectively heating a silver flake–PDMS nanocomposite with an infrared laser, they induced photothermal curing to create conductive pathways with a resolution of 50  $\mu\text{m}$ . The patterned conductor exhibited excellent conductivity, reaching 5,940 S/cm, and maintained electrical stability under strain, with resistance changes ( $R/R_0 \approx 40$ ) remaining minimal even after 5000 cycles at 30% strain. This method demonstrated significant mechanical durability, making it ideal for complex circuit designs in applications like wearable pressure sensors and passive matrix LED arrays (Fig. 7o).

Although not metal-based, LIG has gained attention for forming carbon-based conductive patterns directly with laser irradiation. Lin et al. employed this technique to produce porous graphene films by laser scribing on commercial PI films<sup>168</sup>. By converting  $\text{sp}^3$  carbon in PI to  $\text{sp}^2$  carbon using a  $\text{CO}_2$  laser under ambient conditions, they formed a 3D porous graphene network. The process achieved a resolution of approximately 120  $\mu\text{m}$  (Fig. 8p). The resulting LIG exhibited a sheet resistance as low as 15  $\Omega/\text{sq}$  at higher laser power (5.4 W), alongside excellent mechanical flexibility, allowing the material to endure bending and stretching without loss of conductivity. This scalable, one-step process is particularly suitable for energy storage applications, such as microsupercapacitors, where high surface area and conductivity are critical for performance.

These examples illustrate the versatility of laser patterning in creating precise, durable, and high-performance structures for next-generation soft electronics. From conductive pathways on elastomers to carbon-based films for energy devices, laser patterning continues to expand the possibilities for integrating soft materials into advanced electronic systems.

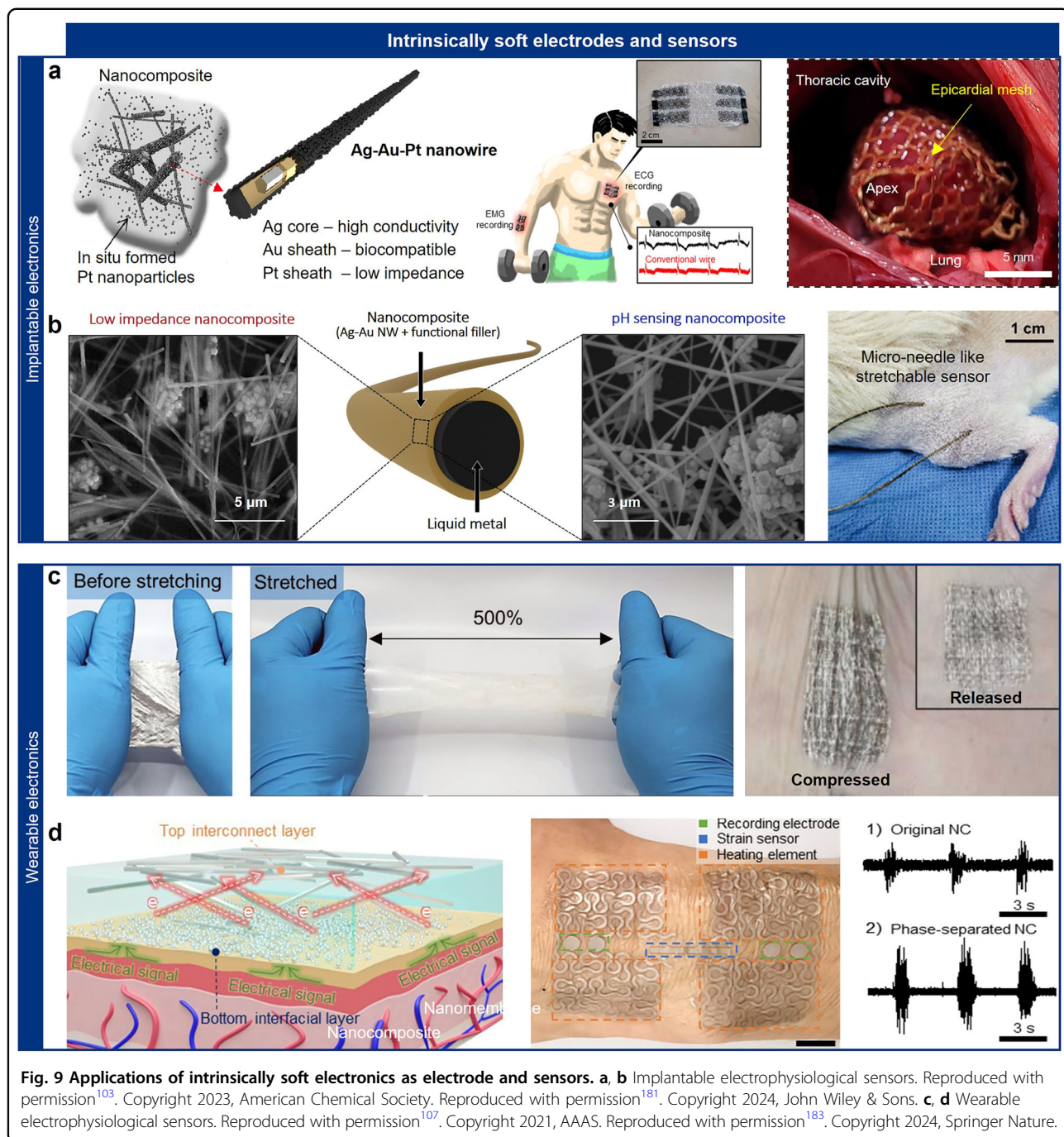
## Applications of intrinsically soft electronics

Driven by advancements in material engineering and assembly strategies, intrinsically soft electronics have rapidly evolved, emerging as promising alternatives to traditional electronics in applications where adaptability and comfort are essential. These devices have been employed in diverse applications, including intrinsically soft interfacing electrodes, sensors, interconnections, displays, antennas, batteries, and computing elements. This section delves into various intrinsically soft electronic components and their applications, highlighting their transformative potential in wearable technologies, flexible devices, and electronic skins.

### Intrinsically soft electrodes and sensors

Intrinsically soft interfacing electrodes play a critical role in monitoring physiological electrical signals such as those generated by muscles or organs, including electroencephalography (EEG), electrocorticography (ECoG), ECG, and electromyography (EMG)<sup>65</sup>. These electrodes facilitate precise physiological monitoring and disease diagnosis while also enabling targeted electrical stimulation for treating and rehabilitating conditions like cerebrovascular diseases, cognitive impairments<sup>12</sup>, cardiac disorders<sup>39,169,170</sup>, and movement disorders<sup>5,171</sup>. Their design focuses on ensuring high-quality signal acquisition and minimizing impedance, which is critical for capturing weak signals ranging from tens of microvolts to several millivolts. High charge-transfer efficiency is essential for smooth charge mobility between the electrode and tissue, while low surface impedance minimizes signal loss, optimizing performance<sup>172–174</sup>. Conductive materials like platinum, Pt black, and PEDOT:PSS have been widely used for their excellent impedance characteristics<sup>13,89</sup>, and liquid metal with intrinsic fluidity and conductivity have emerged as adaptable options for body-conformable electrode designs<sup>175</sup>. Additionally, ultrathin electrodes, less than a few hundred nanometers thick, improve tissue contact and further reduce impedance, enhancing both signal quality and accuracy<sup>107</sup>.

Implantable electrodes, integrated directly with internal organs, eliminate resistance and noise from non-targeted tissues<sup>176,177</sup>, resulting in significantly improved signal quality<sup>178</sup>. For instance, epicardial mesh electrodes fabricated from AgNWs embedded in SBS elastomer have demonstrated high conductivity ( $\sim 10,000 \text{ S/m}$ ) and stretchability up to 60%, adhering seamlessly to the heart surface<sup>179</sup>. These electrodes not only detect abnormal electrical activity but also enhance cardiac contractility through electrical stimulation. However, challenges such as silver ion leaching and NWs oxidation have limited their long-term performance. Innovations in materials, such as incorporating core–shell Ag–Au–PtNWs and SEBS elastomers



integrated with PtNPs, have addressed these issues (Fig. 9a)<sup>103</sup>. The gold shell prevents oxidation and ion leaching, while the platinum enhances charge storage and reduces impedance, significantly improving stability and the signal-to-noise ratio during ECG recordings, while also supporting low-voltage electrical stimulation with greater efficacy<sup>180</sup>.

Another promising design involves fiber-based electrodes that minimize tissue damage during implantation. As

a notable example, Nam et al. discussed the development of a minimally invasive, needle-like microfiber featuring a LM core and a nanocomposite shell for use as an intrinsically soft electrode (Fig. 9b)<sup>181</sup>. The LM core ensures high conductivity ( $\sim 3.4 \times 10^4$  S/cm), stretchability (~800%), and strain-insensitive electrical properties. The nanocomposite shell, comprising Ag-Au NWs, Pt black microparticles, and  $\text{IrO}_2$  NPs, enables multifunctionality, including low impedance and pH sensing.

Wearable intrinsically soft electrodes offer an alternative for measuring physiological signals from the skin surface, avoiding immune responses associated with implantation<sup>52,84</sup>. These electrodes rely on materials with low inherent impedance or designs that maximize the conductive surface area<sup>182,183</sup>. For instance, Jung et al. described a float assembly method to fabricate ultrathin (~250 nm), highly conductive nanomembranes for wearable electronics (Fig. 9c)<sup>107</sup>. Using materials like AgNWs embedded in elastomers, the membranes achieve conductivity of 103,100 S/cm (parallel direction) and maintain performance under strains up to 1000%. Photolithographic patterning and cold welding enhance performance and adaptability. These nanomembranes are applied to multifunctional, reliable skin sensors for electrophysiology, strain, and humidity monitoring, demonstrating reliable, scalable functionality for wearable electronics. In the following work, Lee et al. described a phase-separated nanocomposite for intrinsically soft wearable electronics (Fig. 9d)<sup>184</sup>. Fabricated using AgNWs and AgNPs within a SEBS elastomer matrix, the nanocomposite achieves a conductivity of 18,535 S/cm and stretchability of ~80%. Phase separation improves charge transfer efficiency, reducing contact resistance (~0.132 Ω). Applications include electrophysiology sensors with superior signal-to-noise ratios, strain sensors detecting joint motions with ~80% resistance change, and wearable heaters achieving stable temperature control under motion.

The evolution of intrinsically soft electrodes highlights their potential to transform medical monitoring and wearable technologies. Their adaptability, combined with advanced material and design innovations, ensures high-quality signal acquisition, minimal physiological interference, and enhanced comfort, making them invaluable for a wide range of biomedical applications.

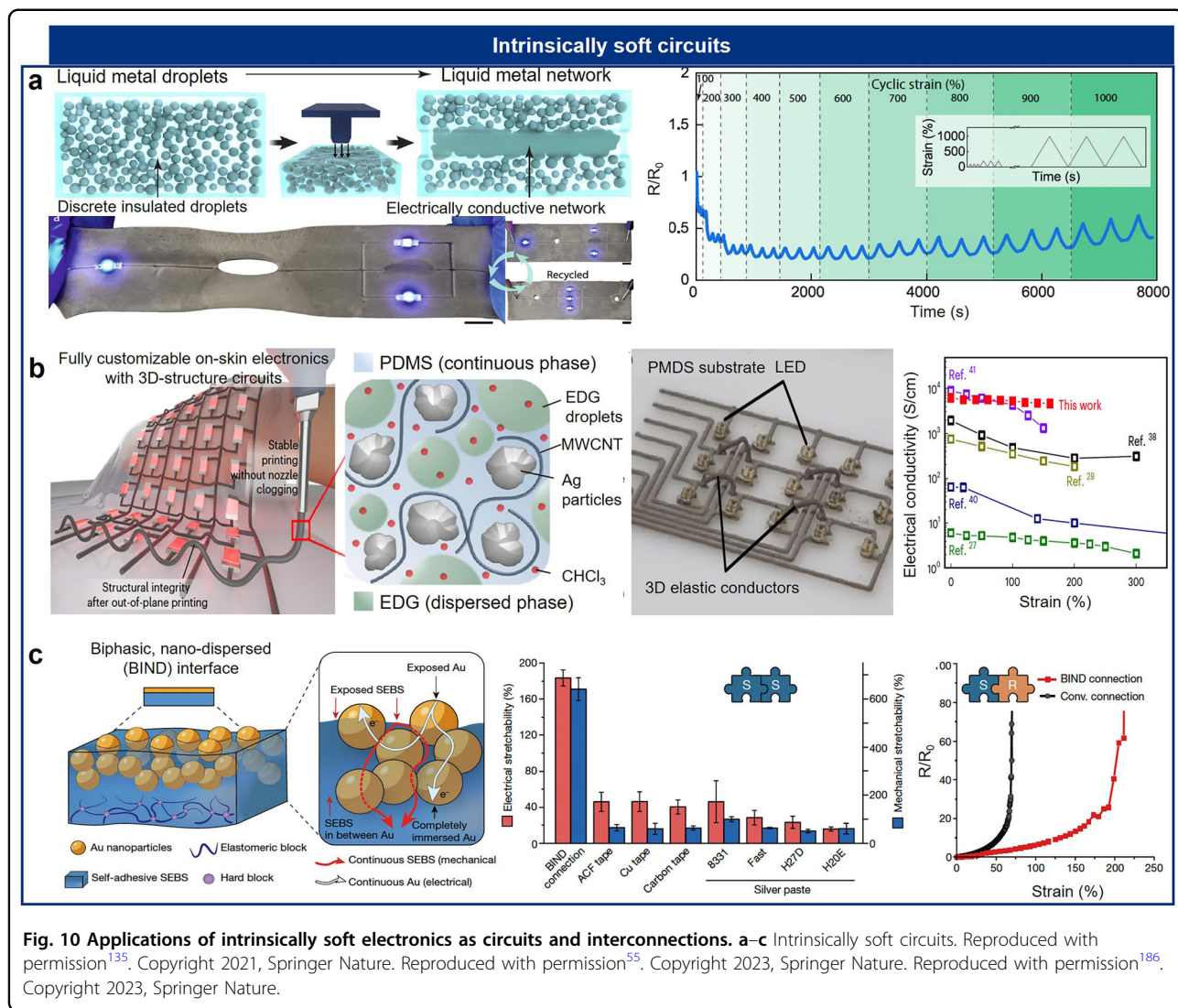
#### Intrinsically stretchable interconnections and circuits

Intrinsically stretchable interconnections are critical components of stretchable circuits, addressing the limitations of traditional structure-based designs like serpentine-shaped thin metal films. These advanced interconnections enable in-plane deformation while surpassing existing constraints on resolution, stretchability, and mechanical stability. One of their key strengths is strain insensitivity, ensuring consistent electrical performance and structural integrity even under significant deformation. Strain insensitivity is achieved by allowing conducting fillers within the matrix to move freely, maintaining the electrical percolation network under applied strain. Various strategies, including the use of LMs<sup>135</sup>, reduction of binding energy between the matrix and fillers<sup>185</sup>, and enabling the free reorganization of fillers, have been employed to achieve these properties.

One innovative approach to intrinsically stretchable interconnections was introduced by Tutika et al., who developed a LM-elastomer composite as a regenerative platform for soft electronics (Fig. 10a)<sup>135</sup>. This composite utilized a styrene–isoprene–styrene block copolymer as the matrix, which is physically crosslinked and reprocessable. The reconfigurable LM droplets within this matrix allowed for self-healing, reconfigurable, and recyclable electrical circuits. Initially dispersed as insulated particles, the LM droplets were restructured into interconnected networks through a scalable embossing technique. The composite demonstrated high conductivity (up to 150 S/cm at 0% strain) and exceptional performance under strain, achieving conductivities as high as 45,400 S/cm at 1200% strain. Additionally, the LM droplets autonomously reconfigured under extreme damage, maintaining conductivity, while the robust polymer matrix exhibited stretchability exceeding 900%, even after substantial damage.

Another approach was introduced by Lee et al., who developed omnidirectional printing for intrinsically stretchable conductors, enabling the creation of out-of-plane 3D structures (Fig. 10b)<sup>55</sup>. Their formulation involved an emulsified ink composed of elastomeric composites with conductive fillers, including silver particles and multiwalled CNTs, in a mixture of diethylene glycol and chloroform. The ink exhibited excellent structural integrity after extrusion, avoiding particle aggregation and nozzle clogging. The printing process produced elastic conductors with freestanding 3D structures, achieving feature sizes below 100 μm and stretchability exceeding 150%. During printing, the evaporation of the immiscible solvent formed self-assembled microstructures with metal particles concentrated at the micropore surfaces, resulting in robust conductive pathways and enhanced electrical conductivity of up to 6682 S/cm. This technology was demonstrated through a skin-mountable electronic device capable of measuring and displaying body temperature using a matrix-type stretchable display.

Bao et al. introduced the BIND (biphasic, nano-dispersed) interface, which enabled robust and highly stretchable connections between soft, rigid, and encapsulated modules in a plug-and-play manner (Fig. 10c)<sup>186</sup>. The BIND interface was created by thermally depositing AuNPs or AgNPs onto a self-adhesive SEBS elastomer, forming an interpenetrating nanostructure. This configuration enhanced contact between NPs and stabilized both mechanical and electrical connections. Under physical pressure, the interface strengthened the bond between modules, providing reliable connectivity. The soft-soft BIND connections achieved over 180% electrical stretchability and more than 600% mechanical stretchability, while soft-rigid BIND connections with substrates like PI, PET, glass, and metal attained approximately 200% electrical stretchability. The soft-encapsulation BIND



connections exhibited interfacial toughness 60 times greater than traditional methods, allowing the fabrication of complex stretchable devices. For instance, a 21-channel on-skin EMG electrode utilizing the BIND interface collected high-quality EMG signals while resisting mechanical interference, showcasing the potential of this approach in practical applications.

#### Intrinsically stretchable optoelectronic devices

Intrinsically stretchable optoelectronic devices, such as LEDs<sup>187,188</sup> and photodetectors (PDs)<sup>189,190</sup>, are revolutionizing human-centric electronics by offering a combination of flexibility and advanced functionality<sup>14,191</sup>. Unlike traditional stretchable devices that rely on rigid-island structures connected by serpentine conductors<sup>192</sup>, these intrinsically soft devices provide seamless adaptability to curvilinear surfaces, even under significant deformation<sup>193</sup>. This soft and flexible nature expands

design possibilities, enhances user interaction, and enables novel applications in areas like smart textiles, flexible smartphones, and implantable medical devices<sup>194</sup>. Current efforts focus on optimizing mechanical properties, resolution, and color reproducibility while ensuring compatibility with other flexible components.

The material used in stretchable active layers—responsible for light emission or absorption—plays a pivotal role in determining device performance. Organic fillers, such as semiconducting polymers, have garnered significant attention due to their excellent stretchability, arising from their ductility, dynamic chain behavior, and interpenetrating polymer networks. These characteristics enable organic fillers to retain their mechanical properties under deformation, making them ideal for stretchable optoelectronic applications.

A notable example is the work by Kim et al., who developed an intrinsically stretchable organic light-

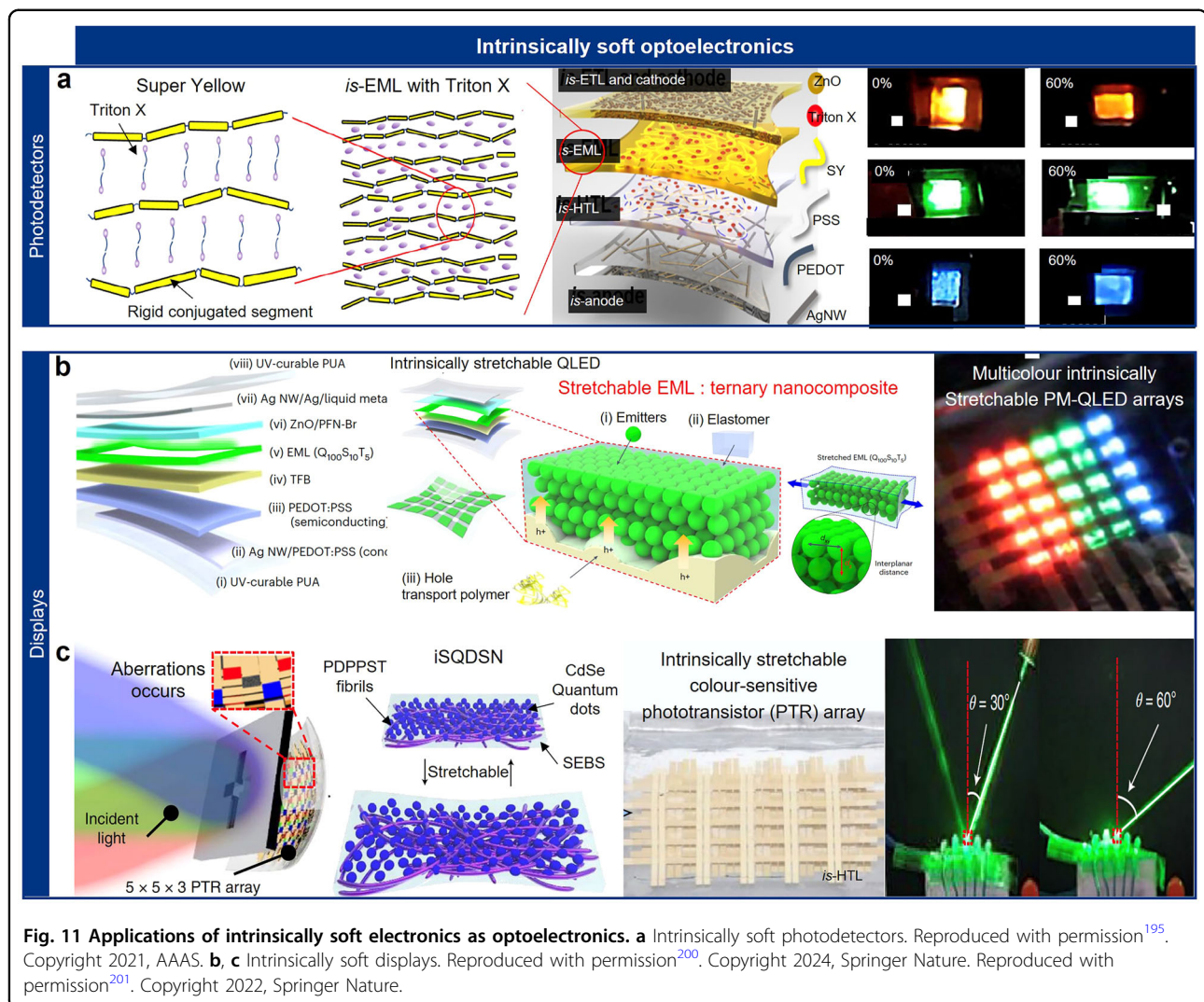


**Fig. 11 Applications of intrinsically soft electronics as optoelectronics. a** Intrinsically soft photodetectors. Reproduced with permission<sup>195</sup>. Copyright 2021, AAAS. **b, c** Intrinsically soft displays. Reproduced with permission<sup>200</sup>. Copyright 2024, Springer Nature. Reproduced with permission<sup>201</sup>. Copyright 2022, Springer Nature.

emitting diode (OLED) fabricated entirely from stretchable materials (Fig. 11a)<sup>195</sup>. Their design employed a blend of the emissive material SuperYellow and Triton X, a nonionic surfactant that acted as a plasticizer. This combination increased the free volume in the polymer matrix, enhancing its flexibility and stretchability. The resulting OLED achieved a turn-on voltage of 8 V and a maximum luminance of 4,400 cd/m<sup>2</sup>, maintaining stable light emission even under 80% strain and over 200 stretching cycles. Other strategies, such as blending SuperYellow with elastomers like polyurethane, have also proven effective in achieving stretchable emissive layers.

Inorganic fillers, including colloidal QDs and perovskite nanocrystals, have emerged as alternatives due to their superior electrical conductivity, high quantum efficiency, and narrow emission spectra<sup>196–199</sup>. However, these nanocrystals require embedding within elastomeric matrices to impart stretchability. Achieving the right balance between filler content and elastomer properties is

crucial for maintaining both mechanical integrity and electrical performance.

For instance, Kim et al. developed intrinsically stretchable QD-based light-emitting diodes (QLEDs) using a ternary nanocomposite emissive layer comprising colloidal QDs, an elastomeric polymer, and a charge-transport polymer (Fig. 11b)<sup>200</sup>. This design ensured stable interparticle spacing and enhanced hole transport to the QDs, enabling the device to maintain consistent performance under 50% strain. The QLEDs achieved a turn-on voltage of 3.2 V, a maximum luminance of 15,170 cd/m<sup>2</sup> at 6.2 V, and stable brightness under deformation. This approach facilitated the development of full-color passive-matrix QLED arrays with red, green, and blue emissive layers, advancing flexible and stretchable display technologies.

Colloidal QDs have also been employed in stretchable light-absorbing layers, enabling the creation of intrinsically stretchable photodetectors. Song et al. introduced a stretchable phototransistor array using a QD-based

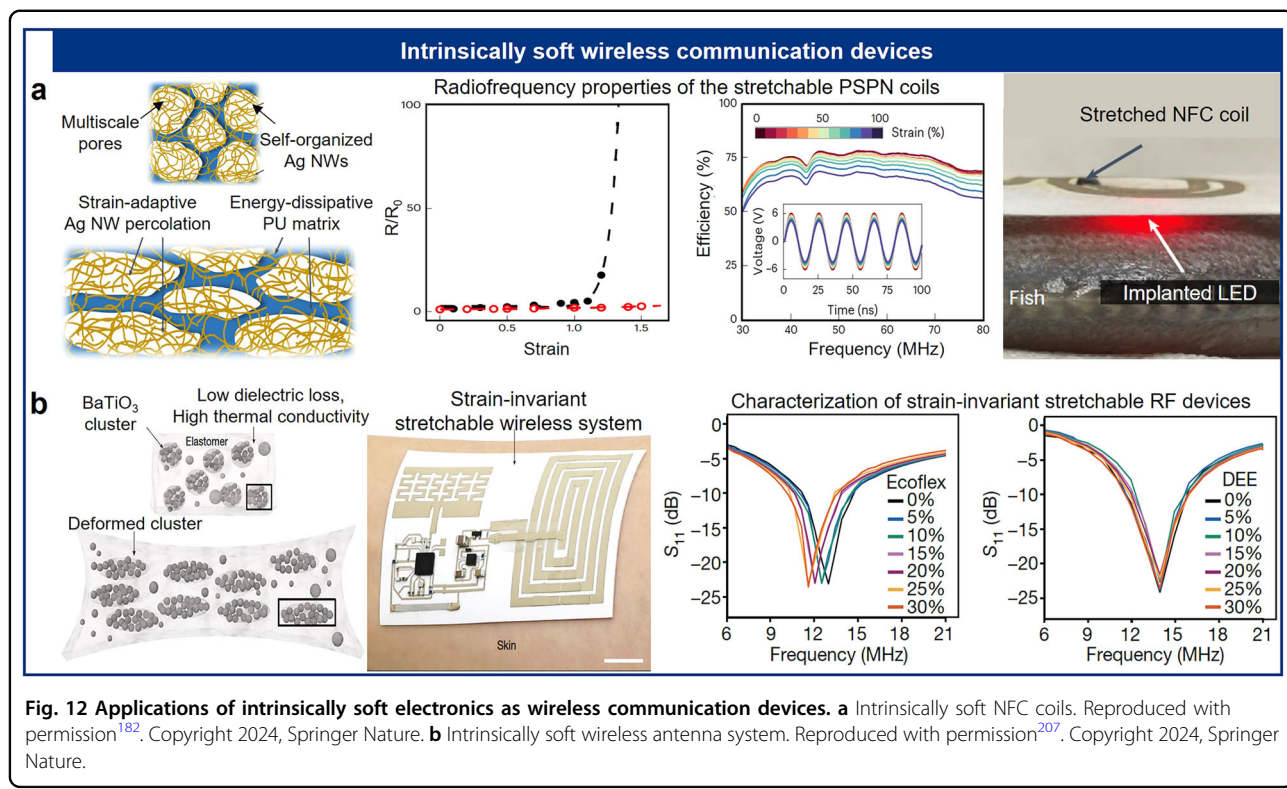


**Fig. 12 Applications of intrinsically soft electronics as wireless communication devices.** **a** Intrinsically soft NFC coils. Reproduced with permission<sup>182</sup>. Copyright 2024, Springer Nature. **b** Intrinsically soft wireless antenna system. Reproduced with permission<sup>207</sup>. Copyright 2024, Springer Nature.

semiconducting nanocomposite that integrated organic semiconducting polymers with size-tuned QDs and elastomeric matrices (Fig. 11c)<sup>201</sup>. By leveraging the surface energy mismatch between QDs and the elastomer, the design enhanced charge-transfer efficiency, achieving high photosensitivity and color resolution. To counter optical aberrations and mechanical deformation noise, a deep neural network algorithm was used, enabling accurate detection of red, green, and blue patterns in both flat and deformed states.

#### Intrinsically stretchable wireless communication components

For fully integrated electronic systems, components for wireless communication are essential to ensure efficient signal transmission and reception under mechanical deformation, enabling reliable wireless data transfer and energy harvesting. Intrinsically stretchable antennas play a crucial role in incorporating wireless communication and energy transfer into flexible and adaptable electronic systems, making them indispensable for applications such as wearable devices and electronic skin<sup>202,203</sup>. Their ability to maintain performance while bending, stretching, or twisting is critical for advancing energy transfer systems, particularly in scenarios where flexibility and durability are critical<sup>204</sup>.

To achieve these properties, various advanced nanomaterials, including metallic NPs, ceramic NPs, and

carbon-based materials like graphene and CNTs, have been employed<sup>205,206</sup>. These materials are chosen for their high electrical conductivity and mechanical flexibility, ensuring that antennas can adapt to deformations without compromising signal integrity or power transfer efficiency.

For example, Kim et al. developed a stretchable near-field communication (NFC) system that demonstrates robust wireless power and data transmission capabilities, even under significant mechanical deformation<sup>182</sup>. Using an innovative *in situ* phase separation technique, the researchers assembled microscale AgNWs within a polymer matrix, creating self-organized percolation networks along the surfaces of pores (Fig. 12a). This approach minimized the required filler content while achieving highly conductive and strain-insensitive nanocomposites. The multiscale porous polymer matrix enhanced flexibility and mechanical resilience, ensuring stable electrical conductivity. The stretchable NFC system exhibited reliable performance with less than a 10% variation in wireless power and data transmission under strains of up to 50%, showcasing its potential for wearable communication devices.

In another study, Kim et al. introduced strain-invariant stretchable radio frequency (RF) components using a novel dielectroelastic elastomer (DEE) (Fig. 12b)<sup>207</sup>. DEE was synthesized by embedding high-dielectric-constant ( $\kappa$ ) ceramic NPs, specifically barium titanate oxide

(BaTiO<sub>3</sub>), into an elastomeric matrix, resulting in enhanced electrical, mechanical, and thermal properties compared to conventional stretchable substrates. A unique feature of DEE is its ability to maintain consistent RF characteristics by tuning its dielectric properties under strain, effectively minimizing resonance frequency shifts and improving performance in dynamic environments, such as on the human skin. Stretchable RF electronics fabricated with DEE demonstrated wireless operation over distances of up to 30 m, maintaining excellent performance even under significant strain.

### Intrinsically stretchable energy device

Powering components, encompassing energy storage systems and nanogenerators, are foundational for the evolution of portable and wearable electronics<sup>208</sup>. These components enable the seamless integration of energy storage and harvesting functionalities into devices designed for dynamic environments. Stretchable energy storage materials, such as CNTs, graphene, conductive polymers, and specialized alloys<sup>209</sup>, are designed to combine mechanical flexibility with high electrochemical performance<sup>210,211</sup>. By employing innovative material strategies and structural designs, researchers have significantly advanced the flexibility and efficiency of these systems.

A notable development in the field is the creation of aqueous zinc-ion batteries capable of maintaining efficiency at subzero temperatures, where the freezing of water in the electrolyte typically disrupts ion transport and hinders performance. To address this, Kim et al. developed an antifreezing gel electrolyte composed of PAAm, graphene oxide (GO), and EG (Fig. 13a)<sup>212</sup>. This composite gel leverages the mechanical strength provided by GO and the 3D macroporous network it forms, which enhances ion transport. Meanwhile, EG prevents freezing, ensuring reliable operation in extreme conditions. The resulting pAAM/GO/EG electrolyte demonstrated impressive ionic conductivity (14.9 mS/cm at -20 °C) and superior mechanical properties compared to conventional pAAM-based gels. When applied in a quasisolid-state zinc–manganese dioxide (Zn–MnO<sub>2</sub>) battery, this electrolyte enabled robust electrochemical performance, even under harsh temperature conditions, showcasing its potential for use in flexible and cold-resistant energy storage devices.

Stretchable nanogenerators, on the other hand, harness mechanical energy and convert it into electrical energy through piezoelectric or triboelectric mechanisms<sup>213</sup>. These devices capture energy from movements, vibrations, or environmental forces, leveraging materials like piezoelectric polymers, thermoelectric polymers, NWs, and conductive elastomers<sup>214,215</sup>. However, the application of piezoelectric nanogenerators (PENGs) has been

limited by their low output current density, reducing their effectiveness in ambient mechanical energy harvesting. Gu et al. addressed this limitation with an innovative 3D intercalation electrode (IENG) design (Fig. 13b)<sup>216</sup>. This design incorporates numerous boundary interfaces within a high-piezoelectric-coefficient material, thereby enhancing surface polarization charges and significantly increasing current density. The IENG achieved a peak short-circuit current of 320 μA and a current density of 290 μA/cm<sup>2</sup>, marking a 1.93-fold improvement over previous PENGs and a 1.61-fold increase over triboelectric nanogenerators (TENGs). Additionally, it charged a 1 μF capacitor from 0 V to 8 V in just 21 cycles and exhibited an equivalent surface charge density of 1690 μC/m<sup>2</sup>, surpassing TENGs by 1.35 times. Demonstrating its potential, the IENG powered 100 red commercial LEDs, representing a significant milestone in mechanical energy harvesting technology.

### Intrinsically stretchable memory devices

Intrinsically stretchable memory devices are a vital component of next-generation stretchable electronics, addressing the growing need for data storage solutions that can withstand mechanical deformation while maintaining reliable performance. Unlike conventional rigid memory devices, these stretchable counterparts are designed to endure repeated stretching, bending, and twisting without compromising their electrical functionality or data retention capabilities. Their unique combination of mechanical flexibility and high-performance data storage makes them indispensable for applications in wearable devices, electronic skin, and soft robotics, where adaptability to dynamic environments is crucial. These devices must maintain reliable performance under mechanical deformation while providing the durability and flexibility required for dynamic environments.

Addressing the challenges of integrating memory technologies into flexible systems, Kim et al. introduced a novel self-healing stretchable resistive random-access memory (SS-RRAM) (Fig. 13c)<sup>217</sup>. The SS-RRAM utilized a bilayer structure composed of Ag-gradient nanocomposites, which ensured a stable metal–insulator–metal configuration essential for reliable data storage and resistive switching performance. A key innovation in this design was the incorporation of a tough, self-healing polymer matrix combined with Ag microflakes and nanoflakes. This matrix provided both mechanical resilience and electrical stability, enabling the device to endure substantial deformation while maintaining functionality. The SS-RRAM demonstrated exceptional electrical endurance and data retention, even under strains of up to 100%. It achieved a high on/off ratio during resistive switching, highlighting its suitability for advanced memory applications. Additionally, the device exhibited robust durability, retaining performance over

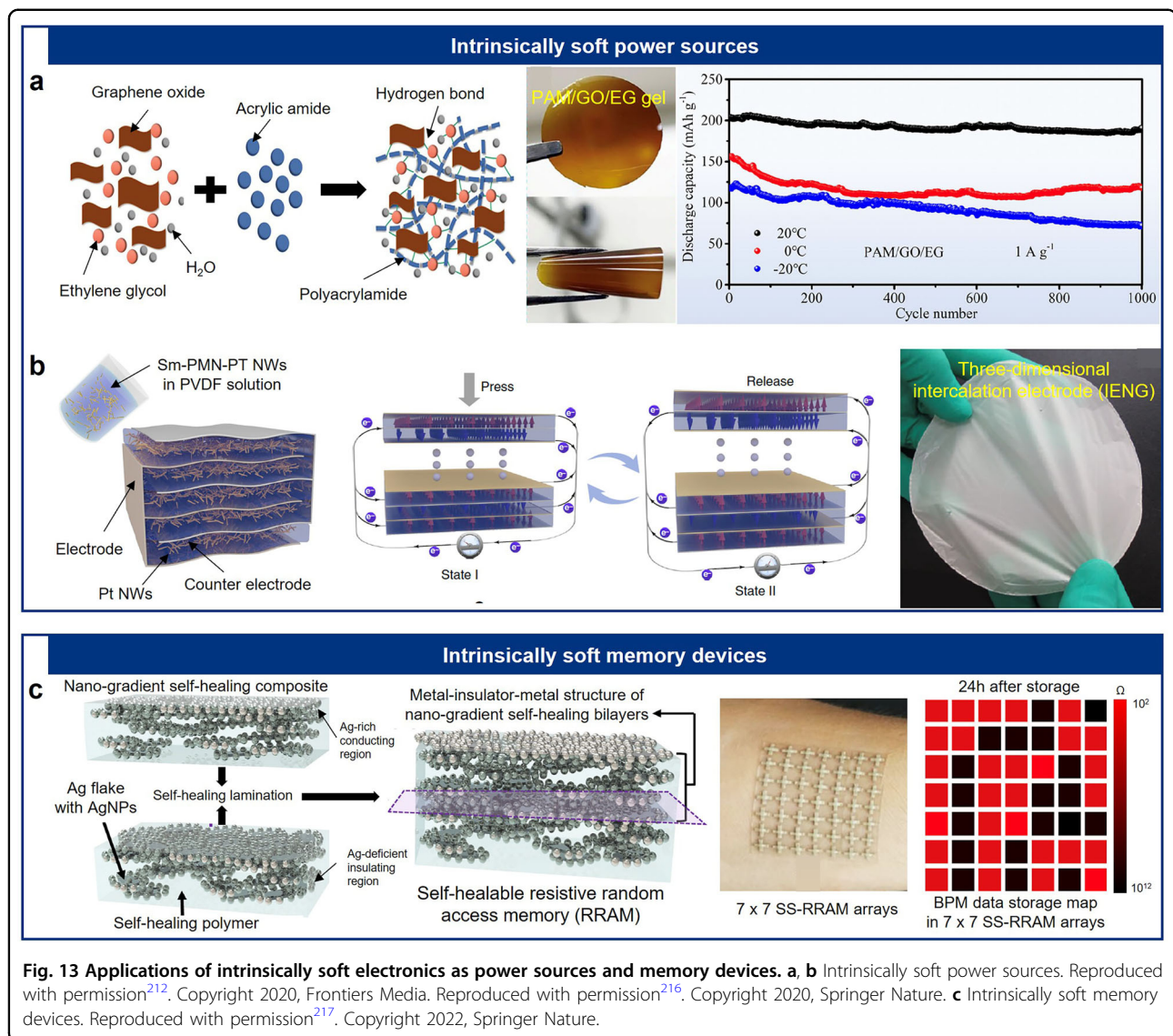


**Fig. 13 Applications of intrinsically soft electronics as power sources and memory devices.** **a, b** Intrinsically soft power sources. Reproduced with permission<sup>212</sup>. Copyright 2020, Frontiers Media. Reproduced with permission<sup>216</sup>. Copyright 2020, Springer Nature. **c** Intrinsically soft memory devices. Reproduced with permission<sup>217</sup>. Copyright 2022, Springer Nature.

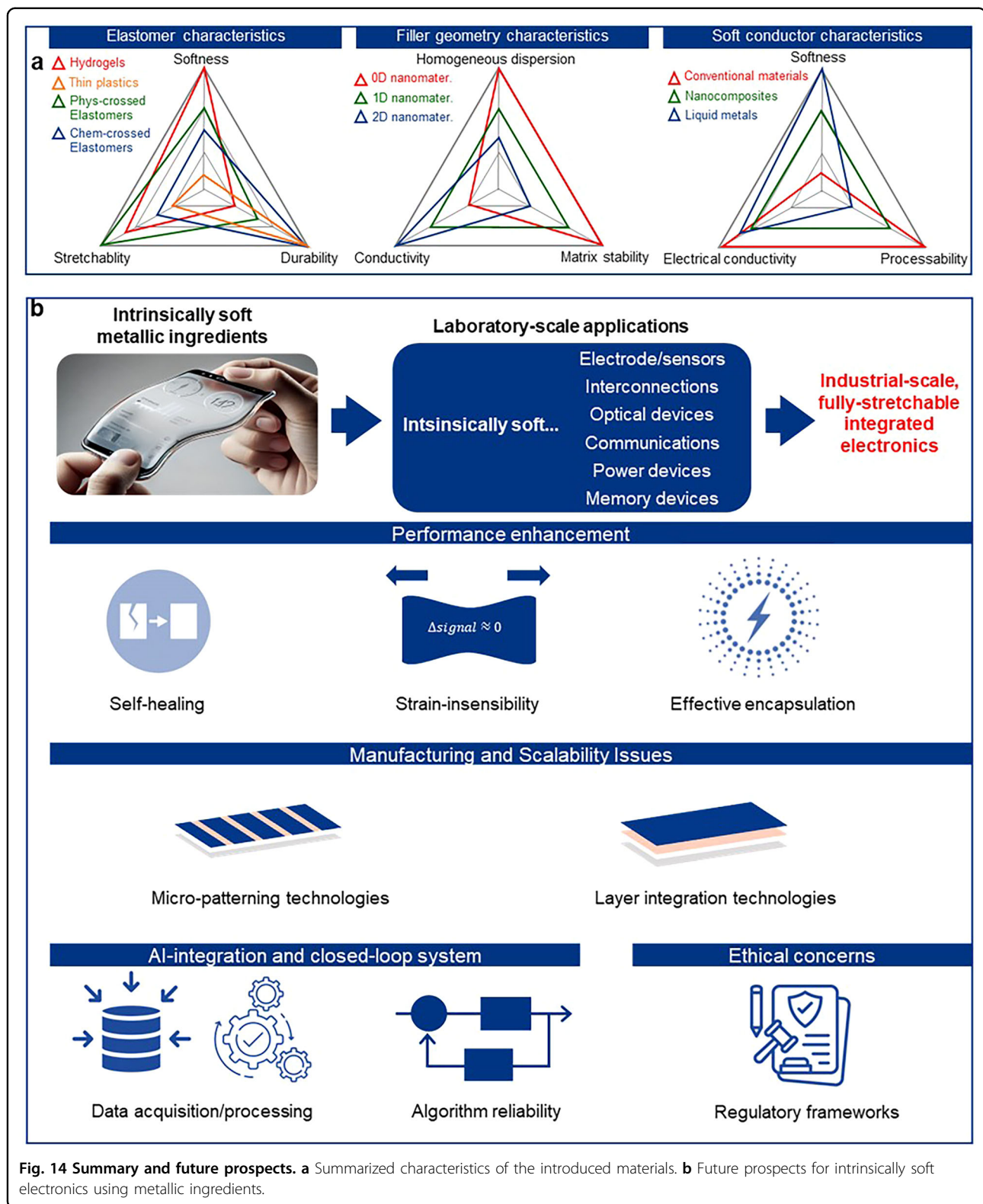
extended use and deformation cycles. These features make the SS-RRAM a significant step forward in creating intrinsically stretchable memory devices for next-generation flexible electronics. Recently, Nam et al. presented intrinsically stretchable floating-gate memory transistors for use in electronic skin<sup>218</sup>. These devices use AgNPs embedded in an elastomer as the floating gate and a dual-stimuli writing system (optical and electrical). They exhibit a high memory on/off ratio ( $>10^5$ ), retention time ( $>10^6$  s), and mechanical durability under strains of 50% uniaxial and 30% biaxial. Applications include personalized data storage in E-skin systems, demonstrating reliability in dynamic environments.

### Conclusion and future perspectives

Intrinsically soft electronics have gained prominence for their capacity to seamlessly integrate flexibility with

functionality, driving advancements in biomedicine, wearable technology, and energy systems. These devices encompass a variety of components, including electrodes, batteries, displays, memory devices, energy storage systems, and communication modules, each offering distinct benefits and addressing unique challenges. To meet the performance requirements for specific applications, researchers must carefully select materials that align with the intended function of these components. A thorough evaluation of the advantages and limitations of candidate materials is essential for achieving the desired balance between mechanical, electrical, and functional properties. Representative characteristics of the materials commonly used in intrinsically soft electronics are concisely summarized in Fig. 14a, serving as a reference for their suitability across various applications.

While intrinsically soft electronic materials incorporating metallic ingredients have demonstrated remarkable



potential as individual components, further advancements in material development and enhanced interaction among identical components are essential to achieve fully

integrated, industrial-scale soft electronics (Fig. 14b). These advancements are crucial for transitioning from isolated functionalities to cohesive systems capable of

operating as complete, practical devices. In the subsequent sections, we will explore the future directions and research endeavors necessary to overcome current limitations and enable the realization of advanced, fully soft electronic systems. These discussions will highlight the critical challenges in material optimization, component integration, manufacturing scalability, and system-level functionality, outlining the roadmap for the next generation of intrinsically soft electronics.

Soft electrodes are particularly valuable in bridging the interface between electronic devices and biological systems. Their ability to conform to tissue surfaces enhances their capacity to monitor and stimulate physiological processes, offering improved solutions for health monitoring and disease treatment. Meanwhile, soft batteries and energy storage devices ensure the reliable operation of implants and wearable devices by maintaining consistent performance under mechanical deformation. Soft displays, on the other hand, provide real-time feedback in applications such as health monitoring, enhancing user interaction, and patient care by adapting seamlessly to body contours for both comfort and functionality. These advancements in soft electrodes, batteries, and displays are driving the evolution of wearable health monitors, fitness trackers, and smart clothing, making devices more versatile and effective.

Soft memory devices and communication modules contribute significantly to the versatility of electronic systems. Memory devices in soft electronics need to maintain reliability and data retention while accommodating mechanical deformation, ensuring seamless integration into flexible systems. Soft communication modules facilitate efficient data transfer and wireless communication, enabling the development of fully integrated systems with advanced connectivity. The potential applications of these components extend to everyday objects, where they can enable highly adaptable, connected, and efficient electronic systems.

Despite these advancements, the field faces significant challenges. For instance, soft electrodes require further improvements in biocompatibility, dynamic stability, and electrical performance. Current research has aimed to enhance their ability to minimize immune responses, maintain long-term reliability, and optimize their interaction with biological systems. Specifically, applying a biohybrid system would dramatically improve biocompatibility and biological interfacing. Similarly, soft batteries must overcome challenges related to energy density, mechanical flexibility, and performance stability under stress. Energy storage devices require materials that can balance high storage capacity with flexibility and durability, while soft displays must address issues of resolution and mechanical resilience to expand their applications<sup>219</sup>.

Memory devices in soft electronics face challenges in achieving high storage density, reliability, and processing speed while maintaining their stretchable nature. Energy storage devices and generators must ensure mechanical stability and efficiency, even under significant deformation. Novel materials and structures are essential to address these requirements. Communication modules must ensure robust signal transmission and data integrity in dynamic environments, necessitating advancements in materials and design to improve their overall performance.

A critical area of focus for soft electronics lies in enhancing long-term durability and stability under dynamic conditions. Devices need to withstand mechanical stresses such as bending, stretching, and compression without losing functionality. Self-healing materials and strain-insensitive composites have emerged as promising solutions to extend the lifespan of these devices, enabling them to autonomously repair minor damage and adapt to mechanical strain. Additionally, addressing challenges related to nanomaterial toxicity and oxidation is essential to prevent performance degradation and ensure safety.

Transitioning from laboratory prototypes to scalable, mass-produced devices presents its own set of challenges. The development of reproducible and cost-effective manufacturing processes is vital to achieving consistent quality and performance in large-scale production. Advances in patterning technologies and layer-integration techniques will be crucial for the commercialization of soft electronics.

The integration of artificial intelligence (AI) and closed-loop systems represents a significant step forward in the functionality of soft electronics. AI enables advanced data analysis, predictive modeling, and personalized treatments, enhancing the capabilities of these systems, including self-monitoring and calibration. Closed-loop designs, which rely on real-time sensing, data processing, and feedback mechanisms, offer the potential for responsive and adaptive applications in areas like physiological monitoring and therapeutic interventions. However, challenges related to data accuracy, security, and algorithm transparency must be addressed to fully realize these possibilities.

To transition laboratory-scale advances into practical, commercially viable applications, the development of scalable, large-area fabrication techniques is essential. Prominent large-scale manufacturing methods include roll-to-roll printing, extrusion-based additive manufacturing, and continuous casting, all of which enable high-throughput production of soft electronic devices with uniform quality. Roll-to-roll printing, for instance, has demonstrated potential in fabricating stretchable conductive films using metallic nanowire-based inks, achieving consistent electrical and mechanical

performance over large areas. Extrusion-based additive manufacturing facilitates precise three-dimensional patterning of conductive elastomer composites at industrial scales, suitable for customized wearable and implantable devices. However, these large-scale fabrication methods face critical challenges such as maintaining material homogeneity, controlling ink rheology for uniform deposition, and managing curing processes to preserve desired mechanical and electrical properties. Addressing these hurdles requires further research into optimized ink formulations, advanced quality control systems, and process automation. Bridging these gaps will significantly enhance the reliability and reproducibility of intrinsically soft electronics, accelerating their integration into healthcare monitoring, soft robotics, and flexible consumer electronics. Lastly, ethical and regulatory considerations are paramount to ensuring the responsible development and deployment of soft electronics. Establishing clear guidelines and frameworks can help address concerns about data privacy, security, and informed consent, while balancing innovation with ethical responsibilities.

In conclusion, the continued development of intrinsically soft electronics requires addressing a range of technical, manufacturing, and ethical challenges. By overcoming these obstacles, these technologies can unlock their full potential, revolutionizing applications in healthcare, wearable devices, and beyond.

#### Acknowledgements

This research was supported by the Institute for Basic Science (IBS-R006-A1), the National Research Foundation of Korea (2021R1C1C2004400, RS-2025-00555824), the Korea Health Industry Development Institute (RS-2025-02263839), and the Regional Innovation System & Education (RISE) program through the Gangwon RISE Center (2025-RISE-10-006, 2025-RISE-10-005).

#### Author details

<sup>1</sup>Department of Chemical Engineering, Kumoh National Institute of Technology, Gumi, Republic of Korea. <sup>2</sup>Center for Nanoparticle Research, Institute for Basic Science (IBS), Seoul, Republic of Korea. <sup>3</sup>Department of Chemical Engineering, Inha University, Incheon, Republic of Korea. <sup>4</sup>Department of Biomedical Engineering, Yonsei University, Wonju, Republic of Korea. <sup>5</sup>Department of Chemical, Biological, and Battery Engineering, Gachon University, Gyeonggi-do, Republic of Korea. <sup>6</sup>Department of Semiconductor Engineering, Gachon University, Gyeonggi-do, Republic of Korea. <sup>7</sup>School of Chemical and Biological Engineering, and Institute of Chemical Processes, Seoul National University, Seoul, Republic of Korea. <sup>8</sup>Department of Materials Science and Engineering, Seoul National University, Seoul, Republic of Korea

#### Author contributions

S.H.S. and H.J.K. contributed equally to this work. S.H.S., H.J.K. wrote the manuscript. J.H.K. modified the figure images. D.C.K. and D.H.K. revised the overall manuscript.

#### Competing interests

The authors declare no competing interests.

#### Publisher's note

Springer Nature remains neutral with regard to jurisdictional claims in published maps and institutional affiliations.

Received: 31 January 2025 Revised: 16 July 2025 Accepted: 1 August 2025. Published online: 10 October 2025

#### References

1. Ceruzzi, P. E. Chapter from *NASA Spaceflight* 89-127 (2018).
2. Kim, D. H., Lu, N., Ghaffari, R. & Rogers, J. A. Inorganic semiconductor nanomaterials for flexible and stretchable bio-integrated electronics. *NPG Asia Mater.* **4**, e15 (2012).
3. Fischer, A. C. et al. Integrating MEMS and ICs. *Microsyst. Nanoeng.* **1**, 15005 (2015).
4. Kim, J. et al. Stretchable silicon nanoribbon electronics for skin prosthesis. *Nat. Commun.* **5**, 5747 (2014).
5. Son, D. et al. Multifunctional wearable devices for diagnosis and therapy of movement disorders. *Nat. Nanotechnol.* **9**, 397–404 (2014).
6. Xu, S. et al. Stretchable batteries with self-similar serpentine interconnects and integrated wireless recharging systems. *Nat. Commun.* **4**, 1543 (2013).
7. Myny, K. The development of flexible integrated circuits based on thin-film transistors. *Nat. Electron.* **1**, 30–39 (2018).
8. Sunwoo, S.-H., Ha, K.-H., Lee, S., Lu, N. & Kim, D.-H. Wearable and implantable soft bioelectronics: Device designs and material strategies. *Annu. Rev. Chem. Biomol. Eng.* **12**, 359–391 (2021).
9. Wang, W. et al. Strain-insensitive intrinsically stretchable transistors and circuits. *Nat. Electron.* **4**, 143–150 (2021).
10. Wang, S. et al. Skin electronics from scalable fabrication of an intrinsically stretchable transistor array. *Nature* **555**, 83–88 (2018).
11. Sunwoo, S.-H. et al. Soft bioelectronics for the management of cardiovascular diseases. *Nat. Rev. Bioeng.* **2**, 8–24 (2023).
12. Sunwoo, S. H. et al. Advances in soft bioelectronics for brain research and clinical neuroengineering. *Matter* **3**, 1923–1947 (2020).
13. Lim, C. et al. Tissue-like skin-device interface for wearable bioelectronics by using ultrasoft, mass-permeable, and low-impedance hydrogels. *Sci. Adv.* **7**, eabd3716 (2021).
14. Chang, S. et al. Flexible and stretchable light-emitting diodes and photodetectors for human-centric optoelectronics. *Chem. Rev.* **124**, 768–859 (2024).
15. Kim, D.-H. et al. Epidermal electronics. *Science* **333**, 838–843 (2011).
16. Zhang, Y. et al. Buckling in serpentine microstructures and applications in elastomer-supported ultra-stretchable electronics with high areal coverage. *Soft Matter* **9**, 8062–8070 (2013).
17. Jiao, R. et al. Vertical serpentine interconnect-enabled stretchable and curved electronics. *Microsyst. Nanoeng.* **9**, 149 (2023).
18. Sun, Y., Choi, W. M., Jiang, H., Huang, Y. Y. & Rogers, J. A. Controlled buckling of semiconductor nanoribbons for stretchable electronics. *Nat. Nanotechnol.* **1**, 201–207 (2006).
19. Xu, S. et al. Assembly of micro/nanomaterials into complex, three-dimensional architectures by compressive buckling. *Science* **347**, 154–159 (2015).
20. Woo, J. et al. Ultrastretchable helical conductive fibers using percolated Ag nanoparticle networks encapsulated by elastic polymers with high durability in omnidirectional deformations for wearable electronics. *Adv. Funct. Mater.* **30**, 1910026 (2020).
21. Stanley, J., Kunovski, P., Hunt, J. & Wei, Y. Stretchable electronic strips for electronic textiles enabled by 3D helical structure. *Nat. Sci. Rep.* **14**, 11065 (2024).
22. Kim, Y. G., Song, J. H., Hong, S. & Ahn, S. H. Piezoelectric strain sensor with high sensitivity and high stretchability based on kirigami design cutting. *npj Flex. Electron.* **6**, 52 (2022).
23. Guan, Y. S., Zhang, Z., Tang, Y., Yin, J. & Ren, S. Kirigami-Inspired Nanoconfined Polymer Conducting Nanosheets with 2000% Stretchability. *Adv. Mater.* **30**, 1706390 (2018).
24. Cho, Y. et al. Engineering the shape and structure of materials by fractal cut. *Proc. Natl. Acad. Sci. USA* **111**, 17390–17395 (2014).
25. Lee, Y., Kim, B. J., Hu, L., Hong, J. & Ahn, J. H. Morphable 3D structure for stretchable display. *Mater. Today* **53**, 51–57 (2022).
26. Kumar, S., Mishra, T. & Mahata, A. Manipulation of mechanical properties of monolayer molybdenum disulfide: Kirigami and hetero-structure based approach. *Mater. Chem. Phys.* **252**, 123280 (2020).
27. Hong, S., Lee, S. & Kim, D. H. Materials and design strategies of stretchable electrodes for electronic skin and its applications. *Proc. IEEE* **107**, 2185–2197 (2019).

28. Correia, R. et al. Biocompatible polyimide-C laser-induced graphene electrodes for microsupercapacitor applications. *ACS Appl. Mater. Interfaces.* **14**, 46427–46438 (2022).
29. Werkmeister, F. & Nickel, B. Towards flexible organic thin film transistors (OTFTs) for biosensing. *J. Mater. Chem. B* **1**, 3830–3835 (2013).
30. Dong, Z. et al. Microfabrication of functional polyimide films and microstructures for flexible MEMS applications. *Microsyst. Nanoeng.* **9**, 31 (2023).
31. Jin, H. et al. Flexible surface acoustic wave resonators built on disposable plastic film for electronics and lab-on-a-chip applications. *Sci. Rep.* **3**, 2140 (2013).
32. Zardetto, V., Brown, T. M., Reale, A. & Di Carlo, A. Substrates for flexible electronics: A practical investigation on the electrical, film flexibility, optical, temperature, and solvent resistance properties. *J. Polym. Sci. B Polym. Phys.* **49**, 638–648 (2011).
33. Shan, S. et al. Flexibility characteristics of a polyethylene terephthalate chemiresistor coated with a nanoparticle thin film assembly. *J. Mater. Chem. C Mater.* **2**, 1893–1903 (2014).
34. Li, N. et al. Large-scale flexible and transparent electronics based on monolayer molybdenum disulfide field-effect transistors. *Nat. Electron.* **3**, 711–717 (2020).
35. Skafi, Z. et al. Flexible perovskite solar cells on polycarbonate film substrates. *Adv. Energy Mater.* **14**, 2400912 (2024).
36. Wang, C., Hu, Y. & Li, L. Phase transition and electrical conversion properties of Ge/Sb nano-multilayer films on flexible substrates. *npj Flex. Electron.* **8**, 8 (2024).
37. Quereda, J. et al. Scalable and low-cost fabrication of flexible WS<sub>2</sub> photodetectors on polycarbonate. *npj Flex. Electron.* **6**, 23 (2022).
38. Shim, H. J., Sunwoo, S. H., Kim, Y., Koo, J. H. & Kim, D. H. Functionalized Elastomers for Intrinsically Soft and Biointegrated Electronics. *Adv. Healthc. Mater.* **10**, 2002105 (2021).
39. Han, W. B. et al. Ultra-stretchable and biodegradable elastomers for soft, transient electronics. *Nat. Commun.* **14**, 2263 (2023).
40. Takamatsu, S., Sato, S. & Itoh, T. Stress concentration-relocating interposer in electronic textile packaging using thermoplastic elastic polyurethane film with via holes for bearing textile stretch. *Sci. Rep.* **12**, 9269 (2022).
41. Chen, H. et al. A new route to fabricate flexible, breathable composites with advanced thermal management capability for wearable electronics. *npj Flex. Electron.* **7**, 24 (2023).
42. Zhou, J., Zhao, S., Tang, L., Zhang, D. & Sheng, B. Programmable and Weldable Superelastic EGaN/TPU composite fiber by wet spinning for flexible electronics. *ACS Appl. Mater. Interfaces.* **15**, 57533–57544 (2023).
43. Cao, J. et al. Anti-friction gold-based stretchable electronics enabled by interfacial diffusion-induced cohesion. *Nat. Commun.* **15**, 1116 (2024).
44. Lv, J. et al. Printed sustainable elastomeric conductor for soft electronics. *Nat. Commun.* **14**, 7132 (2023).
45. Li, Y. et al. Achieving tissue-level softness on stretchable electronics through a generalizable soft interlayer design. *Nat. Commun.* **14**, 4488 (2023).
46. Koo, J. H. et al. A vacuum-deposited polymer dielectric for wafer-scale stretchable electronics. *Nat. Electron.* **6**, 137–145 (2023).
47. Miwa, Y., Kurachi, J., Kohbara, Y. & Kutsumizu, S. Dynamic ionic crosslinks enable high strength and ultrastretchability in a single elastomer. *Commun. Chem.* **1**, 5 (2018).
48. Ariati, R., Sales, F., Souza, A., Lima, R. A. & Ribeiro, J. Polydimethylsiloxane composites characterization and its applications: A review. *Polymers* **13**, 4258 (2021).
49. Nishikawa, T., Yamane, H., Matsuhashi, N. & Miki, N. Stretchable Strain Sensor with Small but Sufficient Adhesion to Skin. *Sensors* **23**, 1774 (2023).
50. Park, H. et al. Facile strategy for uniform gold coating on silver nanowires embedded PDMS for soft electronics. *npj Flex.* **8**, 63 (2024).
51. Jeong, S. H., Zhang, S., Hjort, K., Hilborn, J. & Wu, Z. G. PDMS-based elastomer tuned soft, stretchable, and sticky for epidermal electronics. *Adv. Mater.* **28**, 5830–5836 (2016).
52. Park, C. et al. Stretchable conductive nanocomposites and their applications in wearable devices. *Appl. Phys. Rev.* **9**, 21312 (2022).
53. Firpo, G., Angeli, E., Repetto, L. & Valbusa, U. Permeability thickness dependence of polydimethylsiloxane (PDMS) membranes. *J. Memb. Sci.* **481**, 1–8 (2015).
54. Lu, Y. et al. Stretchable graphene–hydrogel interfaces for wearable and implantable bioelectronics. *Nat. Electron.* **7**, 51–65 (2024).
55. Lee, B. et al. Omnidirectional printing of elastic conductors for three-dimensional stretchable electronics. *Nat. Electron.* **6**, 307–318 (2023).
56. Kim, J. Y., Park, K. S., Kim, Z. S., Baek, K. H. & Do, L. M. Fabrication of low-cost submicron patterned polymeric replica mold with high elastic modulus over a large area. *Soft Matter* **8**, 1184–1189 (2012).
57. Liu, J. et al. Fully stretchable active-matrix organic light-emitting electrochemical cell array. *Nat. Commun.* **11**, 3362 (2020).
58. Li, S. et al. Digital light processing of liquid crystal elastomers for self-sensing artificial muscles. *Sci. Adv.* **7**, eabg3677 (2021).
59. Cha, G. D. et al. Multifunctional Injectable Hydrogel for in Vivo Diagnostic and Therapeutic Applications. *ACS Nano* **16**, 554–567 (2022).
60. Cha, G. D. et al. Minimally-Invasive and In-Vivo Hydrogel Patterning Method for In Situ Fabrication of Implantable Hydrogel Devices. *Small Methods* **7**, 2300032 (2023).
61. Cha, G. D., Lee, W. H., Lim, C., Choi, M. K. & Kim, D. H. Materials engineering, processing, and device application of hydrogel nanocomposites. *Nanoscale* **12**, 10456–10473 (2020).
62. Ohm, Y. et al. An electrically conductive silver–polyacrylamide–alginate hydrogel composite for soft electronics. *Nat. Electron.* **4**, 185–192 (2021).
63. Liu, Y. et al. Soft and elastic hydrogel-based microelectronics for localized low-voltage neuromodulation. *Nat. Biomed. Eng.* **3**, 58–68 (2019).
64. Huang, W. et al. Design of stretchable and self-powered sensing device for portable and remote trace biomarkers detection. *Nat. Commun.* **14**, 5221 (2023).
65. Kim, H. J., Choi, H., Kim, D.-H. & Son, D. Stretchable Functional Nanocomposites for Soft Implantable Bioelectronics. *Nano Lett.* **24**, 8453–8464 (2024).
66. Ram, R., Rahaman, M., Aldalbahi, A. & Khastgir, D. Determination of percolation threshold and electrical conductivity of polyvinylidene fluoride (PVDF)/short carbon fiber (SCF) composites: Effect of SCF aspect ratio. *Polym. Int.* **66**, 573–582 (2017).
67. Shi, Y. D., Li, J., Tan, Y. J., Chen, Y. F. & Wang, M. Percolation behavior of electromagnetic interference shielding in polymer/multi-walled carbon nanotube nanocomposites. *Compos. Sci. Technol.* **170**, 70–76 (2019).
68. Choi, H. J., Kim, M. S., Ahn, D., Yeo, S. Y. & Lee, S. Electrical percolation threshold of carbon black in a polymer matrix and its application to antistatic fibre. *Sci. Rep.* **9**, 6338 (2019).
69. Zhang, Z. et al. Advances in monte carlo method for simulating the electrical percolation behavior of conductive polymer composites with a carbon-based filling. *Polymers* **16**, 545 (2024).
70. Mutiso, R. M., Sherratt, M. C., Rathmell, A. R., Wiley, B. J. & Winey, K. I. Integrating simulations and experiments to predict sheet resistance and optical transmittance in nanowire films for transparent conductors. *ACS Nano* **7**, 7654–7663 (2013).
71. Jagota, M. & Tansu, N. Conductivity of nanowire arrays under random and ordered orientation configurations. *Sci. Rep.* **5**, 10219 (2015).
72. Jung, D. et al. Adaptive Self-Organization of Nanomaterials Enables Strain-Insensitive Resistance of Stretchable Metallic Nanocomposites. *Adv. Mater.* **34**, 2200980 (2022).
73. Amina, S. J. & Guo, B. A review on the synthesis and functionalization of gold nanoparticles as a drug delivery vehicle. *Int. J. Nanomed.* **15**, 9823–9857 (2020).
74. Lee, W., Yun, H., Song, J.-K., Sunwoo, S.-H. & Kim, D.-H. Nanoscale materials and deformable device designs for bioinspired and biointegrated electronics. *Acc. Mater. Res.* **2**, 266–281 (2021).
75. Liu, Y. et al. Silver nanoparticle enhanced metal-organic matrix with interface-engineering for efficient photocatalytic hydrogen evolution. *Nat. Commun.* **14**, 541 (2023).
76. Zhang, Q., Lee, J. Y., Yang, J., Boothroyd, C. & Zhang, J. Size and composition tunable Ag–Au alloy nanoparticles by replacement reactions. *Nanotechnology* **18**, 245605 (2007).
77. Lee, H. E. et al. Amino-acid- A nd peptide-directed synthesis of chiral plasmonic gold nanoparticles. *Nature* **556**, 360–365 (2018).
78. Wang, C. et al. Characterization and antimicrobial application of biosynthesized gold and silver nanoparticles by using *Microbacterium resistens*. *Artif. Cells Nanomed. Biotechnol.* **44**, 1714–1721 (2016).
79. Chung, K. et al. Non-oxidized bare copper nanoparticles with surface excess electrons in air. *Nat. Nanotechnol.* **17**, 285–291 (2022).
80. Khan, M. A. R., Mamun, M. S. A. & Ara, M. H. Review on platinum nanoparticles: Synthesis, characterization, and applications. *Microchem. J.* **171**, 106840 (2021).
81. Proppe, A. H., Berkinsky, D. B., Zhu, H., Šverko, T. & Kaplan, A. E. K. Horowitz, et al. Highly stable and pure single-photon emission with 250 ps optical

coherence times in InP colloidal quantum dots. *Nat. Nanotechnol.* **18**, 993–999 (2023).

82. Kim, T. et al. Efficient and stable blue quantum dot light-emitting diode. *Nature* **586**, 385–389 (2020).
83. Korte, K. E., Skrabalak, S. E. & Xia, Y. Rapid synthesis of silver nanowires through a CuCl- or CuCl<sub>2</sub>-mediated polyol process. *J. Mater. Chem.* **18**, 437–441 (2008).
84. Jung, D. et al. Metal-like stretchable nanocomposite using locally-bundled nanowires for skin-mountable devices. *Adv. Mater.* **35**, 2303458 (2023).
85. Bardet, L. et al. Silver nanowire networks: Ways to enhance their physical properties and stability. *Nanomaterials* **11**, 2785 (2021).
86. Nam, S. et al. Soft conductive nanocomposites for recording biosignals on skin. *Soft Sci.* **3**, 28 (2023).
87. Qian, F. et al. Ultralight conductive silver nanowire aerogels. *Nano Lett.* **17**, 7171–7176 (2017).
88. Dertli, E., Coskun, S. & Esenturk, E. N. Gold nanowires with high aspect ratio and morphological purity: Synthesis, characterization, and evaluation of parameters. *J. Mater. Res.* **28**, 250–260 (2013).
89. Sunwoo, S. H. et al. Stretchable low-impedance nanocomposite comprised of Ag–Au core–shell nanowires and Pt black for epicardial recording and stimulation. *Adv. Mater. Technol.* **5**, 1900768 (2020).
90. Sunwoo, S.-H. et al. Stretchable low-impedance conductor with Ag–Au–Pt core–shell–shell nanowires and in situ formed Pt nanoparticles for wearable and implantable device. *ACS Nano* **17**, 7550–7561 (2023).
91. Miyamoto, A. et al. T. Inflammation-free, gas-permeable, lightweight, stretchable on-skin electronics with nanomeshes. *Nat. Nanotechnol.* **12**, 907–913 (2017).
92. Liu, Y. Q., Zhang, M., Wang, F. X. & Pan, G. B. Facile microwave-assisted synthesis of uniform single-crystal copper nanowires with excellent electrical conductivity. *RSC Adv.* **2**, 11235–11237 (2012).
93. Duong, T. H. & Kim, H. C. Extremely simple and rapid fabrication of flexible transparent electrodes using ultralong copper nanowires. *Ind. Eng. Chem. Res.* **57**, 3076–3082 (2018).
94. Won, Y., Kim, A., Yang, W., Jeong, S. & Moon, J. A highly stretchable, helical copper nanowire conductor exhibiting a stretchability of 700. *NPG Asia Mater.* **6**, e132 (2014).
95. Luc, W. et al. Two-dimensional copper nanosheets for electrochemical reduction of carbon monoxide to acetate. *Nat. Catal.* **2**, 423–430 (2019).
96. Yoon, I. S., Kim, S. H., Oh, Y., Ju, B. K. & Hong, J. M. Ag flake/silicone rubber composite with high stability and stretching speed insensitive resistance via conductive bridge formation. *Sci. Rep.* **10**, 5036 (2020).
97. Seo, H. et al. Durable and fatigue-resistant soft peripheral neuroprosthetics for in vivo bidirectional signaling. *Adv. Mater.* **33**, 2007346 (2021).
98. Lv, J. et al. Printable elastomeric electrodes with sweat-enhanced conductivity for wearables. *Sci. Adv.* **7**, eabg8433 (2021).
99. Lim, G. H., Lee, N. E. & Lim, B. Highly sensitive, tunable, and durable gold nanosheet strain sensors for human motion detection. *J. Mater. Chem. C. Mater.* **4**, 5642–5647 (2016).
100. Heo, S., Jeong, S., Kim, K. H. & Kim, H. J. Mechanically resilient integrated electronics realized using interconnected 2D gold-nanosheet elastomeric electrodes. *NPG Asia Mater.* **14**, 37 (2022).
101. Lim, C. et al. Facile and Scalable Synthesis of Whiskered Gold Nanosheets for Stretchable, Conductive, and Biocompatible Nanocomposites. *ACS Nano* **16**, 10431–10442 (2022).
102. Matsuhisa, N. et al. Printable elastic conductors by in situ formation of silver nanoparticles from silver flakes. *Nat. Mater.* **16**, 834–840 (2017).
103. Sunwoo, S. H. et al. Stretchable low-impedance conductor with Ag–Au–Pt core–shell–shell nanowires and in situ formed Pt nanoparticles for wearable and implantable device. *ACS Nano* **17**, 7550–7561 (2023).
104. Zhang, J., Tang, Y., Lee, K. & Ouyang, M. Nonepitaxial growth of hybrid core–shell nanostructures with large lattice mismatches. *Science* **327**, 1634–1638 (2010).
105. Choi, S. et al. Highly conductive, stretchable and biocompatible Ag–Au core–sheath nanowire composite for wearable and implantable bioelectronics. *Nat. Nanotechnol.* **13**, 1048–1056 (2018).
106. Kim, Y. et al. Stretchable nanoparticle conductors with self-organized conductive pathways. *Nature* **500**, 59–63 (2013).
107. Jung, D. et al. Highly conductive and elastic nanomembrane for skin electronics. *Science* **373**, 1022–1026 (2021).
108. Garnett, E. C. et al. Self-limited plasmonic welding of silver nanowire junctions. *Nat. Mater.* **11**, 241–249 (2012).
109. Lu, Y., Huang, J. Y., Wang, C., Sun, S. & Lou, J. Cold welding of ultrathin gold nanowires. *Nat. Nanotechnol.* **5**, 218–224 (2010).
110. Liu, Y. et al. Capillary-Force-Induced Cold Welding in Silver-Nanowire-Based Flexible Transparent Electrodes. *Nano Lett.* **17**, 1090–1096 (2017).
111. Lim, G. H., Ahn, K., Bok, S., Nam, J. & Lim, B. Curving silver nanowires using liquid droplets for highly stretchable and durable percolation networks. *Nanoscale* **9**, 8938–8944 (2017).
112. Li, Y. et al. One-step synthesis of ultra-long silver nanowires of over 100 μm and their application in flexible transparent conductive films. *RSC Adv.* **8**, 8057–8063 (2018).
113. Zhu, J. et al. Formation of chiral branched nanowires by the Eshelby Twist. *Nat. Nanotechnol.* **3**, 477–481 (2008).
114. Lee, G. H. et al. Rapid meniscus-guided printing of stable semi-solid-state liquid metal microgranular-particle for soft electronics. *Nat. Commun.* **13**, 2643 (2022).
115. Zhang, Y. et al. Global health effects of future atmospheric mercury emissions. *Nat. Commun.* **12**, 3035 (2021).
116. Kim, I. et al. Removal of radioactive cesium from an aqueous solution via bioaccumulation by microalgae and magnetic separation. *Sci. Rep.* **9**, 10149 (2019).
117. Cui, J., Jin, B., Xu, A., Li, J. & Shao, M. Single-Atom Metallophilic Sites for Liquid NaK Alloy Confinement toward Stable Alkali-Metal Anodes. *Adv. Sci.* **10**, 2206479 (2023).
118. Zhang, J., Sheng, L. & Liu, J. Synthetically chemical-electrical mechanism for controlling large scale reversible deformation of liquid metal objects. *Sci. Rep.* **4**, 7116 (2014).
119. Wang, B., Maslik, J., Hellman, O., Gumiero, A. & Hjort, K. Supercooled Liquid Ga Stretchable Electronics. *Adv. Funct. Mater.* **33**, 2300036 (2023).
120. Dejace, L., Chen, H., Furfaro, I., Schiavone, G. & Lacour, S. P. Microscale Liquid Metal Conductors for Stretchable and Transparent Electronics. *Adv. Mater. Technol.* **6**, 2100690 (2021).
121. Khan, M. R., Eaker, C. B., Bowden, E. F. & Dickey, M. D. Giant and switchable surface activity of liquid metal via surface oxidation. *Proc. Natl. Acad. Sci. USA* **111**, 14047–14051 (2014).
122. Kim, J. H. et al. Imbibition-induced selective wetting of liquid metal. *Nat. Commun.* **13**, 4763 (2022).
123. Li, G. et al. Three-dimensional flexible electronics using solidified liquid metal with regulated plasticity. *Nat. Electron.* **6**, 154–163 (2023).
124. Ren, L. et al. Nanodroplets for Stretchable Superconducting Circuits. *Adv. Funct. Mater.* **26**, 8111–8118 (2016).
125. Ota, H. et al. Highly deformable liquid-state heterojunction sensors. *Nat. Commun.* **5**, 5032 (2014).
126. Lin, R. et al. Digitally-embroidered liquid metal electronic textiles for wearable wireless systems. *Nat. Commun.* **13**, 2190 (2022).
127. Guo, H. et al. Fabrication of a Flexible Strain Sensor with High-Aspect-Ratio Liquid-Metal Galinstan. *Adv. Mater. Technol.* **8**, 2200749 (2023).
128. Blum, J. D. Mesmerized by mercury. *Nat. Chem.* **5**, 1066 (2013).
129. Zhang, L. et al. Exploring Self-Healing Liquid Na–K Alloy for Dendrite-Free Electrochemical Energy Storage. *Adv. Mater.* **30**, 1804011 (2018).
130. Lu, X. et al. Liquid-metal electrode to enable ultra-low temperature sodium–beta alumina batteries for renewable energy storage. *Nat. Commun.* **5**, 4578 (2014).
131. Li, X. et al. Evaporation-induced sintering of liquid metal droplets with biological nanofibrils for flexible conductivity and responsive actuation. *Nat. Commun.* **10**, 3514 (2019).
132. Park, J. E., Kang, H. S., Koo, M. & Park, C. Autonomous Surface Reconciliation of a Liquid-Metal Conductor Micropatterned on a Deformable Hydrogel. *Adv. Mater.* **32**, 2002178 (2020).
133. Zhu, H. et al. Fully solution processed liquid metal features as highly conductive and ultrastretchable conductors. *npj Flex. Electron.* **5**, 25 (2021).
134. Yan, J. et al. Solution processable liquid metal nanodroplets by surface-initiated atom transfer radical polymerization. *Nat. Nanotechnol.* **14**, 684–690 (2019).
135. Tutika, R., Haque, A. B. M. T. & Bartlett, M. D. Self-healing liquid metal composite for reconfigurable and recyclable soft electronics. *Commun. Mater.* **2**, 64 (2021).
136. Ma, Z. et al. Permeable superelastic liquid-metal fibre mat enables biocompatible and monolithic stretchable electronics. *Nat. Mater.* **20**, 859–868 (2021).
137. Wu, Q. et al. Suspension printing of liquid metal in yield-stress fluid for resilient 3D constructs with electromagnetic functions. *npj Flex. Electron.* **6**, 50 (2022).

138. Kim, M. et al. Nanowire-assisted freestanding liquid metal thin-film patterns for highly stretchable electrodes on 3D surfaces. *npj Flex. Electron.* **6**, 99 (2022).

139. Liu, Y. et al. Recent advances in inkjet-printing technologies for flexible/wearable electronics. *Nanoscale* **15**, 6025–6051 (2023).

140. Song, O. et al. All inkjet-printed electronics based on electrochemically exfoliated two-dimensional metal, semiconductor, and dielectric. *NPJ 2D Mater. Appl.* **6**, 64 (2022).

141. Yu, Y. et al. Photoreactive and metal-platable copolymer inks for high-throughput, room-temperature printing of flexible metal electrodes for thin-film electronics. *Adv. Mater.* **28**, 4926–4934 (2016).

142. Molina-Lopez, F. et al. Inkjet-printed stretchable and low voltage synaptic transistor array. *Nat. Commun.* **10**, 2676 (2019).

143. Hui, Y. et al. Three-dimensional printing of soft hydrogel electronics. *Nat. Electron* **5**, 893–903 (2022).

144. Hubbard, J. D. et al. Fully 3D-printed soft robots with integrated fluidic circuitry. *Sci. Adv.* **7**, 5257 (2021).

145. Lei, I. M., Sheng, Y., Lei, C. L., Leow, C. & Huang, Y. Y. S. A hackable, multi-functional, and modular extrusion 3D printer for soft materials. *Sci. Rep.* **12**, 12294 (2022).

146. Zhao, J., Li, X., Ji, D. & Bae, J. Extrusion-based 3D printing of soft active materials. *ResearchGate* **60**, 7414–7426 (2024).

147. Li, J., Cao, J., Lu, B. & Gu, G. 3D-printed PEDOT:PSS for soft robotics. *Nat. Rev. Mater.* **8**, 604–622 (2023).

148. Park, Y. G. et al. High-resolution 3D printing for electronics. *Adv. Sci.* **9**, 2104623 (2022).

149. Wang, B. et al. Foundry-compatible high-resolution patterning of vertically phase-separated semiconducting films for ultraflexible organic electronics. *Nat. Commun.* **12**, 4937 (2021).

150. Valle, J. J., Sánchez-Chiva, J. M., Fernández, D. & Madrenas, J. Design, fabrication, characterization and reliability study of CMOS-MEMS Lorentz-force magnetometers. *Microsyst. Nanoeng.* **8**, 103 (2022).

151. Kang, S. H. et al. Full integration of highly stretchable inorganic transistors and circuits within molecular-tailored elastic substrates on a large scale. *Nat. Commun.* **15**, 1–12 (2024).

152. Wang, P. et al. Well-defined in-textile photolithography towards permeable textile electronics. *Nat. Commun.* **15**, 887 (2024).

153. Zhong, D. et al. High-speed and large-scale intrinsically stretchable integrated circuits. *Nature* **627**, 313–320 (2024).

154. Qin, D., Xia, Y. & Whitesides, G. M. Soft lithography for micro- and nanoscale patterning. *Nat. Protoc.* **5**, 491–502 (2010).

155. Lee, S. H. et al. A soft lithographic approach to fabricate InAs nanowire field-effect transistors. *Sci. Rep.* **8**, 3204 (2018).

156. Lee, S. H. et al. Multifunctional self-assembled monolayers via microcontact printing and degas-driven flow guided patterning. *Sci. Rep.* **8**, 16763 (2018).

157. Zheng, S. et al. Pressure-stamped stretchable electronics using a nanofibre membrane containing semi-embedded liquid metal particles. *Nat. Electron.* **7**, 576–585 (2024).

158. Wang, Y. et al. Benchtop micromolding of polystyrene by soft lithography. *Lab Chip* **11**, 3089–3097 (2011).

159. Liu, Y., Zheng, M., O'Connor, B., Dong, J. & Zhu, Y. Curvilinear soft electronics by micromolding of metal nanowires in capillaries. *Sci. Adv.* **8**, 6996 (2022).

160. Li, W., Meredov, A. & Shamim, A. Coat-and-print patterning of silver nanowires for flexible and transparent electronics. *npj Flex. Electron.* **3**, 19 (2019).

161. Marchiori, B., Delattre, R., Hannah, S., Blayac, S. & Ramuz, M. Laser-patterned metallic interconnections for all stretchable organic electrochemical transistors. *Sci. Rep.* **8**, 8477 (2018).

162. Ham, J., Han, A. K., Cutkosky, M. R. & Bao, Z. UV-laser-machined stretchable multi-modal sensor network for soft robot interaction. *npj Flex. Electron.* **6**, 94 (2022).

163. Yang, Q. et al. High-speed, scanned laser structuring of multi-layered eco/bioresorbable materials for advanced electronic systems. *Nat. Commun.* **13**, 6518 (2022).

164. Park, S., Lee, H., Kim, Y. J. & Lee, P. S. Fully laser-patterned stretchable microsupercapacitors integrated with soft electronic circuit components. *NPJ Asia Mater.* **10**, 959–969 (2018).

165. Harper, A. F., Diemer, P. J. & Jurchescu, O. D. Contact patterning by laser printing for flexible electronics on paper. *npj Flex. Electron.* **3**, 11 (2019).

166. Huang, Z. et al. Three-dimensional integrated stretchable electronics. *Nat. Electron* **1**, 473–480 (2018).

167. Song, S. et al. Photothermal Lithography for Realizing a Stretchable Multilayer Electronic Circuit Using a Laser. *ACS Nano* **17**, 21443–21454 (2023).

168. Lin, J. et al. Laser-induced porous graphene films from commercial polymers. *Nat. Commun.* **5**, 5714 (2014).

169. Hong, Y. J., Jeong, H., Cho, K. W., Lu, N. & Kim, D. H. Wearable and Implantable Devices for Cardiovascular Healthcare: from Monitoring to Therapy Based on Flexible and Stretchable Electronics. *Adv. Funct. Mater.* **29**, 1808247 (2019).

170. Choi, S., Han, S. I., Kim, D., Hyeon, T. & Kim, D. H. High-performance stretchable conductive nanocomposites: Materials, processes, and device applications. *Chem. Soc. Rev.* **48**, 1566–1595 (2019).

171. Jin, S. et al. Injectable tissue prosthesis for instantaneous closed-loop rehabilitation. *Nature* **623**, 58–65 (2023).

172. Huang, Z. & Wang, M. A review of electroencephalogram signal processing methods for brain-controlled robots. *Cogn. Robot.* **1**, 111–124 (2021).

173. Reaz, M. B. I., Hussain, M. S. & Mohd-Yasin, F. Techniques of EMG signal analysis: Detection, processing, classification and applications. *Biol. Proced. Online* **8**, 11–35 (2006).

174. Karnewar, J. S., Shandilya, D. R. V. K. & Tambakhe, M. D. A study on ECG signal analysis and ECG databases. *Int. J. Res. Advent. Technol.* **7**, 2321–9637 (2019).

175. Deng, Y. et al. Stretchable liquid metal based biomedical devices. *npj Flex. Electron.* **8**, 12 (2024).

176. Gao, W. & Yu, C. Wearable and implantable devices for healthcare. *Adv. Health Mater.* **10**, 2101548 (2021).

177. Koo, J. H. et al. Electronic skin: Opportunities and challenges in convergence with machine learning. *Annu. Rev. Biomed. Eng.* **26**, 331–355 (2024).

178. Yoo, S., Kim, M., Choi, C., Kim, D. H. & Cha, G. D. Soft bioelectronics for neuroengineering: New horizons in the treatment of brain tumor and epilepsy. *Adv. Healthc. Mater.* **13**, 2303563 (2023).

179. Park, J. et al. Electromechanical cardioplasty using a wrapped elastocoductive epicardial mesh. *Sci. Transl. Med.* **8**, 344 (2016).

180. Han, S. I. et al. Next-generation cardiac interfacing technologies using nanomaterial-based soft bioelectronics. *ACS Nano* **18**, 12025–12048 (2024).

181. Nam, S. et al. Needle-like multifunctional biphasic microfiber for minimally invasive implantable bioelectronics. *Adv. Mater.* **36**, 2404101 (2024).

182. Xu, Y. et al. Phase-separated porous nanocomposite with ultralow percolation threshold for wireless bioelectronics. *Nat. Nanotechnol.* **19**, 1158–1167 (2024).

183. Kim, H. J. et al. Integration of conductive nanocomposites and nanomembranes for high-performance stretchable conductors. *Adv. Nanobiomed. Res.* **3**, 2200153 (2023).

184. Lee, H., Kim, H. J., Shin, Y. & Kim, D. H. Phase-separated stretchable conductive nanocomposite to reduce contact resistance of skin electronics. *Sci. Rep.* **14**, 1393 (2024).

185. Jung, D. et al. Adaptive self-organization of nanomaterials enables strain-insensitive resistance of stretchable metallic nanocomposites. *Adv. Mater.* **34**, 2200980 (2022).

186. Jiang, Y. et al. A universal interface for plug-and-play assembly of stretchable devices. *Nature* **614**, 456–462 (2023).

187. Kim, D. C. et al. Three-dimensional foldable quantum dot light-emitting diodes. *Nat. Electron* **4**, 671–680 (2021).

188. Lee, M. et al. Nanomaterial-based synaptic optoelectronic devices for in-sensor preprocessing of image data. *ACS Omega* **8**, 5209–5224 (2023).

189. Choi, C., Lee, G. J., Chang, S., Song, Y. M. & Kim, D. H. Nanomaterial-based artificial vision systems: From bioinspired electronic eyes to in-sensor processing devices. *ACS Nano* **18**, 1241–1256 (2024).

190. Kim, M. et al. Cuttlefish eye-inspired artificial vision for high-quality imaging under uneven illumination conditions. *Sci. Robot.* **8**, eade4698 (2023).

191. Park, T. et al. Advances in flexible, foldable, and stretchable quantum dot light-emitting diodes: Materials and fabrication strategies. *Korean J. Chem. Eng.* **41**, 3517–3543 (2024).

192. Koo, J. H. et al. Recent advances in soft electronic materials for intrinsically stretchable optoelectronic systems. *Opto-Electron. Adv.* **5**, 210131 (2022).

193. Hong, J. H., Yoon, J., Kim, Y. & Lee, C. Embracing stretchable “Form Factor-Free” displays. *Inf. Disp. (1975)* **39**, 6–10 (2023).

194. Park, J., Seung, H., Kim, D. C., Kim, M. S. & Kim, D. H. Unconventional image-sensing and light-emitting devices for extended reality. *Adv. Funct. Mater.* **31**, 2009281 (2021).

195. Kim, J. H. & Park, J. W. Intrinsically stretchable organic light-emitting diodes. *Sci. Adv.* **7**, 9715 (2021).

196. Kim, J., Roh, J., Park, M. & Lee, C. Recent advances and challenges of colloidal quantum dot light-emitting diodes for display applications. *Adv. Mater.* **36**, 2212220 (2024).

197. Sun, Y., Jiang, Y., Sun, X. W., Zhang, S. & Chen, S. Beyond OLED: Efficient quantum dot light-emitting diodes for display and lighting application. *Chem. Rec.* **19**, 1729–1752 (2019).

198. Meng, X. et al. Stretchable perovskite solar cells with recoverable performance. *Angew. Chem. Int. Ed.* **59**, 16602–16608 (2020).

199. Bade, S. G. R. et al. Stretchable Light-Emitting Diodes with Organometal-Halide-Perovskite-Polymer Composite Emitters. *Adv. Mater.* **29**, 1607053 (2017).

200. Kim, D. C. et al. Intrinsically stretchable quantum dot light-emitting diodes. *Nat. Electron.* **7**, 365–374 (2024).

201. Song, J. K. et al. Stretchable colour-sensitive quantum dot nanocomposites for shape-tunable multiplexed phototransistor arrays. *Nat. Nanotechnol.* **17**, 849–856 (2022).

202. Yoo, S. et al. Wireless power transfer and telemetry for implantable bioelectronics. *Adv. Health Mater.* **10**, 2100614 (2021).

203. Kim, H. et al. Wide-range robust wireless power transfer using heterogeneously coupled and flippable neutrals in parity-time symmetry. *Sci. Adv.* **8**, eab04610 (2023).

204. Joo, H. et al. Soft implantable drug delivery device integrated wirelessly with wearable devices to treat fatal seizures. *Sci. Adv.* **7**, eabd4639 (2021).

205. Wang, C. et al. New Advances in Antenna Design toward Wearable Devices Based on Nanomaterials. *Biosensors* **14**, 35 (2024).

206. Shekhawat, S., Singh, S. & Kumar Singh, S. A review on bending analysis of polymer-based flexible patch antenna for IoT and wireless applications. *Mater. Today Proc.* **66**, 3511–3516 (2022).

207. Kim, S. H. et al. Strain-invariant stretchable radio-frequency electronics. *Nature* **629**, 1047–1054 (2024).

208. Lee, M. H. et al. A biodegradable secondary battery and its biodegradation mechanism for eco-friendly energy-storage systems. *Adv. Mater.* **33**, 2004902 (2021).

209. Hong, S. et al. Stretchable electrode based on laterally combed carbon nanotubes for wearable energy harvesting and storage devices. *Adv. Funct. Mater.* **27**, 1704353 (2017).

210. Song, W. et al. The strategy of achieving flexibility in materials and configuration of flexible lithium-ion batteries. *Energy Technol.* **9**, 2100539 (2021).

211. Lee, W. H. et al. Floatable photocatalytic hydrogel nanocomposites for large-scale solar hydrogen production. *Nat. Nanotechnol.* **18**, 754–762 (2023).

212. Quan, Y., Chen, M., Zhou, W., Tian, Q. & Chen, J. High-Performance Anti-freezing Flexible Zn-MnO<sub>2</sub> Battery Based on Polyacrylamide/Graphene Oxide/Ethylene Glycol Gel Electrolyte. *Front. Chem.* **8**, 603 (2020).

213. Park, K. I. L., Jeong, C. K., Kim, N. K. & Lee, K. J. Stretchable piezoelectric nanocomposite generator. *Nano Convergence* **3**, 12 (2016).

214. Vallem, V., Sargolzaeival, Y., Ozturk, M., Lai, Y. C. & Dickey, M. D. Energy Harvesting and Storage with Soft and Stretchable Materials. *Adv. Mater.* **33**, 2004832 (2021).

215. Xiao, X., Chen, G., Libanori, A. & Chen, J. Wearable triboelectric nanogenerators for therapeutics. *Trends Chem.* **3**, 279–290 (2021).

216. Gu, L. et al. Enhancing the current density of a piezoelectric nanogenerator using a three-dimensional intercalation electrode. *Nat. Commun.* **11**, 1030 (2020).

217. Park, J. et al. D. Reversible electrical percolation in a stretchable and self-healable silver-gradient nanocomposite bilayer. *Nat. Commun.* **13**, 5233 (2022).

218. Nam, T. U. et al. Intrinsically stretchable floating gate memory transistors for data storage of electronic skin devices. *ACS Nano* **18**, 14558–14568 (2024).

219. Shimanoe, S., Fukuda, K., Someya, T. & Yokota, T. Development of air-stable photomultiplication-type organic photodetector and analysis of active layer using removable top electrode. *Adv. Electron. Mater.* **8**, 2200651 (2022).